Assessing and Characterizing the Efficacy of the Constructed Wetland for Treating Pollutants in Landfill Leachate

A thesis presented to

the faculty of

the College of Arts and Sciences of Ohio University

In partial fulfillment

of the requirements for the degree

Master of Science

Chadaporn Busarakum

August 2016

This thesis titled

Assessing and Characterizing the Efficacy of the Constructed Wetland for Treating Pollutants in Landfill Leachate

by

CHADAPORN BUSARAKUM

has been approved for

the Department of Geological Sciences

and the College of Arts and Sciences by

Eung Soek Lee

Associate Professor of Geological Sciences

Robert Frank

Dean, College of Arts and Sciences

ABSTRACT

BUSARAKUM, CHADAPORN., M.S., August 2016, Geological Sciences

Assessing and Characterizing the Efficacy of the Constructed Wetland for Treating Pollutants in Landfill Leachate

Director of Thesis: Eung Seok Lee

Constructed wetlands are one of the effective wastewater treatment systems which have been utilized since 1950s. Characterizing landfill leachate and monitoring the treatment system are important for operation and development of the system. The objectives of this study were to delineate hydrologic and chemical processes occurring in the constructed wetland which has been treating landfill leachate from Athens 691 Landfill in Ohio since 1996. The treatment system consisted of six wetland cells. The leachate has high levels of BOD_5, COD, ammonia, and metals, and low pH and low DO. Field parameters, inflow and outflow rates between wetland cells, and water isotopes were measured monthly to monitor water quality, flow, and storage change. The storage change in each month was corresponded to inflow and outflow rates. Seasonal water samples were collected from the wetland cells and analyzed for water chemistry and water isotopes to evaluate removal efficiencies. The results indicate that the average removal efficiencies of iron, manganese, ammonia, and sulfate were 99 %, 94 %, 84 %, and 69 %, respectively. The results from PHREEQCI indicated that iron and sulfide minerals were precipitating. The modeled data were in keeping with the observed metal concentrations which were decreasing as the water flows through the treatment cells. The removal efficiencies of ammonia, nitrate, BOD_5, and COD were influenced by the

seasonal variations of water temperature which constrains biological processes. Results of this study suggest that the constructed wetland could provide efficient and long-term option for treating landfill leachate in cost effective manner.

DEDICATION

To my mother, family and friends.

ACKNOWLEDGEMENTS

Accomplishing this research could not have been done without the devote support of my advisor Dr. Eung Soek Lee. Since my research began he has put forth great effort to see that all the required tools and resources were made available. His unwavering dedication to all of his advisees is a testament to the strength of the Ohio University, department of geology. I would also like to thank my thesis committee members Dr. Douglas Green, Dr. Dina L. Lopez, and Dr. Craig Grimes for offering their supplementary support whenever it was needed. None of this would be possible without the generous Royal Thai Government who provided me with a scholarship to travel to Ohio University and further my graduate education. I would like to thank the Office of the Civil Service Commission who managed the logistics of that scholarship. In addition to the contributions from the Royal Thai Government, the Geological Sciences Graduate Alumni Research Grant also provided ample funding to make this research possible.

I would like to thank Rachel Taulbee, Randy Spencer, and David Hunt, from the Ohio Environmental Protection Agency's Division of Surface Water for providing field assistance, sample analyses, and access to resources. Thank you to Mike Cooper from the Athens County Health Department for providing me with necessary technical publications from the construction of the landfill and for his time spent helping me acquire data and in the field. Finally, I would like to thank my graduate student companions, family, and friends for offering their knowledge, experience, and support throughout my graduate studies experience at Ohio University.

TABLE OF CONTENTS

Page

LIST OF TABLES

Page

LIST OF FIGURES

Page

CHAPTER 1: INTRODUCTION

Pollutants in leachate from improperly structured or operated landfills can contaminate surface and groundwater (Bulc, 2006). In characterizing leachates, it is important to characterize the quantity and compositions of leachate at specific sites and understand the long-term impacts through continued monitoring of leachate composition after landfill closure because the refuse will continue to decompose and increase the quantity of leachate (Kjeldson et al., 2002; Bulc, 2006). Treating landfill leachate is a challenge because the leachate may remain in the underlain rock and soil layers in the area for extended time periods. Traditional treatment methods involve collection and transport of leachate to off-site facilities. However, such approaches may be dangerous and costly, thus development of more affordable on-site treatment facilities is warranted (Bulc, 2006).

Constructed wetlands provide one of the lower-cost on-site wastewater treatment solutions (Hammer, 1993). The application of constructed wetlands for wastewater treatment has been increasing in Europe since 1950s and in the U.S. since the late 1960s (USEPA, 2000). They were built to treat pollutants in urban, municipal, industrial, and agricultural applications, acid mine drainage, and to solve flood problems. Although the treatment systems of constructed wetlands are based on ecological systems found in natural wetlands, constructed wetlands require a higher degree of control than natural wetlands (May and Edwards, 2001). Therefore, the detailed study of hydrologic and chemical processes occurring within these treatment systems is useful for developing remedial plans and further improving remedial efficacy of the wetland systems.

The Athens County 691 landfill was constructed in an area affected by acid mine drainage (AMD) and reclaimed after its closure in 1984. Wetlands were constructed around the landfill area in 1996, and they have been used to treat the AMD and landfill leachate. However, the systematics and efficacy of the constructed wetland treatment system have not been investigated in detail.

The hypothesis for this study is environmental and engineering conditions such as pH, temperature, precipitation, residence time, and flow rates of the constructed wetland control the hydrologic and chemical processes and the efficacy of the wetland in treating pollutants in landfill leachates and acid mine drainage.

The overall purpose of this study is to delineate hydrologic and chemical processes occurring in wetlands constructed for treating landfill leachate and AMD. This study aims to characterize the constructed wetland comprising six treatment cells regarding their flows, water balance, water quality, types and impacts of controlling factors, and efficiency in treating landfill leachate and acid mine drainage at the 691 Landfill in York Township, Athens County. Specific objectives include the following:

1. To characterize types, structure, and design specifications of the constructed wetland cells through a literature review.
2. To identify key pollutants in the landfill leachate through analyses of existing data.
3. To monitor temporal and spatial variations in flow and quality of water within each treatment cell through field measurements, sampling, and chemical analyses.

4. To delineate speciation and processes occurring in each treatment cell through hydrochemical modeling.
5. To characterize treatment efficiencies of the constructed wetland cells.

The detailed study of hydrologic and chemical processes occurring within these treatment systems will be useful for developing remedial plans and optimizing the wetland system.

CHAPTER 2: BACKGROUND

2.1 Landfill Leachates

Landfill leachate is the wastewater discharge from landfill that is generated through percolation of rainwater through the layers of rocks and soils in a landfill (Kjeldsen et al., 2002). Solid waste materials transfer their pollutants to the percolating water by physical, chemical, and microbial processes. The leachate exits the landfill as seeps or discharge to surface water and recharge to groundwater.

The waste materials collected from households, stores, restaurant, and offices, e.g., municipal solid waste (MSW) are disposed at municipal sanitary landfills. In landfills, organic wastes are decomposed by bacteria consuming oxygen and producing CO_2 and wastewater. When oxygen is completely depleted, anaerobic decomposition occurs to produce volatile fatty acids, amino acids, alcohols, ammonia, sulfides, and methane gas, and yield acidic leachate with high biological oxygen demand (BOD) and chemical oxygen demand (COD). Landfill leachate can also include all kinds of toxic organic compounds and metals depending on types of wastes accepted by the landfills (Niessen and Chansky, 1970).

2.2 Wetlands

Wetlands are the land areas that have the presence of surface water at periodically or all of the year due to their geographic settings (Kadlec and Wallace, 2008). Plants and microbes in wetlands have the ability to adapt themselves to transform and eliminate pollutants in the water flowing through the wetlands. Wetland terrain is considered as one

of the best environments that can naturally and cost-effectively reduce pollutants in surface water resources (Kadlec and Knight, 1996).

Constructed wetlands or engineered wetlands are often used as treatment systems that can effectively improve water quality of waste water (USEPA, 2000). Because biogeochemical processes occurring in natural wetlands can also occur in constructed wetlands, and the flow rates, water depths, and other hydrologic and biogeochemical conditions can be controlled, constructed wetlands can be more effective in treating wastewater compared to natural wetlands (USEPA, 2000). Constructed wetlands are classified into two types; free water surface and vegetated submerged bed wetlands. Both types have some characteristics in common, but they are distinguished by the location of the hydraulic grade line. In general, constructed wetlands are lined with impermeable materials to prevent infiltration (USEPA, 2000).

2.2.1 Free Water Surface Constructed Wetlands

Free water surface (FWS) constructed wetlands are designed to have function and appearance similar to natural wetlands (USEPA, 1999). Their typical features comprise open-water areas, emergent vegetation, and varying water depths. The aerobic zone is near the surface layer while the deeper water is anaerobic zone. The main components include a basin or channels with some liner to enclose the treatment cells, soil to support inlet structures that control influent wastewater, the areas of open-water and fully vegetated surface, and outlet structures that maintain shallow depth of water within the treatment cell. Figure 1 illustrates the main components of an FWS constructed wetland.

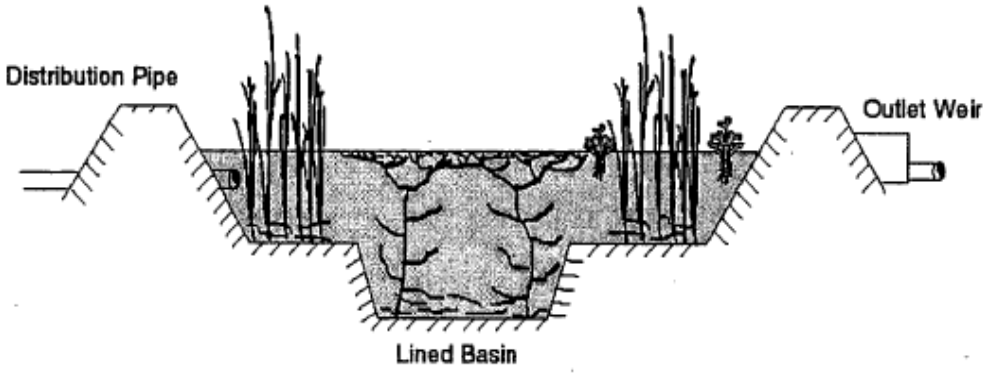

Figure 1. Definition sketch for free water surface constructed wetland with open water zone (USEPA, 1999).

2.2.2 Vegetated Submerged Bed Wetlands

Vegetated submerged bed (VSB) wetlands also consist of a basin with liners. The bedding of a porous substrate contains gravels which allow water flows through the media and also support the root structure of the emergent vegetation (USEPA, 1993) as shown in Figure 2. The water level is designed to remain below the top of gravel media and generates a horizontal flow path. The porous medium in a VSB wetland provides large surface area for treatment. Therefore, the VSB wetland requires a small area for treatment processes and a short retention time within the system (Vymazal, 2005). Also, waste water in a VSB wetland is not exposed to the surface because the water surface is maintained below the gravel media. It is possible to reduce odor problems, insect vectors as well as tolerate to a cold climate (USEPA, 1993).

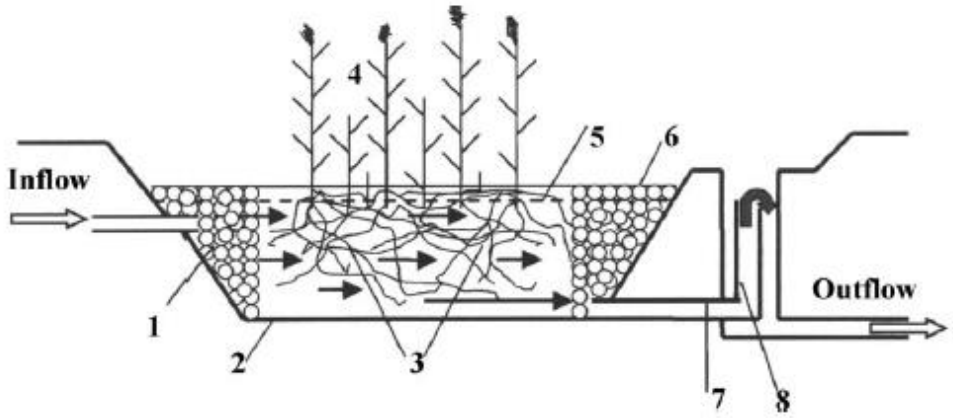

Figure 2. Components of VSB wetland.
1, distribute zone filled with gravel; 2, impermeable liner; 3, filtration medium (gravel, crushed rock); 4, vegetation; 5, water level in bed; 6, collection zone filled with gravel; 7, collection drainage pipe; 8, outlet structure for maintaining of water level in the bed (Vymazal, 2005).

2.3 Wetland Hydrology

The hydrology of wetlands is often considered the primary factor controlling water and nutrient availability, aerobic and anaerobic conditions, water chemistry, soil conditions, and water depth and velocity (USEPA, 1999). Since the hydrology is associated with all functions of wetlands, it is also the important design factor in constructed wetlands treatment efficiency (Mitsch and Gosselink, 2000). Therefore, it is crucial to understand the components affecting the hydrology of wetlands to properly design and construct wetlands.

2.3.1 Water Balance

The water balance determines inflows, outflows, and storage of water within wetland cells (USEPA, 1999). The flows and storage volume affect the length of time water spends in the wetland cells. In the case of constructed wetlands, the primary source

of water is continuous wastewater inflow, precipitation, runoff, and groundwater infiltration (in unlined wetland cells) while they lose water from outflow, evapotranspiration, and exfiltration to groundwater. The components of water balance are illustrated in Figure 3, and the water balance equation is expressed as equation 1:

$$\frac{\Delta V}{\Delta t} = [P + S_i + G_i] - [ET + S_o + G_o] \quad (1)$$

where $\frac{\Delta V}{\Delta t}$ is change in volume of water storage in wetland per unit time, P is precipitation, S_i is surface water inflow, G_i is groundwater inflow, ET is evapotranspiration, S_o is surface water outflow, and G_o is groundwater outflow (Mitsch and Gosselink, 2000). The terms of the water balance in equation 1 are expressed as volume per unit time (cm^3/month or m^3/month).

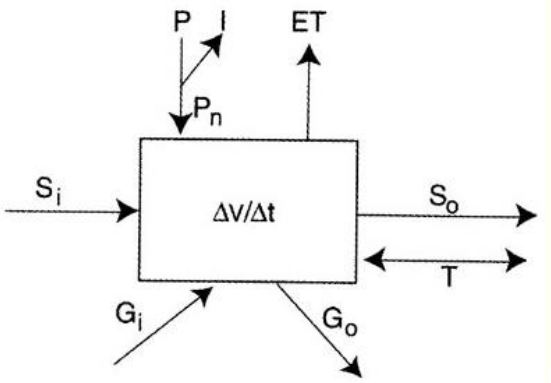

Figure 3. Diagram of water balance for a wetland with corresponding terms as in equation 1 (Mitsch and Gosselink, 2000).

Assuming that the diagram in Figure 3 represents the constructed wetland treatment cells, the water balance can be calculated using the parameters in (1). The variability of inflows caused by atmosphere effects can produce changes in hydrology in the wetlands (Mitsch and Gosselink, 2000; Neuhaus, 2013).

To calculate water balance of the constructed wetland, the detailed study of the components and estimation are discussed below.

2.3.1.1 Precipitation

Precipitation includes rainfall, snowfall, and any form of water that fall from the atmosphere (Mitsch and Gosselink, 2000). It is a source of water for landfill leachate which is wastewater flowing to the treatment system and the direct precipitation which increase water levels in treatment cells. The weather data sources such as the National Oceanic and Atmospheric Administration (NOAA) or National Climatic Data Center (NCDC) provided precipitation data for the study area.

2.3.1.2 Water Inflows and Outflows

The second component for calculating the water balance is surface inflow and outflow. Surface inflow is the main source of the water flowing into natural wetlands (Mitsch and Gosselink, 2000). The main surface inflows and outflows of constructed wetlands are confined to the inlet and outlet structures which were installed on each constructed wetland cell. The variation of inflow rates depends on seasonal effects and inflow rates into the collection systems (USEPA, 1999). The outflows are the amount of treated wastewater leaving the treatment cells at the outlet structures. The measurement of the inflows can be conducted where those structures were installed.

2.3.1.3 Groundwater Inflows and Outflow

Groundwater can either flow into the wetland to supply water or flow out of the wetland to the aquifer, depending on the relative elevation of the wetland and local groundwater level. In the constructed wetland, it is important to identify the groundwater

interactions in the system to understand the effect of these interactions on the treatment system.

2.3.1.4 Evapotranspiration

Water that vaporizes from water bodies or soil in a wetland is called evaporation and water that passes through plants to the atmosphere is called transpiration. The combination of these two processes is called evapotranspiration (Mitsch and Gosselink, 2000). Meteorological factors such as solar radiation, temperature, humidity, and wind speed have an influence on the amount of evapotranspiration (Mitsch and Gosselink, 2000). According to Neuhaus (2013), for surface water bodies, potential evaporation estimated by FAO-56 Penman-Monteith method were more accurate than using Thornthwaite method. The combined Penman-Monteith method as described by Zotarelli et al., (2009) is expresses as:

$$ET = \frac{0.408\Delta(R_n - G) + \gamma \frac{900}{T+273} U_2 (e_a - e_d)}{\Delta + \gamma(1 + 0.34U_2)} \quad (2)$$

where ET = evapotranspiration (mm/day)

U_2 = wind speed measured at 2-meter height (m/s)

R_n = net radiation flux at surface (MJ/m^{2}s)

G = soil heat flux (often estimated) (MJ/m^{2}s)

γ = psychometric constant (kPa /°C)

e_a = Saturation vapor pressure (kPa)

e_d = Actual Vapor Pressure (kPa)

T = Temperature (°C)

Δ = Slope of saturation vapor pressure curve (kPa/°C)

2.3.2 Stable Water Isotopes for Tracing the Hydrological Cycle

The stable isotropic composition of water provides a powerful tool for investigating water flow and mixing in surface and groundwater bodies (Clark and Fritz, 1997). Meteorological processes such as evaporation and condensation changes stable isotopes in water, i.e., ^{2}H and ^{18}O of water molecule. During precipitation, the heavy isotopes ^{2}H and ^{18}O fractionate out of water vapor into meteoric water and the water vapor becomes increasingly depleted with distance from their source water. The stable isotopes are measured as the ratio of two most abundance isotopes of a given element. Isotropic concentrations are expressed as parts per thousand or per mil (‰) which is the difference between ratios of the sample and reference from Vienna Standard Mean Ocean Water (VSMOW). The concentration value is expressed as delta (δ) notation. In this case, $\delta^{18}O$ and $\delta^{2}H$ values can by calculated by:

$$\delta^{18}O = \left[\frac{(\frac{^{18}O}{^{16}O})_{sample}}{(\frac{^{18}O}{^{16}O})_{VSMOW}} - 1\right] x\ 1000 \quad (3)$$

$$\delta^{2}H = \left[\frac{(\frac{^{2}H}{^{1}H})_{sample}}{(\frac{^{2}H}{^{1}H})_{VSMOW}} - 1\right] x\ 1000 \quad (4)$$

The values of $\delta^{18}O$ and $\delta^{2}H$ in fresh water vary depending on the hydrological cycle (Craig, 1961). The global meteoric water line defines the relationship between ^{18}O and ^{2}H in global scale using linear equation:

$$\delta^{2}H = 8\delta^{18}O + 10 \quad (5)$$

Local or regional meteoric water lines are different from the global line in both slope and deuterium intercept because of climatic and geographic differences. In a standing body of water, decrease in the slope of the $\delta^2 H$ v. $\delta^{18} O$ graph compared to the local meteoric water line indicates evaporation of water (Craig, 1961).

Isotope fractionation is the change in relative proportions of isotopes which occurs in thermodynamic reactions due to differences in the rates of reaction for different molecular species (Clark and Fritz, 1997). The partitioning of stable isotopes is expressed by the fractionation factor (α), which is the ratio of the isotope ratios for reactant and product. Reaction temperature has a significant effect on isotope fractionation. Therefore, equilibrium fractionation factors for water and vapor can be determined at different temperature as shown in Table 1. According to Rayleigh distillation, the process of rainout partitions ^{18}O and ^{2}H from the water vapor to the rain or snow. The general form of Rayleigh distillation is expressed as:

$$R = R_0 f^{(\alpha-1)} \tag{6}$$

where R is the isotope ratio in a decreasing reservoir of the reactant, R_0 is the initial isotopic ratio, f is the remaining fraction of that reservoir, and α is the equilibrium fractionation factor for the reaction.

In case of the constructed wetland, evaporation can be estimated by using Rayleigh distillation equation. When $\delta^{18} O$ values of water in the wetland cells are known, the remaining fraction of water can be calculated by equation 7 and 8.

Table 1 Values for fractionation relationship of ^{18}O and ^{2}H in water-vapor reaction (Clark and Fritz, 1997).

Temperature (°C)	$10^3 \ln \alpha^{18}O$	$10^3 \ln \alpha^{2}H$
-10	12.8	122
0	11.6	106
5	11.1	100
10	10.6	93
15	10.2	87
20	97	82
25	9.3	76
30	8.9	71
40	8.2	62
50	7.5	55
75	6.1	39
100	5.0	27

$$ln\left(\frac{\delta^{18}O+1000}{\delta^{18}O_0+1000}\right) = (\alpha - 1) \cdot \ln f \quad (7)$$

$$\delta^{18}O - \delta^{18}O_{\ 0} = 1000\ (\alpha - 1) \cdot lnf \quad (8)$$

where $\delta^{18}O$ is the isotope ratio of water from the outlet, $\delta^{18}O_{\ 0}$ is the isotope ratio of water from the inlet, f is the remaining fraction of the water in the wetland cell, and α is the equilibrium fractionation factor for the reaction depending on air temperature.

Faure (1986) established the relationship between $\delta^{18}O$ and $\delta^{2}H$ which represented the global meteoric water line (Figure 4). Deviation of $\delta^{18}O$ and $\delta^{2}H$ data from the meteoric water line indicates water that subjected to significant evaporation. The data plotted to the right of meteoric water line showing higher enrichment of $\delta^{18}O$ than $\delta^{2}H$.

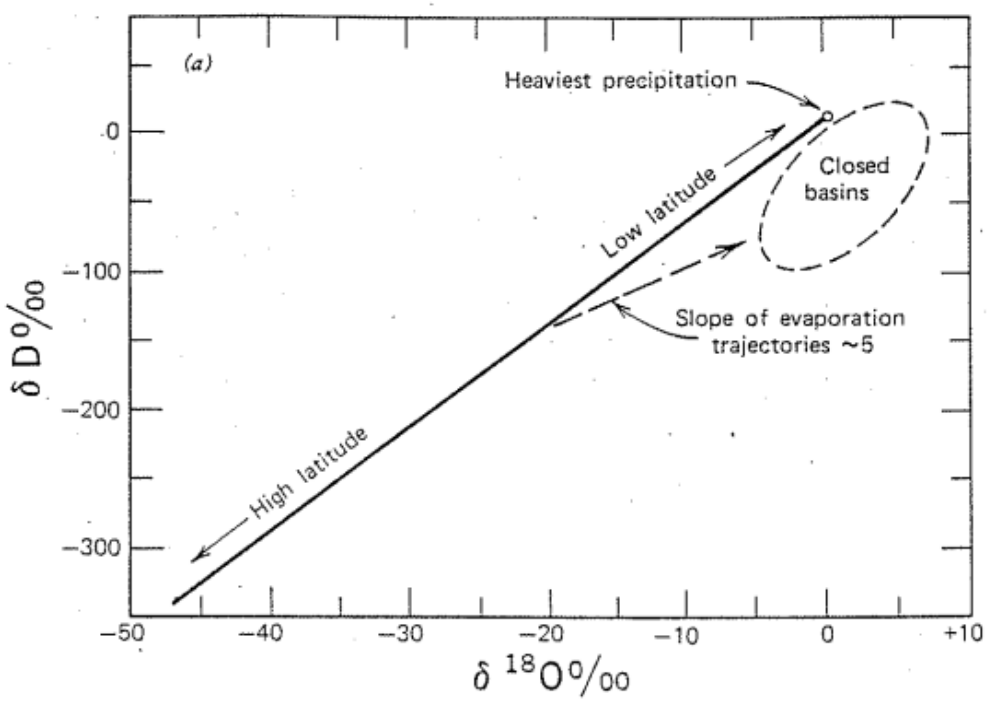

Figure 4. The relationship of $\delta^{18}O$ and $\delta^{2}H$ in meteoric water samples. The linear best fit represents meteoric water line (Faure, 1986).

2.3.3 Hydraulic Residence Time

Wetland hydraulics refer to the movement of water through the FWS constructed wetlands, which are water depth, volume, wetland porosity, average wastewater flow, hydraulic retention time, and hydraulic loading rate (USEPA, 1999). Residence time is the time of water moving through each treatment cell. It is one of the factors that play an important role in the pollutants removal efficiencies of wetlands (Shimala, 2000). The equation for calculating residence time is given as:

$$\text{Residence time} = \frac{\text{Volume of wetland cell (ft3)}}{\text{flow in or flow out (cfs)}} \quad (9)$$

2.4 Wetland Biogeochemistry

Constructed wetlands are designed to have similar functions as natural wetlands for the purpose of water quality improvement (Hammer et al., 1989). Therefore, the mechanisms of pollutants removal in natural wetlands have been studied and applied to wastewater treatment in constructed wetlands. The treatment system is a complex function of water, soil, plants, and microorganisms, which contributes to the mechanisms that are available to transform and eliminate pollutants in wastewater while it flows through the wetlands (USEPA, 1999).

The biogeochemical cycle is a key process in the treatment system. It is the transport and transformation of chemicals in ecosystems, which includes physical, chemical, and biological processes (Mitsch and Gosselink, 2000). These processes are related to hydrologic conditions in wetlands which determine the ability to improve water quality. The predominant physical, chemical, and biological mechanisms are liquid/solid separations and constituent transformations, which occur separately in the treatment processes (USEPA, 1999).

2.4.1 Conceptual Partitioning of Treatment Processes

The partitioning of wetland treatment processes occurs in different zones within the wetland volume as illustrated in Figure 5 (USEPA, 1999). Dissolved oxygen concentration determines the zones of aerobic biological processes. In open-water zones where oxygen transfers from the atmosphere to the water column, and sufficient dissolved oxygen is present, nitrification can occur. In contrast, denitrification, sulfate reduction, or methanogenesis can occur in anaerobic conditions where oxygen is

depleted. The suspended solids are more quickly settled down near the inlet zone while finer particulates are removed slowly by flocculent settling farther into the wetland.

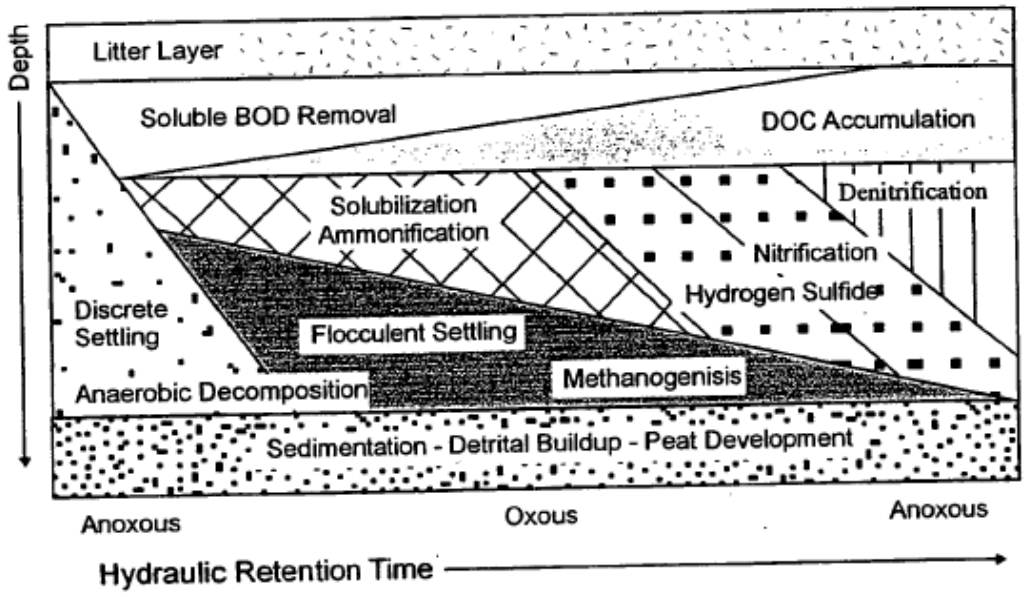

Figure 5. Conceptual partitioning of treatment processes through an FWS wetland (USEPA, 1999).

2.4.2 Metals Considerations

Coal mining processes cause acid mine drainage when metal sulfides are exposed to air and water and oxidized. Microorganisms can greatly accelerate oxidation, especially at low pH conditions. Iron is the main metal present in acid mine drainage (Ibanez, 2007). Oxidation of sulfide minerals such as pyrite can be represented by the equation:

$$FeS_{2(S)} + H_2O_{(l)} + 7/2O_{2(g)} \rightarrow Fe^{2+} + 2SO_4^{2-} + 2H^+ \quad (10)$$

Ferrous iron (Fe^{2+}) is then oxidized to become ferric iron (Fe^{3+}). Therefore, the removal of ferrous iron is limited by the rate of oxidation.

$$2Fe^{2+} + 1/2O_2 + H^+ \rightarrow 2Fe^{3+} + H_2O \quad (11)$$

Next, Fe^{3+} can be hydrolyzed and form insoluble ferric hydroxide precipitate. Hydrogen ions are released during the oxidation process causing the drainage pH decrease and become acidic.

$$Fe^{3+} + 3H_2O \rightarrow Fe(OH)_3 + 3H^+ \quad (12)$$

2.4.3 Roles of Wetland Plants in Controlling Treatment Processes

Wetland plants also play an important role in the water quality improvement. They provide a large surface area for suspended solid attachment and growth of microbes. The physical components of the plants help stabilize the surface of the beds and slow down the velocity of water which contributes to sediment settling and trapping process (Zhang et al., 2010). Photosynthesis by plants balances the oxygen within wetlands. Moreover, the oxygen can be transported from the leaves to the root zone and enhance microbial activities in decomposing organic matters (Akinbile et al., 2012). The typical wetland plants that can effectively uptake nutrients are Reed *Phragmites karka* and Cattail *Typha angustifolia* (USEPA, 1999).

2.4.4 Biochemical Oxygen Demand

Biochemical oxygen demand (BOD) is the parameter that influenced by biogeochemical cycle. It is the amount of oxygen consumed by microorganisms to decompose organic waste. If there is a large quantity of organic waste in water, the BOD level will be high. In the treatment of BOD, the physical processes including filtration and gravitational settlement remove particulate matters as illustrated in Figure 6 (USEPA, 1999). The microbial decomposition and removal of BOD are the processes that balance

BOD concentration within the wetlands (USEPA, 1999). Moreover, Karathanasis (2003) concluded that planted constructed wetlands with a variety of flowering plants provide the best treatment for BOD during warmer months of the year. Vegetation in wetlands can enhance substrate attenuation capacity through dense rooting which allows more microbial populations to transport extra oxygen.

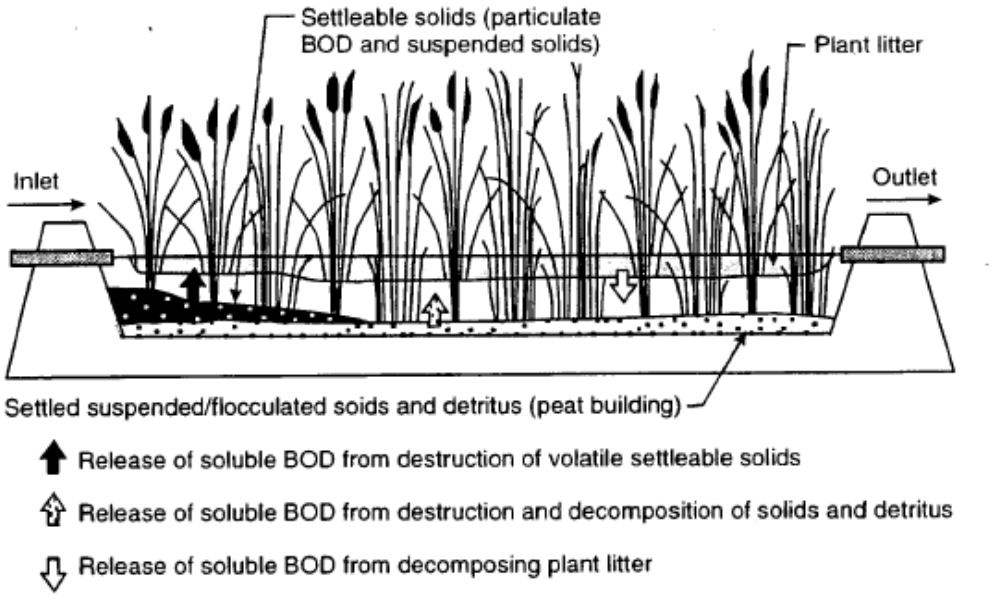

Figure 6. The balancing of BOD concentration within wetlands.
Incoming BOD is reduced by deposition of particulate forms near the inlet zones while decomposition processes create a return flux (USEPA, 1999).

2.4.5 Nitrogen Removal

Nitrogen occurs in various forms in wetlands including ammonium nitrogen, nitrate, and nitrite. Ammonium nitrogen is one of the pollutants of concern in the landfill. Nitrification is an aerobic process in which bacteria oxidize ammonia to nitrate nitrogen. It occurs in aerobic conditions with sufficient alkalinity and within a suitable temperature

range (Kadlec and Wallace, 2008). Nitrate nitrogen is transformed into nitrogen gas through nitrification of bacteria, which occurs in wetland plants where dissolved oxygen is depleted and organic carbon is high (USEPA, 1999).

2.5 Estimating Efficiency of Constructed Wetland Treatment Systems

To evaluate the ability to remove contaminants of constructed wetlands, researchers have been using similar methods that determine the treatment efficiency. The performance of each treatment system is specific and mainly dependent on the compositions of the pollutants that were being treated, as well as regional climate (Speer, 2012). The acceptable monitoring methods to investigate the treatment performance that was conducted is evaluating removal efficiency for the long-term maintenance of the system. In order to calculate removal efficiency, water samples need to be collected and analyzed for concentration of pollutants before and after being treated (Dunne et al., 2005; Bulc, 2006; Speer, 2012). Removal efficiencies of the leachate constituents can be calculated based on concentrations (mg/l) and flow (m^3/day) measurements using the equation:

$$\text{RE} = \frac{(Q_{inf} \text{ x } C_{inf}) - (Q_{eff} \text{ x } C_{eff})}{(Q_{inf} \text{ x } C_{inf})} x\ 100\% \qquad (13)$$

where Q_{inf} is the inflow rate (volume/time), C_{inf} is the influent concentration (mass/volume), Q_{eff} is the outflow rate (volume/time), and C_{eff} is the effluent concentration (mass/volume),

2.6 Statistical Analyses

Statistical analyses are often used to evaluate the results and examine the correlations between parameters before and after treatment. In general research, data

distributions are tests for normality. If the data are not normally distributed, log transformation is required to transform before proceeding statistical analysis. Then, statistically significant differences are determined. For instance, Speer et al. (2012) conducted Wilcoxon rank sum tests with software to determine statistically significant differences in the influent and effluent concentration data. Dunne et al. (2005) performed paired Student t-test. Statistical significance was based on a 95% confidence interval ($p < 0.05$). In order to examine the impact of seasonal and spatial variation in the system performance, Nzengy and Wishitemi (2001) plotted concentration data against time (months) for temporal analysis and sampling stations for spatial analysis. The best line of fit was fitted in each plot and One-way analysis of variance (ANOVA) was used to determine whether variations between and within stations were significant (Nzengy and Wishitemi, 2001). Moreover, the correlation between parameters in the inlets and outlets of wetland cells were tested by Pearson correlation coefficient at $p < 0.05$ and 0.01 (Bulc, 2006).

2.7 Hydrochemical Modeling

Although the removal mechanisms in wastewater treatment systems have been described in the literature (Hammer, 1993; Nzengy and Wishitemi, 2001; Dunne, 2005; Speer, 2012), the hydrochemical modeling for chemical species in the treatment processes are rarely evaluated because precipitation and dissolution of certain minerals that occur the treatment system need to be calculated.

A hydrochemical model PHREEQC interactive (PHREEQCI) is based on the equilibrium chemistry of aqueous solutions and simulates chemical reactions and

transport processes through a one- dimensional flow path in natural or polluted waters (Parkhurst and Appelo, 2013). The primary functions of the program can be used to perform all modeling aspects of chemical speciation, batch-reaction, forward modeling, and inverse modeling. The powerful inverse modeling capability allows identification of reactions that occur as water evolves along a flow path (Parkhurst and Appelo, 2013). This program was used to calculate chemical budgets for chemical species to investigate the evolution of stream chemistry in Hewett Fork watershed (Schleich, 2014). The inputs are chemical analyses of water at different points along the flow path. A mole-balance model can be calculated from the analyses and phases.

An example of inverse modeling for the chemical evolution of spring-water compositions in the Sierra Nevada was described by Parkhurst and Appelo (2013). The differences in composition between two spring-waters were assumed to be caused by reactions between the water, the minerals and the gases it has contacted. The analytical data for two springs were input in the program. The SOLUTION_SPREAD data block was used to investigate the two spring waters. The INVERSE_MODELING data block defined the inverse-modeling calculations, including the solutions and phases to be used, the mole-balance equations, and the uncertainty limits. The program generated two inverse models in the output. The results show the relative fractions of each solution, which were derived from the mole balance on water. For two solutions in the model, the fraction for each solution will be 1.0. The positive phase mole transfers indicate dissolution while negative mole transfers indicate precipitation. Through inverse modeling using PHREEQCI, it was concluded that the main reactions in the first model

were the dissolution of calcite, plagioclase and carbon dioxide; kaolinite. In the second model Ca-montmorillonite precipitate, and kaolinite and chalcedony were precipitated. Small amounts of halite, gypsum, and biotite dissolution were required in the models. For this study, analytical data for inflow and outflow water samples of each cell will be used as input data.

Glynn and Brown (1996) performed inverse modeling to help identify the mass transfer reactions and the extent of the mass transfer reactions of contaminants in groundwater. The site is located at the Pinal Creek site where had been affected by acid mine drainage. They suggested that the flow path indicate the mass transfer reactions when acidic groundwater is treated by aquifer materials as flow through the aquifer. The research used eleven mass balance constrains on Cl, Ca, Mg, Na, Al, Si, Fe, Mn, C, redox state, and S. The mineral phases were constrained in at least one phase. Fourteen minerals were considered in the model; calcite, goethite, gypsum, dolomite, SiO_2, MnO_2, $MnCO_3$, anorthite, gibbsite, $Mn(OH_3)$, tremolite, $AlOHSO_4$, biotite, and K-montmorillonite. PHREEQCI produced seven tentative inverse mass balance models. According to their results, the modeling depended on the mineral and gas phases assumed for the input.

CHAPTER 3: STUDY SITE

3.1 Site Location

The Athens County 691 Landfill is in York Township, Athens County approximately 6.5 kilometers south of Nelsonville, Ohio (Figure 7). The constructed wetland is located on Glen Ebon Road down from the intersection of State Route 691 and Glen Ebon Road.

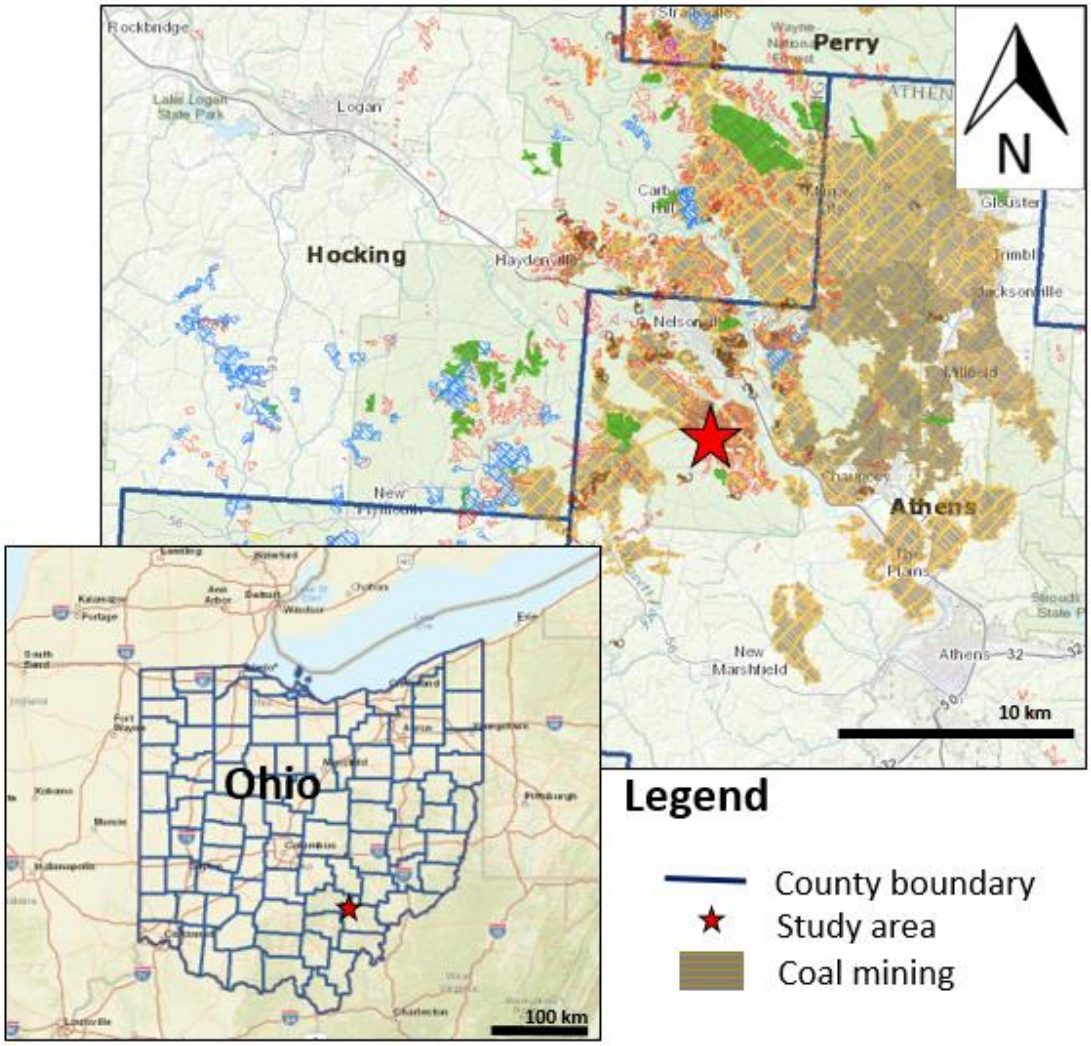

Figure 7. A map showing the study area and the location of abandoned coal mining. (Retrieved from https://gis.ohiodnr.gov/MapViewer/?config=OhioMines).

3.2 Site History

The Athens 691 landfill is located within Upper Freeport rocks that were strip-mined for coal between 1944 and 1969. The site began operating as a landfill in 1969. During landfill operation, industrial and municipal solid wastes were placed in the area. The landfill was closed in 1984. A clay cap was installed to diminish precipitation infiltration and for leachate treatment process.

In order to reduce the effect of pollutants from the landfill leachate flowing to the Minker's Run tributary and Hocking River, the constructed wetland treatment system was constructed in 1996. The constructed wetland is located on the east side of the landfill (Figure 8). Since the site was originally a coal mine and later operated the landfill, the landfill leachate consists of a combination of acid mine drainage (AMD) and sanitary landfill leachate. The leachate composed of high acidity, ammonia, suspended solids, conductivity, total iron, total manganese, and low in pH and dissolved oxygen (MRB Environmental Services, Inc., 1998).

3.3 Site Geology and Hydrogeology

The study area is part of the Appalachian Plateau Province, in which bedrock dips slightly to the southeast (Sturgeon et al., 1958). Rocks of Pennsylvanian age (Conemaugh and Allegheny Groups) underlie the landfill area. The Allegheny Group comprises a cyclothem sequence of The Upper Freeport formations, Bolivar, and The Lower Freeport (Figure 9 and 10). These formations consist of alternating layers of sandstone, shale, limestone, coal, clay, and siltstones. The coal unit of the Upper Freeport and overlying strata were removed by strip-mining.

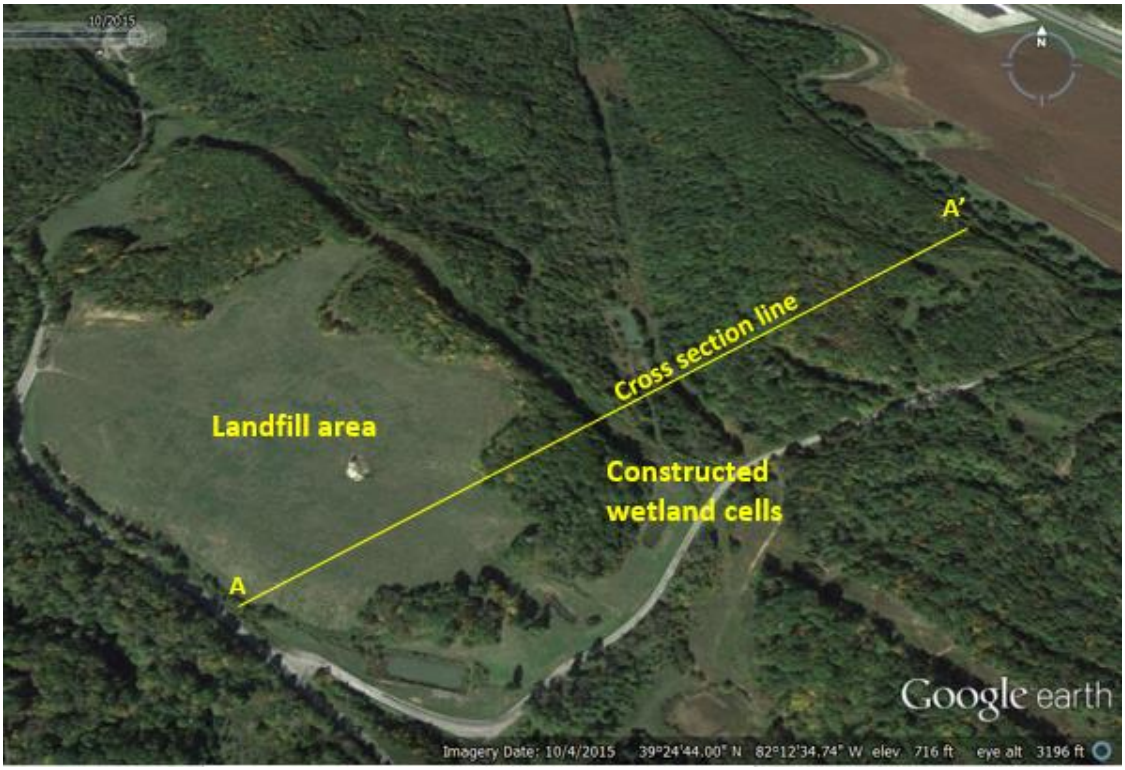

Figure 8. Satellite image showing the location of landfill area and the constructed wetland cells.

The Mahoning Formation of the Conemaugh Group is the youngest formation composing the upper portion of the hills, which have an average height of 240 feet. The Hocking River, located east of the landfill, receives the discharge from the lower Freeport sandstone that underlies the landfill (Seaman, 1984).

The uppermost saturated unit beneath the landfill is the Upper Freeport formation which is composed of sandstone and sandy shale approximately 4 to 18 feet thick (ARCADIS U.S., Inc., 2013). The Upper Freeport saturated zone has been identified as the zone of significant saturation. The Bolivar Shale lies beneath the Upper Freeport saturated zone and thickness ranges from 5 to 22 feet. Based on the results from monitoring program, a limited amount of groundwater is present in isolated fractures

within the Bolivar Shale (ARCADIS U.S., Inc., 2015). This formation is not a zone of significant saturation beneath the site. The Lower Freeport formation is the primary aquifer, comprised of sandstone, and is over 34 feet thick (Seaman, 1984). Both the Upper and Lower Freeport formations are monitored as part of the groundwater quality monitoring and assessment program (ARCADIS U.S., Inc., 2013).

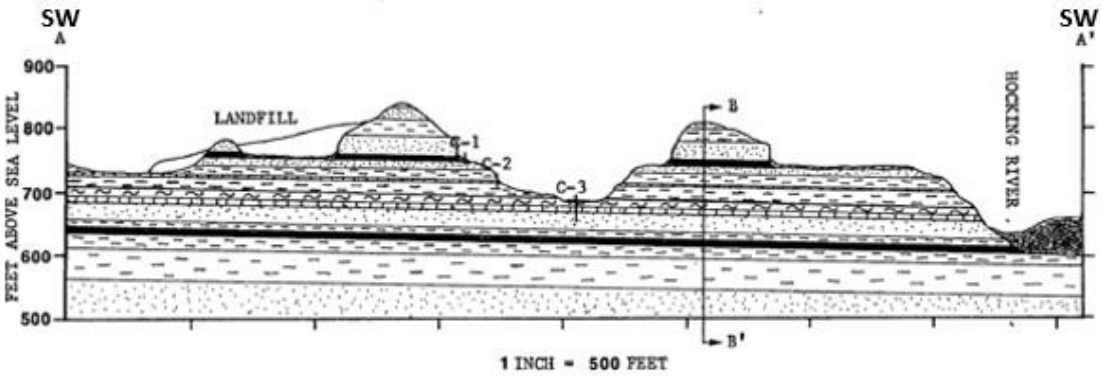

Figure 9. Geologic cross-section of the Athens County 691 landfill in northeast - southwest direction (Seaman, 1984).

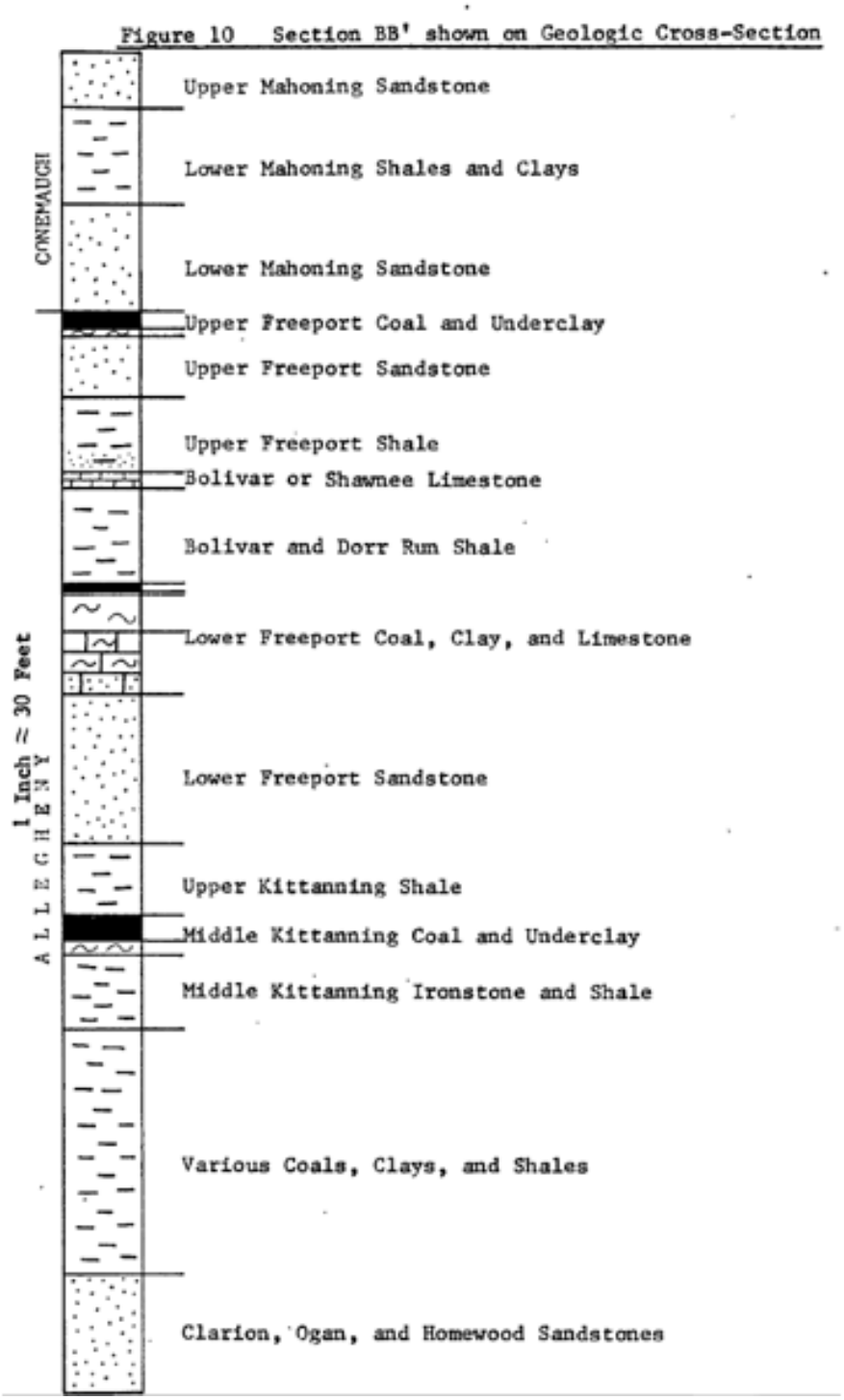

Figure 10. Stratigraphic column of rocks in the Athens County 691 landfill (Seaman, 1984).

3.3.1 Upper Freeport Aquifer

According to hydraulic head data from groundwater monitoring wells, groundwater in the Upper Freeport formation locally flows to the south and west (ARCADIS U.S., Inc., 2015) as shown on the Upper Freeport Potentiometric Surface Map for October 7, 2015 (Figure 11). Average hydraulic conductivity of the Upper Freeport Aquifer determined by pumping tests are 0.87 ft/day (Seaman, 1984). Based on the potentiometric map, the Upper Freeport is at the elevation ranges from 725 to 750 feet. The lateral extent of the Upper Freeport saturated zone is limited because the surface topography of the landfill and groundwater in this aquifer flows to the opposite direction where the constructed wetland are located. Therefore, groundwater in this aquifer could not contribute flow to the constructed wetland.

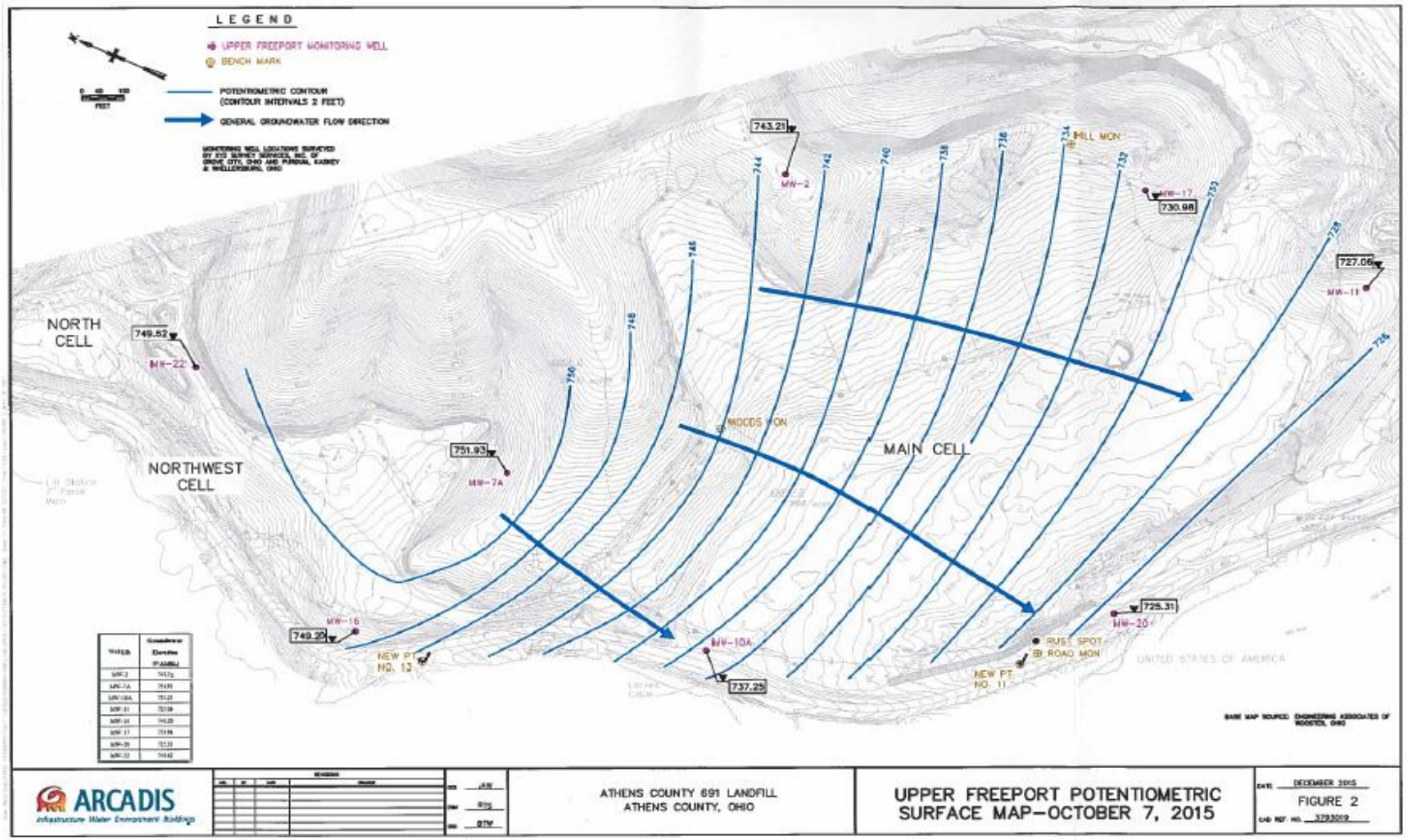

Figure 11. Potentiometric surface map of The Upper Freeport aquifer. (ARCADIS U.S., Inc., 2015).

3.3.2 Lower Freeport Aquifer

Groundwater in the Lower Freeport aquifer flows to the eastern portion of the landfill and discharges into the Hocking River (ARCADIS U.S., Inc., 2015) as shown on the Lower Freeport Potentiometric Map for October 7, 2015 (Figure 12). Average hydraulic conductivity of the aquifer determined by recovery methods are 0.13 ft/day (Seaman, 1984).

Groundwater elevation in the Lower Freeport Aquifer ranges from 707 to 686 feet. The hydraulic heads indicate that the groundwater from this aquifer could not contribute flow to the constructed wetland cells in high elevation; however, the groundwater could discharge to the lower constructed wetland cells near Minker's Run tributary.

3.4 Groundwater Monitoring Well Summary

The groundwater quality data compiled by ARCADIS presents the results from spring 2013 to fall 2015 at the site. According to the report, groundwater quality remained unchanged. A summary of the statistical analyses for the Upper Freeport zone shows that chloride concentrations in monitoring wells are below the corrective measures plan (CMP) concentration limit of 288 mg/l. Sodium concentrations are below the CMP concentration limit of 196 mg/l. Chemical oxygen demand (COD) concentrations are below the CMP concentration limit of 98.8 mg/l. The detected volatile organic compounds (VOCs) are below maximum concentration limits in this zone. The Lower Freeport Formations were sampled for metals, ammonia, chloride, COD, and VOCs. They were detected below the reporting limit (ARCADIS U.S., Inc., 2015).

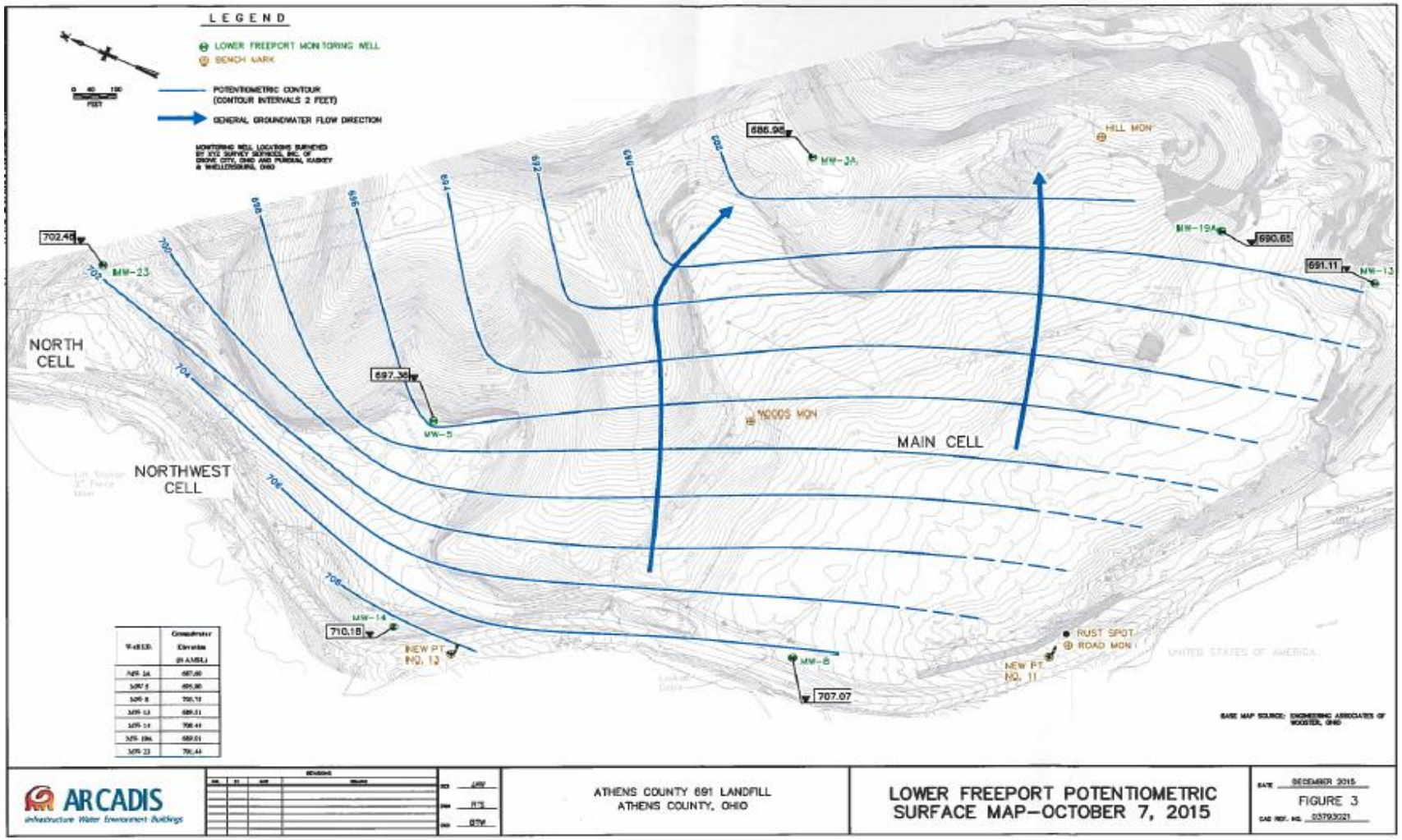

Figure 12. Potentiometric surface map of The Lower Freeport aquifer. (ARCADIS U.S., Inc., 2015).

3.5 The Design of Constructed Wetland Cells

Characteristics of discharge from the landfill contribute to the design of constructed wetland cells. Since the discharge from the landfill is segmented into two categories for treatment; acid mine drainage (AMD) and landfill leachate, the constructed wetland was designed to reduce suspended solids, iron, manganese, and ammonia loading. A pre-treatment system was constructed in the form of settling ponds in order to facilitate precipitation of metals.

Construction of the wetland treatment system began in September, 1996. The wetland system was designed by Mike Crau at MRS Environmental Service, Inc as shown in Figure 13-15. Table 2 provides size and flow rate of each treatment cell.

The treatment ponds were constructed using in-situ material that was composed of Guernsey Upshur soil complex. This soil complex consists of a mixture of silty loam and silty clay loam and has moderately low to low permeability (MRB Environmental Services, Inc., 1998).

Table 2 The design of constructed wetland.

Wetland cell	Elevation (ft)	Size (ft)	Volume (ft^3)	Treatment purpose
1	706.8	70 x 4 x 0.4	112	Iron and manganese removal
2	706	90 x 20 x 4	7,200	Iron and manganese removal
3	705	40 x 20 x 2	1,600	Iron and manganese removal
4	703	130 x 35 x 4	18,200	Iron and manganese removal
5	686.5	160 x 45 x 1	7,200	Aerobic treatment of BOD
6	681.7	150 x 55 x 1	8,250	Aerobic treatment of BOD

The design goal of the sedimentation ponds and free water surface wetland cells 1, 2, 3, and 4 are to remove metals in the leachate. Aerobic wetlands are shallow (1 to 3 feet deep) ponds. They promote oxidation of metals and precipitation of iron, manganese, and other metals (Ford, K.L. 2003). Physical precipitation in cell 1 and 3 is the primary mechanism for removal of iron and manganese from water. Anaerobic wetlands in cell 2 and 4 are lined with sand to reduce metals.

A limestone spillway was placed between cell 2 and 3 to add alkalinity and raise pH values of wastewater when water flows down a steep slope with limestone riprap (Ford, K.L. 2003). Cells 5 and 6 are designed as aerobic wetlands providing a reiteration process to further reduce metals in water.

Figure 13. Photograph of the constructed wetland cell 1

Figure 14. Photographs of the constructed wetland cell 2 and limestone drain (top), and cell 3 (bottom).

Figure 15. Photographs of the constructed wetland cell 4 (top-left), cell 5 (top-right), and cell 6 (bottom).

CHAPTER 4: METHODS

The objectives of this study are; 1) to determine hydrologic and chemical processes occurring in wetlands constructed for treating landfill leachate and AMD, 2) to investigate a constructed wetland comprising six treatment cells in terms of their flow, water balance, water quality, types and impacts of controlling factors, and 3) assess efficiency in treating landfill leachate and acid mine drainage at the 691 Landfill in York Township, Athens County. The study methods required to achieve the objectives were divided into two sections including hydrological and hydrochemical characterization of the constructed wetland.

4.1 Hydrological Characterization of the Constructed Wetland

Hydrology of a constructed wetland is an important factor to consider in estimating the treatment efficiency (Kadlec and Wallace, 2008). Hydrological characterization depends on field measurements of water inflow and outflow rates and on analysis of samples collected at the site. Flow and storage volume determine the length of time that water spends in the wetland cells. Hydrologic factors including water balance and hydraulic residence time were estimated as follows.

4.1.1 Field Data Collection

To investigate the performance of the constructed wetland for landfill leachate treatment, field parameters and water samples were collected at eight sampling locations as describe in Table 3 and Figure 16. The field parameters include flowrates, temperature, pH, electrical conductivity, and dissolved oxygen (DO) measured using meters. Water

samples were collected and analyzed for water quality monitoring and constructing hydrochemical model.

Table 3 Sampling locations.

Station number	Description	Location
601-1	Cell 1influent	Landfill leachate from influent manhole
601-2	Cell 1 effluent	Discharge from cell 1
602	Cell 2 effluent	Discharge from cell 2
603	Limestone drain	Inlet to cell 3
604	Cell 3 effluent	Metal gate discharge from cell 3
605	Cell 4 effluent	Metal gate discharge from cell 4
606	Cell 5 influent	The inlet PVC pipe in cell 5
001	Final outfall	Final discharge outfall from cell 6

4.1.2 Flow Rate Measurements

Water inflow and outflow rates to and from wetland cells were measured monthly at inlet and outlet points of individual wetland cells as shown in Figure 16. The leachate from the landfill has been collected by underground pipes installed on the west and east side of the landfill that discharge to cell 1. The velocities of water flows into cell 1 were measured at the PVC pipes using FLO-MATE Model 2000 portable flowmeter. The equation 14 and 15 were used to calculate cross sectional area (A) of water in the pipe as shown in Figure 17.

$$a = 2\,cos^{-1}\,\frac{R-h}{R} \tag{14}$$

$$\mathrm{A} = \frac{1}{2}R^2(a - \sin a) \tag{15}$$

where a is angle, R is radius, h is water height, A is cross sectional area of the water in the pipe.

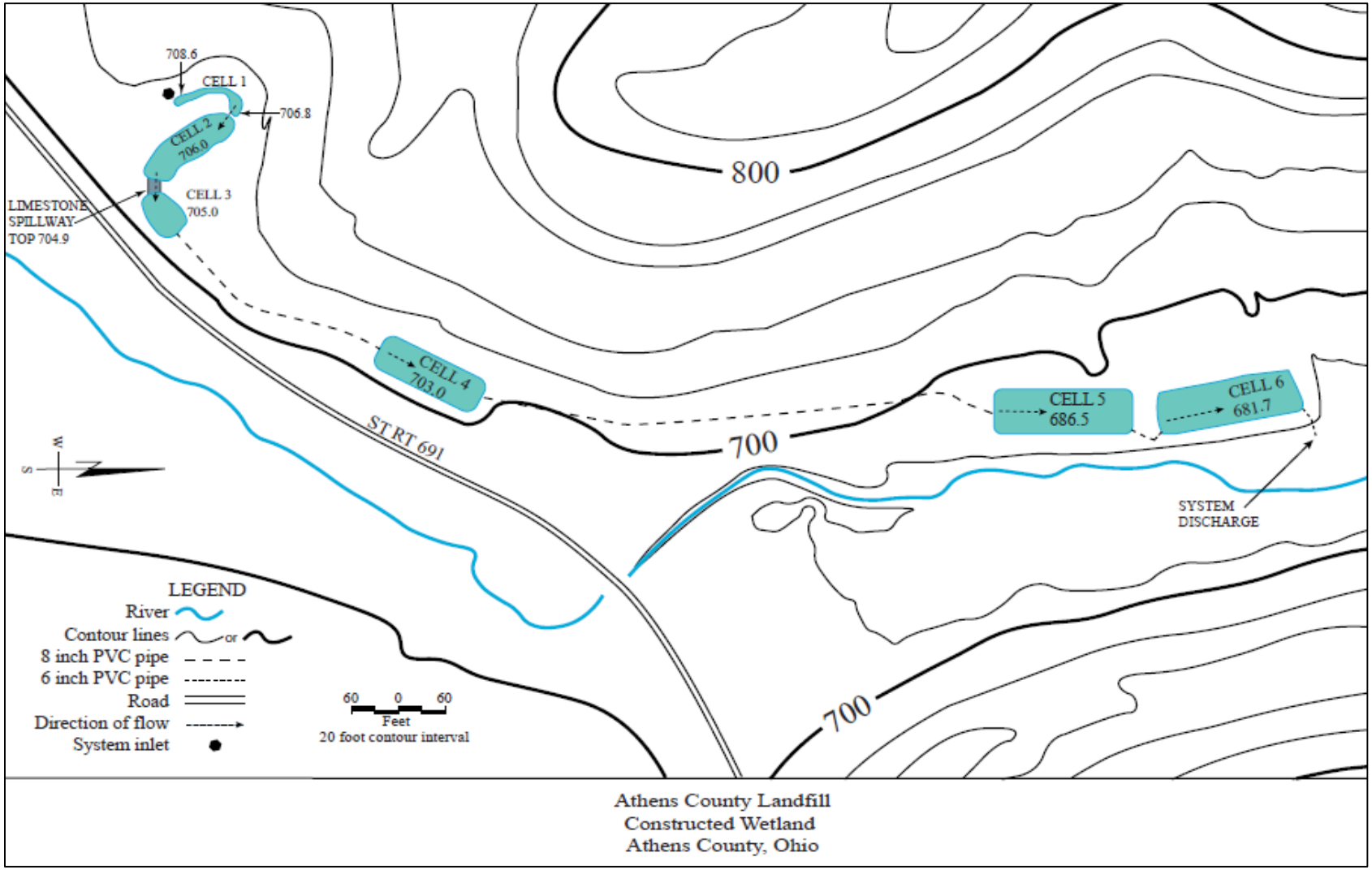

Figure 16. Constructed wetland plan illustrating elevations flow paths between the treatment cells.

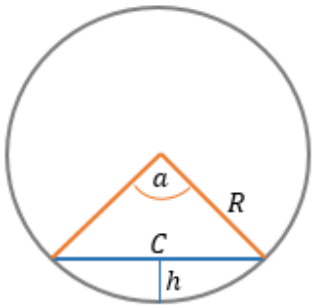

Figure 17. Cross section area of the pipe with the open flow when the height of water (h) less than the radius of the pipe (R).

Volumetric flow rates of the leachate were calculated by:

$$Q = V \times A \quad (16)$$

where Q is volumetric flow rate (m^3/s), V is measured flow velocity, and A is cross sectional area of the water in the pipe (m^2).

Water flow rates between the wetland cells were measured by collecting a liter of water in a period of time by using stopwatch and bucket. The outflow from cell 1 was measured at a foot-height waterfall between cell 1 and 2. Due to the limestone spillway between cells 2 and 3, which allows water seep through the rock or overflow on surface, water outflow from cell 2 was not available to measure. The inflow to cell 5 and outflow rates from cell 6 were measured by using stopwatch and bucket at the PVC pipes.

4.1.3 Water Balance

The movement of water within the constructed wetland cells can be expressed as a water balance. The water balance of the constructed wetland area during the study period (August 2015 – June 2016) was based on a conceptual model in Figure 18. The total volume of water storage is the volume combined for six wetland cells. Therefore, the water

balance in this study is an estimation of overall storage change in the constructed wetland area. Change in water storage was estimated by using equation 17.

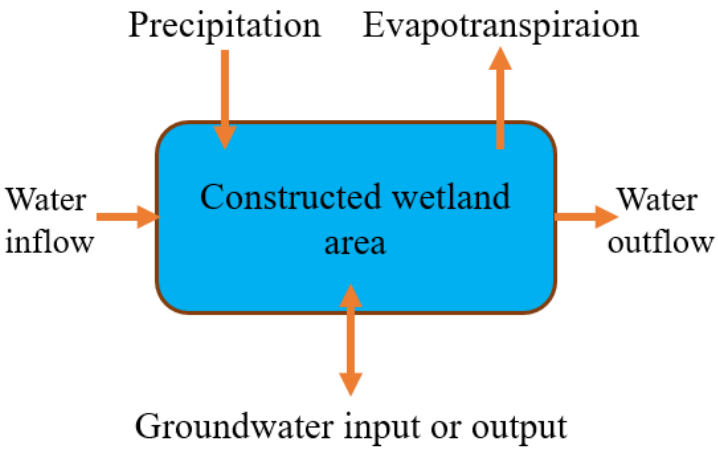

Figure 18. Schematic diagram of the factors contributing water balance of the constructed wetland.

$$\Delta S = [P + W_i + G_i] - [ET + W_o - G_o] \quad (17)$$

where ΔS = storage change, P = precipitation, W_i = surface-water inflow, G_i = groundwater inflow, ET = evapotranspiration, W_o = surface-water outflow, G_o = groundwater outflow

The water balance components in equation 17 were collected and estimated from the sources and the methods described below.

4.1.3.1 Climate Data

Monthly weather data from August 2015 through June 2016 including precipitation (inch) and air temperature (F) were obtained by National Oceanic and Atmospheric Administration (NOAA) at Nelsonville, Ohio weather station. Online climate data, which provides the dataset for monthly averages of temperature and

precipitation, is available through NOAA website (http://www.ncdc.noaa.gov/cdo-web/datasets). Since the treatment system in the study area was constructed in a small area and the wetland cells were connected to each other, the total precipitation was considered to be equal for every wetland cell. The data units were adjusted to the format that can be applied for water balance calculation. Temperature data were converted from units of Fahrenheit to Celsius. Precipitation data unit was converted from inches to meters.

4.1.3.2 Evapotranspiration

Evapotranspiration was estimated using a model based on climate data and water isotopic compositions of wetland water, and Rayleigh distillation model, which will be discussed in section 4.1.4. The CROPWAT 8.0 program was used to estimate evapotranspiration (ET_o). The calculation procedures used in the program are based on FAO Penman-Monteith Method (Zotarelli et al., 2009). The required weather data input for the program include temperature (°C), wind speed (km/day), relative humidity (%), and sunshine hours. Monthly average data for wind speed and relative humidity were collected from Western Regional Climate Center (WRCC) RAWS USA Climate Archive at Zaleski, Ohio station. Sunshine data were obtained by National Research Council (NRC) mean hours of bright sunshine with 30 days in a month for various latitudes (Table 4). The sunshine data are the correction factors that have been used to calculate evapotranspiration in Thornthwaite (1948) method (Gray et al., 1970). Since the study area is located on latitude 39.40 °N, sunshine data at north latitude 40°N is used in this study.

Monthly evapotranspiration values were calculated by selecting “Climate/ETo” icon in the module bar located on the left on the main CROPWAT window. The collected climate data were input to the data window. The output of radiation and ETo data were calculated from the program using the FAO Penman-Monteith approach as shown in Figure 19.

Table 4 NRC mean hours of bright sunshine expressed in units of 30 days of 12 hours each day (Gray et al., 1970).

North Lat.	J	F	M	A	M	J	J	A	S	O	N	D
0	1.04	0.94	1.04	1.01	1.04	1.01	1.04	1.04	1.01	1.04	1.01	1.04
10	1.00	0.91	1.03	1.03	1.08	1.06	1.08	1.07	1.02	1.02	0.98	0.99
20	0.95	0.90	1.03	1.05	1.13	1.11	1.14	1.11	1.02	1.00	0.93	0.94
30	0.90	0.87	1.03	1.08	1.18	1.17	1.20	1.14	1.03	0.98	0.89	0.88
35	0.87	0.85	1.03	1.09	1.21	1.21	1.23	1.16	1.03	0.97	0.86	0.85
40	0.84	0.83	1.03	1.11	1.24	1.25	1.27	1.18	1.04	0.96	0.83	0.81
45	0.80	0.81	1.02	1.13	1.28	1.29	1.31	1.21	1.04	0.94	0.79	0.75
50	0.74	0.78	1.02	1.15	1.33	1.36	1.37	1.25	1.06	0.92	0.76	0.70

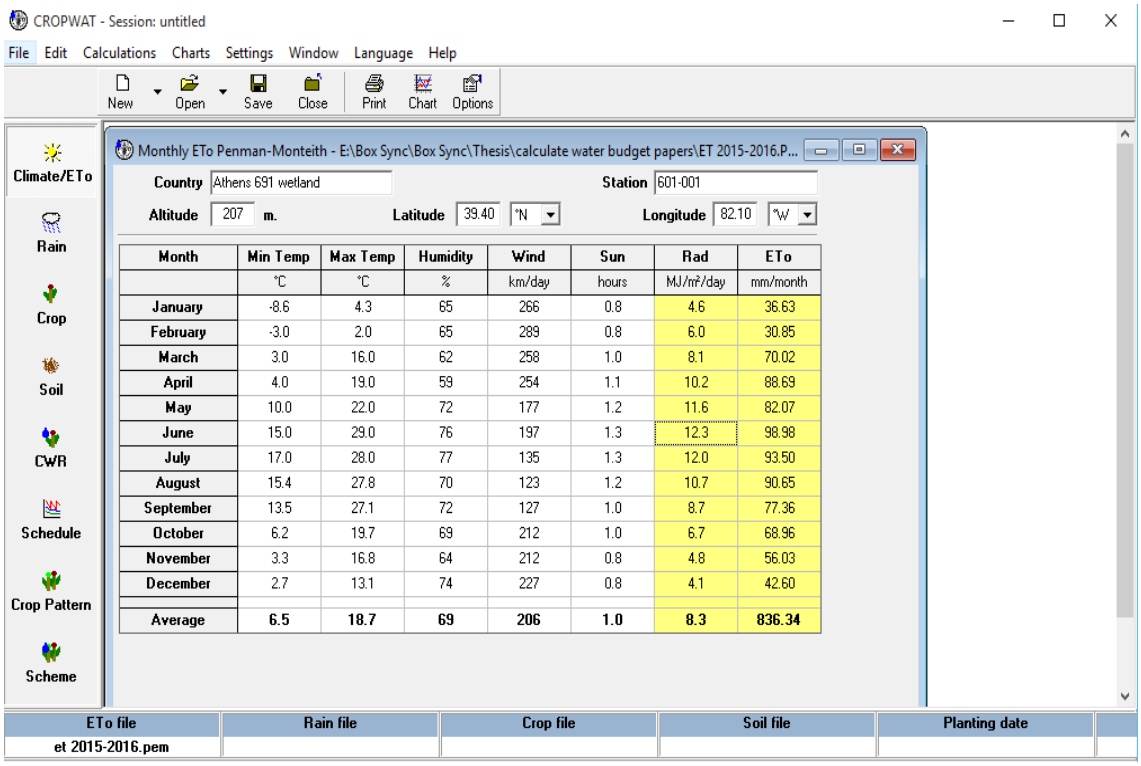

Figure 19. Printout ETo data from CROPWAT 8.0 program.

4.1.3.3 Groundwater Inflow and Outflow

The lateral extent of the Upper Freeport saturated zone is limited because the surface topography of the landfill and groundwater in this aquifer flows to the opposite direction where the constructed wetland are located. Therefore, there appears to be no groundwater interactions from this aquifer to the wetland cells. Groundwater interactions in the constructed wetland cells can be mainly influenced by Lower Freeport Aquifer. The hydraulic heads indicate that the groundwater from the Lower Freeport Aquifer could contribute flow to the constructed wetland cells in low elevations (cell 5 and 6) near Minker's Run tributary. It was estimated that groundwater in Lower Freeport Aquifer was flowing from the landfill toward Hocking River with hydraulic gradient 0.063. Averaged hydraulic conductivity of Lower Freeport Aquifer is 0.0395 m/day. The amount of groundwater flow into and out of the cells was calculated by using Darcy's Law:

$$Q_{in/out} = Kx\ i\ x\ A \tag{18}$$

where $Q_{in/out}$ is volume of groundwater flow in or out of the cells (m^3/day), K is hydraulic conductivity of the aquifer, i is hydraulic gradient, and A is cross section area of cell 5 and 6.

Groundwater in the aquifer flow horizontally into cells 5 and 6 as illustrated in Figure 20. To calculate volume of groundwater flow in and out of the wetland cells, the cross section area in vertical planes (length x depth) of cells 5 and 6 were combined as overall area of 66.4 m^2. The amount of groundwater was estimated using equation 18. It was assumed that the amount of groundwater flow in and out for each month are

identical. Based on the observation, the constructed wetland gained water from groundwater when there was water in cell 5 but lost water when cell 5 was dry.

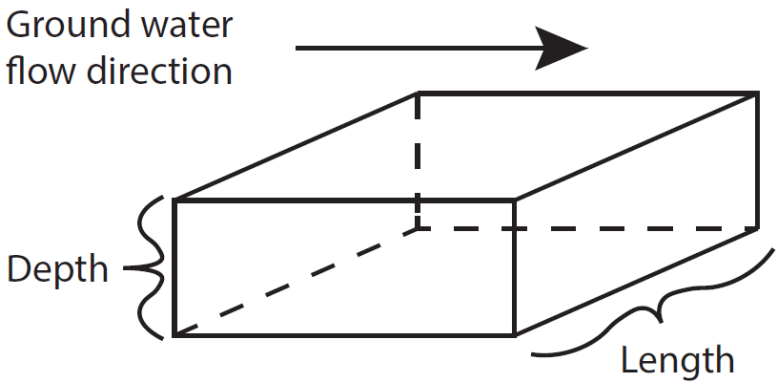

Figure 20. Sketch describing dimensions and groundwater flow direction of the wetland cells 5 and 6.

4.1.4 Isotopic Data Interpretation

The stable isotopic composition of water was also used to estimate water balance of the constructed wetland. Local meteoric water line (LWML) provided by Liston (2014) was used to determine evaporation of water in the wetland cells. The local meteoric water line of $\delta^2H = 7.39\delta^{18}O + 5.1$ was constructed by plotting isotopic data from precipitation in Mansfield, Ohio from 10/18/2012 through 11/17/2013. The isotopic data that was plotted on the local meteoric water line indicate meteoric recharge. Isotopic data of the water were plotted with low δ^2H v. $\delta^{18}O$ slope, may indicate evaporation.

4.1.5 Hydraulic Residence Time

Residence time is the time of water moving through each treatment cell. It is one of the factors that play important role in the pollutants removal efficiencies of wetlands (Shimala, 2000). The equation for calculating residence time is given as:

$$\text{Residence time} = \frac{\text{Volume of wetland cell } (m^3)}{\text{flow in or flow out } (m^3/\text{day})} \quad (19)$$

4.2 Hydrochemical Characterization of the Constructed Wetland

The chemical composition of the water entering and leaving through six wetland cells at different times was determined in order to characterize the hydrochemistry of the constructed wetland. The water chemistry combined with flow regime were used to identify chemical variation occurring within the wetland cells. In addition to the information of chemical variations, hydrochemical modeling was applied to study chemical reactions affecting the treatment processes. Field work associated with chemical data acquisition are described in the following section.

4.2.1 Field Parameters

Field parameters were measured monthly and immediately as the water samples were taken, using YSI 600XLM Multi-parameter Water Quality Sonde. At each sampling site, temperature, pH, electrical conductivity, and dissolved oxygen (DO) were measured.

4.2.2 Water Sampling

Water samplings were conducted seasonally in fall, winter, spring, and summer in 2015-2016. Water samples were collected at each location following EPA standard procedures (USEPA, 2000). The selected sampling sites were the influents and effluents from the constructed wetland cells. The water samples from each site were collected in a four-liter and two one-liter plastic containers. After collection, samples were preserved, stored and transferred to Ohio EPA laboratory for analyses. The samples used for cations analysis were preserved with HNO_3 in one-liter containers. The samples used for the analysis of total organic carbon (TOC), chemical oxygen demand (COD), phosphate were

preserved with H_2SO_4. All samples were stored in an icebox to remain cool between 1°C and 4°C during transportation.

4.2.3 Water Analyses

Water samples from each sampling event were analyzed by Ohio EPA laboratory. The methods for chemical analysis of water samples are illustrated in Table 5.

Table 5 Methods for chemical analysis of water samples at Ohio Environmental Protection Agency laboratory (USEPA,1979).

Parameter	Method	Units	Detection limit
Acidity	USEPA 305.1	mg/L	< 5.0 mg/L
Alkalinity	USEPA 310.1	mg/L	< 5.0 mg/L
Aluminum	USEPA 200.7	µg/L	< 200.0 µg/L
Ammonia	SM 4500-NH3BE	mg/L	< 0.05 mg/L
Arsenic	SM 3113B	µg/L	< 2.0 µg/L
Barium	USEPA 200.7	µg/L	< 15.0 µg/L
Cadmium	SM 5210B	µg/L	< 0.2 µg/L
BOD5	SM 5210B	mg/L	< 2.0 mg/L
Chloride	USEPA 325.1	mg/L	< 5.0 mg/L
Chromium	USEPA 200.7	µg/L	< 2.0 µg/L
COD	SM 5220D	mg/L	< 20.0 mg/L
Copper	SM 3113B	µg/L	< 2.0 µg/L
Hardness, Total	USEPA 200.7	mg/L	< 10.0 mg/L
Iron	USEPA 200.7	µg /L	< 50.0 µg/L
Lead	SM 3113B	µg/L	< 2.0 µg/L
Magnesium	USEPA 200.7	mg/L	< 1.0 mg/L
Manganese	USEPA 200.7	µg/L	< 10.0 µg/L
Nickel	USEPA 200.7	µg/L	< 2.0 µg/L
Nitrate+nitrite	USEPA 350.1	mg/L	< 0.1 mg/L
Nitrite	USEPA 353.2	mg/L	< 0.02 mg/L
Potassium	USEPA 200.7	mg/L	< 2.0 mg/L
Selenium	SM 3113B	µg/L	2.0 µg/L
Sodium	USEPA 200.7	mg/L	< 5.0 mg/L
Sulfate	USEPA 375.2	mg/L	< 10.0 mg/L
Total Dissolved Solids	SM 2540C	mg/L	< 10.0 mg/L
Total Phosphorus	USEPA 365.4	mg/L	< 0.01 mg/L
Total Suspended Solids	SM 2540D	mg/L	< 5.0 mg/L
Zinc	USEPA 200.7	µg/L	< 10.0 µg/L

4.2.4 Hydrochemical Modeling Using the PHREEQCI

Chemical modeling of water chemistry in the wetland cells was conducted using PHREEQCI program. The chemical concentrations were extracted from the analytical data of water samples.

4.2.4.1 Modeling Approach

Concentration data were used for the hydrochemical modeling of the wetland cells. In order to understand the chemical reactions that control deposition of minerals in the constructed wetland cells, forward chemical modeling was performed. Key controlling factors, i.e., temperature and pH, were assigned based on analytical data from each sampling event in order to understand how these factor relates to chemical reactions occurred in the treatment system. The SOLUTION_SPREAD function was used to assign chemical concentration from each wetland cell for the input data. After input of the chemical data, the function RUN was used to simulate chemical reactions and transport in the solutions. The output files displayed chemical species present in the solutions and identified saturation indices of minerals in the solutions. The saturation index of each mineral was calculated by equation:

$$SI = \log(\frac{IAP}{K}) \quad (20)$$

where SI is saturation index, IAP is the ion activity products, and K is the equilibrium constant.

When SI = 0, the solution is at thermodynamic equilibrium with respect to the mineral. If SI > 0, the solution is supersaturated with respect to the mineral meaning that the mineral is precipitated. If SI < 0, the solution is undersaturated with respect to the mineral meaning that the mineral is dissolved (Zhu and Anderson, 2002).

4.2.4.2 Inverse Chemical Modeling

Inverse chemical modeling was used to identify chemical reactions that occurred during the treatment processes and quantify mass transfers. PHREEQCI was used to examine some possible reaction models that could affect changes in wetland water chemistry. The inputs of two water chemistry data sets, i.e., influent and effluent of each wetland cell, were assigned in INVERSE_MODELING function with 0.05 global uncertainty. Phases of selected minerals were selected based on the results from forward modeling. Mass balance of elements including Al, Ba, C, Ca, Cd, Cl, Fe, H, K, Mg, Mn, N, Na, Pb, S, and Zn were assigned with -0.02 uncertainty limits for initial and final solutions. The -0.02 uncertainty limit indicated an uncertainty limit of 2 percent of the moles in solution. The negative uncertainty limit was interpreted as an absolute value in moles to use for the solution in the mole-balance equation. The models predicted chemical reactions within the constructed wetland cells.

The outputs of chemical compositions were given in terms of mol per kilogram of water phase changes. PHREEQCI identified the direction of mass transfer reactions. The negative sign (-) specified precipitation only and positive sign (+) dissolution only.

4.2.5 Hydraulic Loading

Hydraulic loading was calculated by determining the chemical loading on a water volume per unit area using:

$$\text{Hydraulic loading} = parameter\ concentration\ \times \frac{water\ volume}{area} \qquad (21)$$

4.3 Removal Efficiencies

Removal rates (kg/day) were determined for each sampling event. Mass removal rates were calculated for aluminum, iron, acidity, and sulfate using concentration (mg/l) and flow measurements (l/day). The removal efficiencies of the constructed wetland cells were the difference between inflow mass flux and outflow mass flux. The equation for the calculation of removal efficiencies is shown below:

$$RE = \frac{(Qinf \times Cinf) - (Qeff \times Ceff)}{(Qinf \times Cinf)} x\ 100\% \quad (22)$$

where Q is the flow rate (volume/time) of the inflow and outflow, and C is the concentration (mass/volume).

4.4 Data Analyses

Field parameters and water quality data distributions were tested for normality by kurtosis and skewness. When data were distributed normally, statistical analyses were performed. Correlation between parameters in the inlet and outlet of the wetland cells were tested by Pearson correlation coefficient. The statistically significant was based on a 95% confidence interval ($p < 0.05$). The Pearson correlation is able to measure the strength of the linear relationship between two variables. The "r" values were given to identify the strength of relationship which range from -1 to 1. If the value r close to -1, it indicates a strong negative linear relationship between variables while the value r close to 1, it indicates a strong positive linear relationship and the value 0 indicates no linear relationship between variables. Figure 21 shows the scatter plots for $r = 0.4$, $r = 0$, and $r = -0.4$.

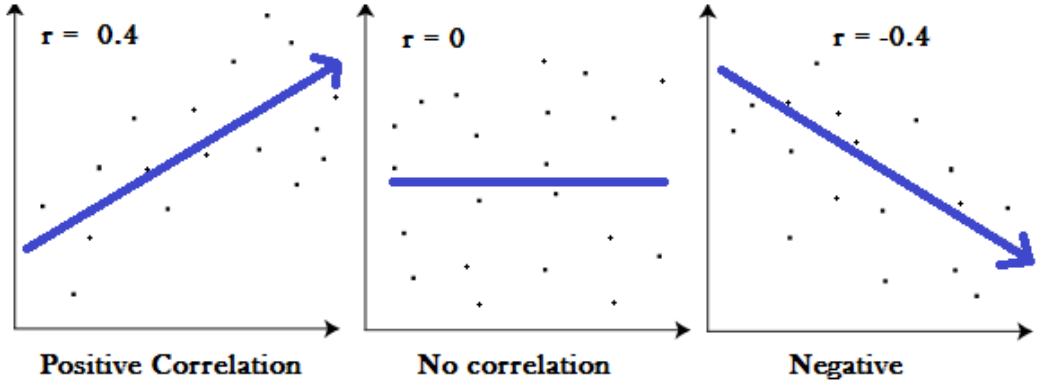

Figure 21. The scatter plots for positive correlation r = 0.4, no correlation r = 0, and for negative correlation r = -0.4 (http://www.statisticshowto.com/what-is-the-pearson-correlation-coefficient).

CHAPTER 5: RESULTS AND DISCUSSION

5.1 Characterization of the Landfill Leachate

The landfill discharge comprises acid mine drainage (AMD) and landfill leachate. The flow and constituents of the leachate were determined by collecting samples from two leachate holding tanks (west and east), which have been used to collect leachate before the constructed wetland cells were installed (MRB Environmental Services, Inc., 1998).

5.1.1 Acid Mine Drainage

The first source of pollutants from landfill leachate is mine drainage. According to Athens County 691 Landfill Annual Post-closure report for 2014, the results of analytical testing of an annual grab sample of leachate showed that the concentrations of dissolved iron and manganese exceeded the maximum contaminant levels (MCLs). Other metals were present but their concentrations were below the MCL.

5.1.2 Landfill Leachate

Degraded organic and inorganic wastes from the landfill are drained by rainfall and other percolated waters to produce leachates. After the landfill closure, pit ponds around the landfill were studied. The leachate discharges were collected at seepage from trenches and analyzed for chemical compositions and a weighted 5-day average flow rate was determined (Table 6). These data indicated that COD, total suspended solids, ammonia, metals, and other pollutants of concern in the leachate exceeded effluent limitations of water quality standard (MRB Environmental Services, Inc.,1998). The pollutant concentrations varied from 1996-2014.

According to table 6, pH values ranged from 6 to 6.9. The levels of alkalinity, nitrate, iron, potassium, and sodium increased over time while TSS, chloride, magnesium, manganese, nickel, and zine decreased.

Table 6 Analytical concentration of collected leachate occurred from 1996 to 2014.

Parameter	Concentration (mg/L)			
	1996	2003	2004	2014
pH	6.0	6.5	6.3	6.9
Alkalinity, Total (CaCo3)	266.0	422.0	230.0	935.0
COD	69.0	55.0	624.0	28.7
TSS	1,036.0	935.0	480.0	740.0
Chloride	80.0	76.0	30.0	26.7
Nitrate, ammonia	9.2	20.2	12.9	25.7
Magnesium	63.0	43.9	39.6	20.0
Manganese	11.0	7.5	7.1	1.9
Lead	<0.002	<0.002	0.042	<0.002
Nickel	0.042	0.035	0.066	0.010
Iron	ND	35.0	75.4	46.0
Potassium	16.3	18.2	19.5	20.1
Sodium	53.7	52.6	68.1	70.4
Zinc	0.77	0.06	ND	0.02

5.2 Hydrological Characterization of the Constructed Wetland

Dynamics of water flowing into and out of the constructed wetland were investigated through characterization of hydrologic factors such as flow rates, residence times, and water balance in the wetland cells.

5.2.1 Climate Data

Monthly accumulated precipitation data (Table 7 and Figure 22) showed that fall 2015 and winter 2015-2016 were dry with average precipitation 67.8 mm/month from September to November and 56.9 mm/month from December to January while spring

2016 had more precipitation with an average precipitation of 105.5 mm/month. The driest month was January 2016 with monthly precipitation of 29.0 mm. Potential evapotranspiration data were estimated using the FAO Penman-Monteith Method, and illustrated in Figure 22. The estimation was based on temperature (°C), wind speed (km/day), relative humidity (%), and sunshine hours. The results show that potential evapotranspiration exceeded precipitation in August and October 2015, and January and April 2016 by 27, 3, 21, and 14 %, respectively.

Table 7 Monthly precipitation and evapotranspiration.

Month	Precipitation (mm/month)	ET (mm/month)
Aug-15	66.0	90.7
Sep-15	80.0	77.4
Oct-15	66.8	69.0
Nov-15	58.4	56.0
Dec-15	78.2	42.6
Jan-16	29.0	36.6
Feb-16	63.5	30.9
Mar-16	106.7	70.0
Apr-16	88.9	88.7
May-16	120.9	82.3
Jun-16	85.0	99.0

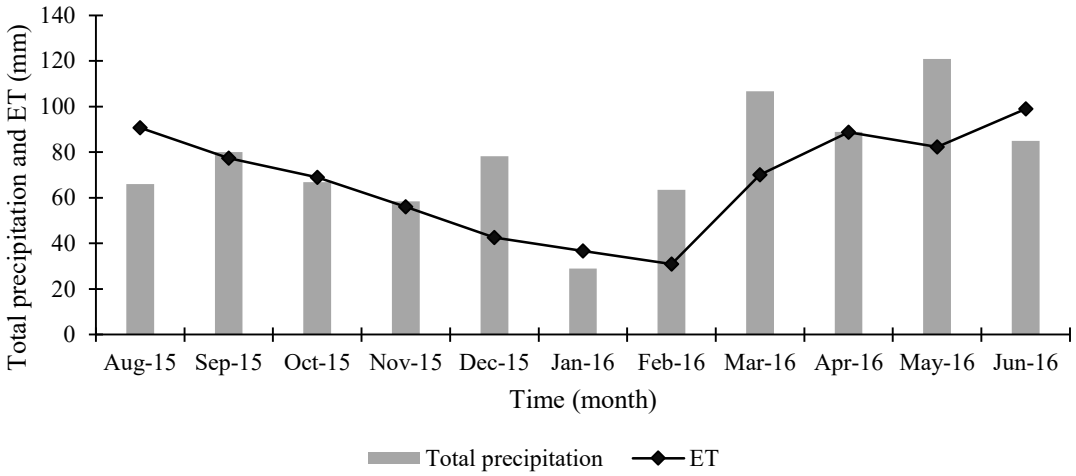

Figure 22. Total precipitation and potential evapotranspiration from August 2015 to June 2016.

5.2.2 Water Balance

Water flow rates in the constructed wetland conformed to the climate which was relatively dry in summer, fall 2015, and early winter and wet in late winter and spring 2016 (Table 8 and Figure 23). The high inflow rates occurred in August, September, and November 2015, and May 2016 with rates ranging from 1,700 to 2,700 m^3/month while the low inflow rates occurred in October 2015 and January 2016 with rates ranging from 443 to 986 m^3/month. The lowest outflow rates occurred in September and October 2015 and June 2016 with rates ranging from 3.5 to 5 m^3/month. The highest outflow rates occurred in December 2015 and January 2016 with 10,769 m^3/month and 9,749 m^3/month, respectively.

The water balance of the entire constructed wetland area with surface area of 3,506 m^2 was estimated by considering precipitation, water inflow and outflow, groundwater inflow and outflow and evapotranspiration. The storage change values, inflow and outflow rates were averaged for each month.

Table 8 The parameters used in water balance calculation.

Month	inflow	outflow	P	ET	GW inflow	GW outflow	Storage
Aug-15	2,18.8	24.2	231.6	317.8	0.2	-	2,208.5
Sep-15	1,716.7	5.3	280.5	271.2	0.2	-	1,720.9
Oct-15	443.5	4.5	234.2	241.8	-	0.2	431.3
Nov-15	2,575.1	103.0	204.8	196.5	0.2	-	2,480.6
Dec-15	1,330.5	10,769.8	274.3	149.4	0.2	-	-9,314.3
Jan-16	986.2	9,749.6	101.5	28.4	0.2	-	-8,790.2
Feb-16	1,659.5	754.2	222.6	108.2	0.2	-	1,010.0
Mar-16	1,774.0	1,925.9	374.0	245.5	0.2	-	-23.2
Apr-16	1,376.1	1,925.9	311.7	311.0	0.2	-	-548.8
May-16	2,704.4	2,954.9	423.9	288.6	-	0.2	-115.3
Jun-16	429.2	3.5	298.0	326.9	0.2	-	397.0

Note: All parameters are in the unit of m^3/month.

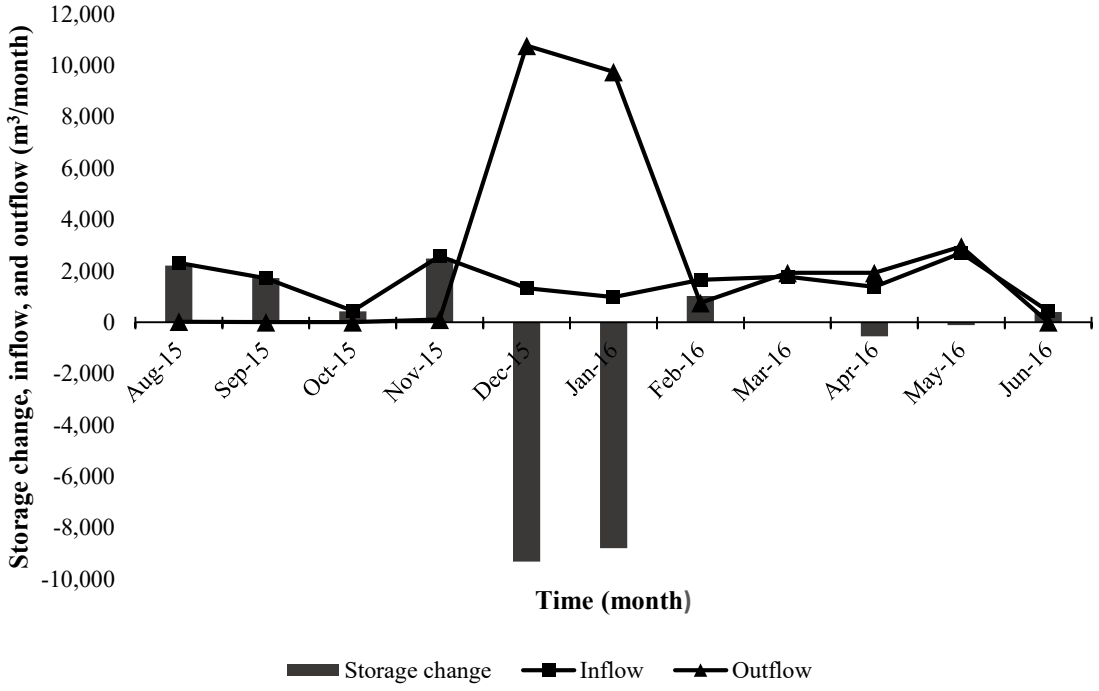

Figure 23. Water balance of the constructed wetland from 2015 to June 2016.

Water in cell 5 was dry in October and May, suggesting that the wetland cell lost water to groundwater during those months whereas gained approximately the same amount of water to groundwater during most of the year. The estimated amount of loss by

flow out to groundwater is 0.2 m^3/month. The water balance calculation result indicates that the constructed wetland lost water in December, January, March, April, and May with the amount of 9,314.3 m^3, 8,790.2 m^3, 23.2 m^3, 548.8 m^3, and 115.3 m^3, respectively. The constructed wetland gained water in August, September, October, November, February, and June with the amount of 2,208.5 m^3, 1,720.9 m^3, 431.3 m^3, 2,480.6 m^3, 1,020.0 m^3, and 397.0 m^3, respectively. In general, the water balance within the wetland corresponded to inflow and outflow rates suggesting that the inflow and outflow rates control the water balance.

The water balance estimation suggested that all of the wetland cells should be dry in December 2015 and January 2016, but this was not observed to be true. The discrepancy between predicted and observed shows that the water balance equation may need to be altered to compensate for freezing temperature during winter months.

5.2.3 Water Balance from Isotopic Data

Isotopic composition of water samples collected in September and October 2015 is illustrated in Table 9 and Figure 24. In both sampling events, the water samples from cells 1, 2, and 5 were isotopically heavier than water samples from limestone drain, cells 3, 4, and final outfall. The data were clustered around LMWL indicating meteoric source of water. Evaporation was observed by higher oxygen isotopic values for water samples collected from the limestone drain, cell 4, and final outfall. Rayleigh distillation model was used to quantify the amount of water lost by evaporation. Low isotopic compositions and low water temperature in cell 5 indicate groundwater flow into the cell, which is suggested by hydrogeological investigation data of Lower Freeport Aquifer.

Based on the calculation of $\delta^{18}O$ values using Rayleigh distillation model, the amounts of water lost by evaporation were estimated to be 561.33 m^3 in September and 593.30 m^3 in October. The amount of water lost by evaporation estimated by isotopic data is approximately 50 % higher than FAO Penman-Monteith method (Table 7). The estimation of evapotranspiration by using FAO Penman-Monteith method is not direct-measurement procedure and subjected to error, since the climate data used in calculation were not obtained from the actual area of study. Although isotopic data of water samples were physical data that could provide more accurate in estimating evaporation, other factors that affected the isotope composition need to be considered. Isotopic concentrations can be changed or fractionated in the water through processes such as sulfate reduction, water-rock exchange, and mineral or gas dissolution along the flow path (Clark and Fritz, 1997).

Table 9 Isotopic data for September and October 2015.

	Sep-15		Oct-15	
Location	$\delta^{18}O$	$\delta^{2}H$	$\delta^{18}O$	$\delta^{2}H$
Cell 1 influent	-7.9	-47	-8	-45
Cell 1 effluent	-7.6	-45	-7.8	-46
Cell 2 effluent	-4.9	-33	-5.4	-39
Limestone drain	-0.7	-15	1.3	-10
Cell 3 effluent	-0.7	-14	ND	ND
Cell 4 effluent	-2.2	-20	-1.6	-20
Cell 5 influent	-4.7	-29	ND	ND
Final outfall	-0.7	-13	-1.1	-18

Note: ND indicates no data. Unit for all values is per mil (‰) VSMOW.

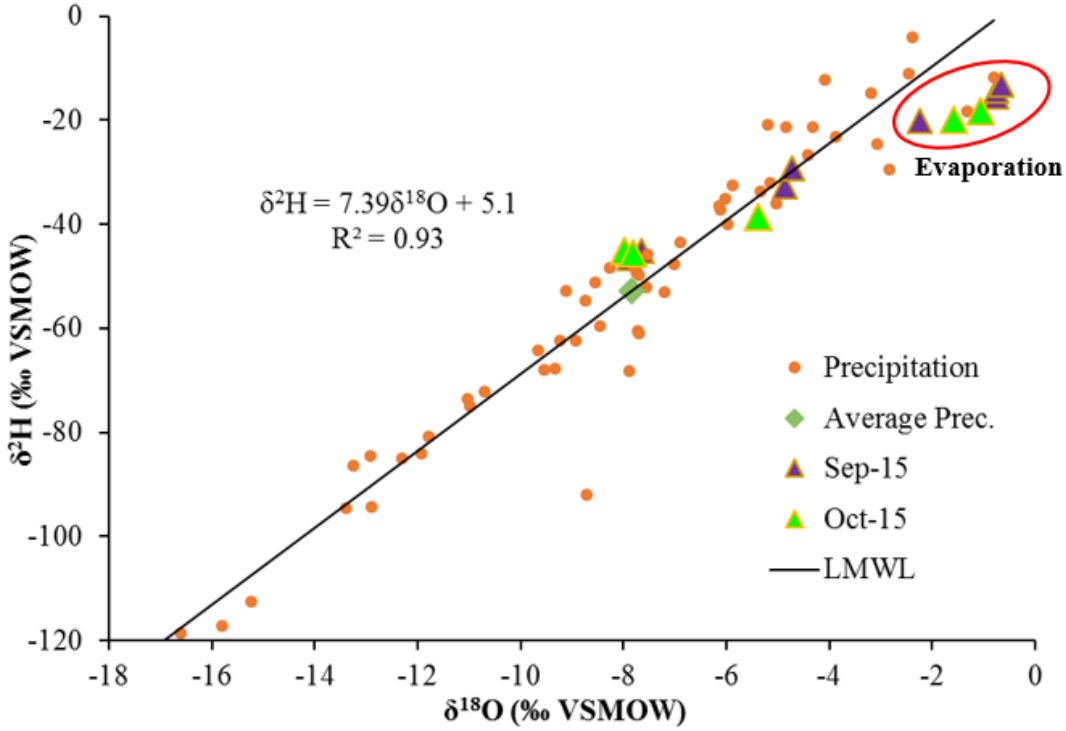

Figure 24. Plot of $\delta^2 H$ vs $\delta^{18} O$ in water samples for September and October 2015.

5.2.4 Hydraulic Residence Time

The time that the water in the treatment system takes to move from the inlet cell to the final outfall was calculated in order to determine pollutants removal efficiencies. The following equation was used to estimate residence time in wetland cells. The residence times were estimated using flow rate data collected in December 2015 when the flow rates were measurable for every wetland cell.

$$\text{Residence time} = \frac{\text{Volume of wetland cell } (m^3)}{\text{flow in or flow out } (m^3/\text{hour})} \quad (23)$$

Table 10 Hydraulic residence time of the constructed wetland cells in December 2015.

Location	Volume (m^3)	Flow rate (m^3/hour)	Residence time (hour)
Cell 1	5.3	1.8	3.0
Cell 2	528.0	7.2	73.3
Cell 3	129.2	0.6	202.7
Cell 4	917.7	3.9	233.8
Cell 5	319.2	4.3	73.9
Cell 6	293.2	14.5	20.3

Residence times in each cell were estimated to be 3, 73.3 202.7, 233.8, 73.9, and 20.3 hours for cells 1, 2, 3, 4, 5, and 6, respectively. The residence time was the longest in cell 4 mainly due to the largest volume of cell. Likewise, residence time was shortest in cell 1 due to the smallest volume of the cell. Because longer residence time in larger cells can provide longer reaction time for pollutants in the cell, large cells may yield better removal efficiencies than smaller cells. Field observations suggest that residence times in the cells could be longer during dry periods when there was no flow between the cells.

5.3 Hydrochemical Characterization of the Constructed Wetland

After the water samples were collected and analyzed, chemical data were used to characterize the hydrochemical aspects of the constructed wetland. This section is divided into three topics; water quality dynamics in the constructed wetland, the PHREECQI modeling, and the hydraulic loading rate of the constructed wetland system.

5.3.1 Water Quality Dynamics in the Constructed Wetland

The seasonal variations in water chemistry within the constructed wetland cells were investigated during the four seasons in 2015-2016. Monthly measurement of field parameters including temperature, pH, conductivity, and dissolved oxygen were plotted

in line graphs (Figure 25 - 28). The chemical data for acidity, alkalinity, ammonia, COD, BOD_5, nitrate, iron, manganese, sulfate, and chloride determined at different sampling locations are illustrated in Figure 29 - 35.

5.3.1.1 Water Temperature

Water temperature data for each wetland cell are presented in Table 11 and Figure 25. Water temperatures in fall 2015 and spring 2016 were highest in cell 4 and lowest in cell 1. Water temperature in cell 1, which is the first receiving body of the landfill leachate was less affected by air temperature compared to other cells. Water temperatures in effluents from cell 3 and cell 4 were sensitive to air temperature suggesting active heat transfer with the air. This observation was attributed to longer residence times in those cells compared to other cells. Water temperatures in cell 5 and final outfall were lower than effluents from cells 3 and 4 indicating the existence of inflow of colder water, i.e. groundwater, to cells 5 and 6.

Table 11 Monthly water temperature (°C) at eight sampling locations.

Month	Cell 1 influent	Cell 1 effluent	Cell 2 effluent	Limestone Drain	Cell 3 effluent	Cell 4 effluent	Cell 5 influent	Final outfall
Aug-15	16.7	18.0	21.6	20.1	23.1	23.5	19.8	20.1
Sep-15	16.5	16.3	14.8	19.1	16.6	20.9	12.9	14.6
Oct-15	15.2	13.1	16.7	-	20.1	17.2	-	13.3
Nov-15	11.5	6.1	5.0	5.3	6.0	5.6	3.8	6.5
Dec-15	10.9	10.0	7.8	8.2	8.3	8.8	8.6	7.9
Jan-16	11.4	10.8	8.2	8.6	8.4	9.1	8.7	8.9
Feb-16	7.2	5.8	3.1	3.8	1.9	3.2	3.2	2.0
Mar-16	8.9	9.8	11.8	12.8	13.6	13.8	13.6	12.4
Apr-16	12.2	18.0	17.6	18.4	20.1	20.1	16.3	13.6
May-16	12.7	14.4	15.0	15.1	15.6	17.3	15.9	13.9
Jun-16	15.8	21.8	26.6	27.7	27.6	28.8	25.5	19.9
Average	12.6	13.1	13.5	13.9	14.7	15.3	12.8	12.1

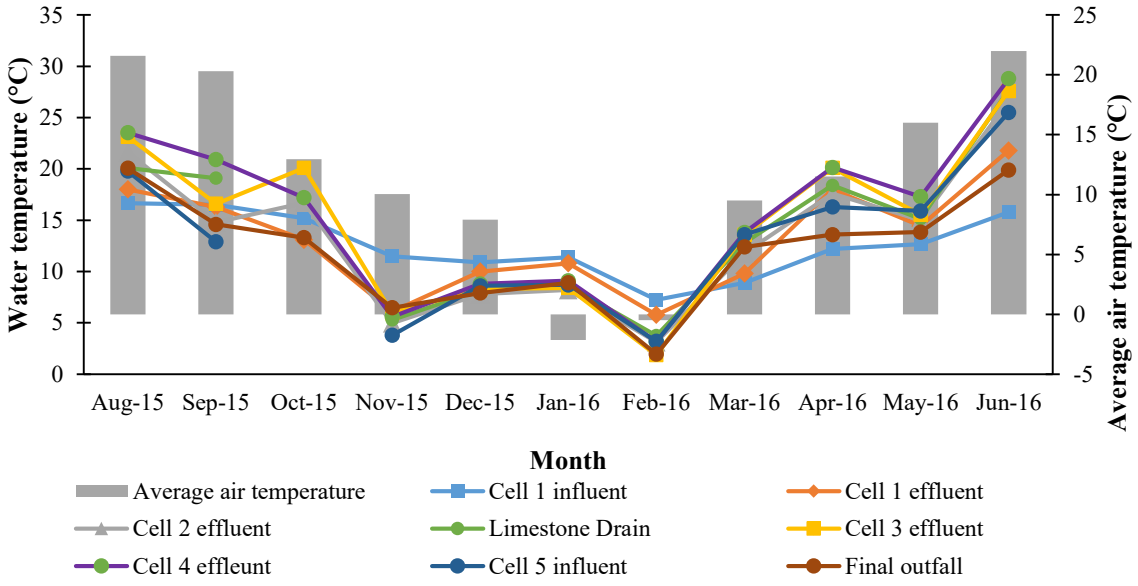

Figure 25. Water temperature at different sampling locations in accordance with average air temperature.

5.3.1.2 Field pH

Table 12 and Figure 26 show field pH values plotted with precipitation data. The pH of water in cell 1 influent ranged from 5 to 6.5 with an average of 6. The values of pH in cell 1 effluent, cell 2, limestone drain, cell 3, cell 4, cell 5 ranged from 6 to 8 due to the carbonate added to water from limestone. The pH data indicated that initially acidic leachate is gradually neutralized as the water flows through the wetland cells by dilution of water. The pH and precipitation data indicated that dilution by precipitation would not greatly affect pH of water in the wetlands.

Table 12 Monthly pH values at eight sampling locations.

Month	Cell 1 influent	Cell 1 effluent	Cell 2 effluent	Limestone Drain	Cell 3 effluent	Cell 4 effluent	Cell 5 influent	Final outfall
Aug-15	6.4	7.0	7.5	7.2	7.7	8.1	7.6	7.9
Sep-15	6.4	6.8	7.5	7.5	7.6	7.5	7.5	7.4
Oct-15	6.3	6.8	7.8	-	8.1	7.3	-	7.1
Nov-15	6.4	7.2	7.8	7.8	7.6	8.1	8.1	7.7
Dec-15	6.3	6.5	6.8	6.8	6.9	6.8	7.0	7.0
Jan-16	6.5	6.6	6.8	7.0	6.9	7.2	7.2	7.4
Feb-16	5.3	5.8	5.5	6.6	5.3	6.7	7.0	7.2
Mar-16	6.3	6.7	6.7	6.6	6.5	7.3	7.5	7.4
Apr-16	6.0	6.9	7.1	7.2	7.3	7.6	7.7	7.6
May-16	6.0	6.6	6.8	6.9	7.1	7.5	7.5	7.6
Jun-16	6.1	6.4	7.1	7.2	7.3	7.4	6.7	6.7
Average	6.2	6.7	7.0	7.1	7.1	7.4	7.4	7.4

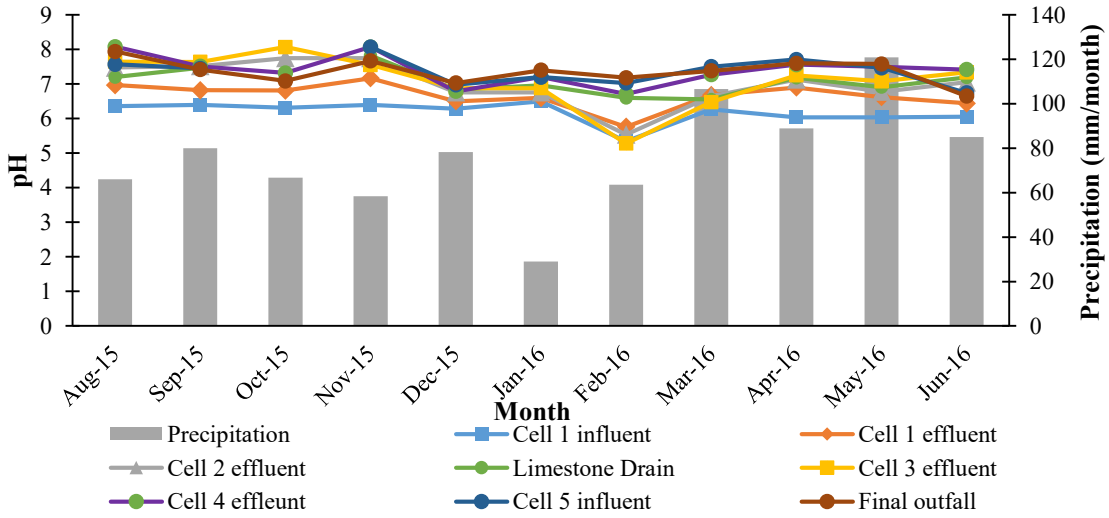

Figure 26. pH values at different sampling locations in accordance with monthly precipitation.

5.3.1.3 Conductivity

Conductivity generally decreased as leachate flows through the cells as shown in Table 13 and figure 27. The average conductivity of cell 1 influent, i.e., leachate from the landfill was 1,065 µs/cm. Average conductivity in the final outfall was 463 µs/cm, showing 56% of overall removal of dissolved constituents in the leachate. Conductivity

in cell 1 was higher in the summer than in the winter, suggesting more active generation of pollutants during the summer months.

Differences in conductivity between the constructed wetland cells were magnified during months of higher precipitation and converge at 600 µs/cm during drier months. Longer hydraulic residence time resulted in the bigger difference in conductivity values observed between cell 1 to cell 2.

Table 13 Monthly conductivity values (µs/cm) at eight sampling locations.

Month	Cell 1 influent	Cell 1 effluent	Cell 2 effluent	Limestone Drain	Cell 3 effluent	Cell 4 effluent	Cell 5 influent	Final outfall
Aug-15	1397	1358	977	667	592	541	473	503
Sep-15	1411	1293	749	535	478	526	497	310
Oct-15	1283	1247	950	-	430	540	-	309
Nov-15	968	863	786	690	679	505	201	316
Dec-15	790	694	590	590	590	600	560	500
Jan-16	815	714	604	612	601	588	590	448
Feb-16	789	713	613	649	560	722	721	616
Mar-16	603	546	545	589	574	574	520	424
Apr-16	1074	1020	882	864	827	789	768	617
May-16	1232	1200	1032	1005	990	925	857	720
Jun-16	1354	1262	851	790	947	574	591	335
Average	1065	992	780	699	661	626	578	463

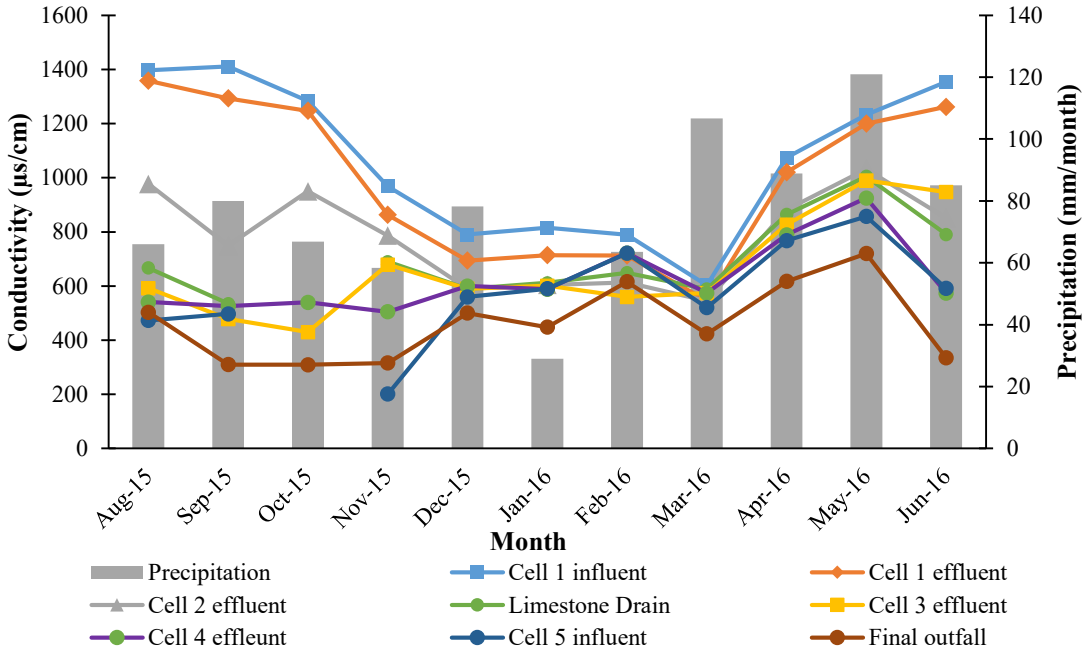

Figure 27. Field conductivity at different sampling locations in accordance with monthly precipitation.

5.3.1.4 Dissolved Oxygen

Concentrations of dissolved oxygen generally increased during dry and cold months and decreased in warm months (Table 14 and Figure 28). The average values of dissolved oxygen concentrations increased as the water flowed through the constructed wetland cells. Cell 1 influent has an average dissolved oxygen concentration of 5.77 mg/l. Average dissolved oxygen concentration in the final outfall was increased by 74 % to 10.06 mg/l. Oxygen was released by plants to the water column during daylight hours through photosynthesis (USEPA, 2000). Dissolved oxygen concentrations were decreased in cells 2, 3, and limestone drain compared to cell 1. This observation was attributed to the fact that the parameter was measured at the outlet where the wetland plants were grown and the oxygen was likely consumed by these plants (Vymazal, 2005).

Table 14 Monthly dissolved oxygen concentrations (mg/l) at eight sampling locations.

Month	Cell 1 influent	Cell 1 effluent	Cell 2 effluent	Limestone Drain	Cell 3 effluent	Cell 4 effluent	Cell 5 influent	Final outfall
Aug-15	2.4	3.2	1.2	3.6	2.5	9.7	2.8	6.6
Sep-15	2.0	3.0	2.7	2.8	3.1	3.5	3.9	4.7
Oct-15	1.9	2.4	2.9	-	3.1	3.3	-	3.8
Nov-15	8.9	11.8	10.0	7.8	7.2	13.2	9.8	14.2
Dec-15	7.6	10.4	8.8	6.9	7.1	12.5	8.7	13.5
Jan-16	7.8	10.8	8.9	7.2	7.5	11.9	9.1	13.8
Feb-16	9.8	11.7	9.9	11.5	8.9	12.3	13.8	15.6
Mar-16	7.4	8.3	7.4	9.4	7.7	10.5	9.4	12.8
Apr-16	4.1	6.8	7.4	8.5	8.2	8.7	8.9	9.4
May-16	5.9	7.8	6.4	7.4	6.3	7.3	7.2	9.2
Jun-16	5.7	3.6	6.3	5.3	4.3	11.0	8.5	7.1
Average	5.8	7.2	6.5	7.0	6.0	9.4	8.2	10.1

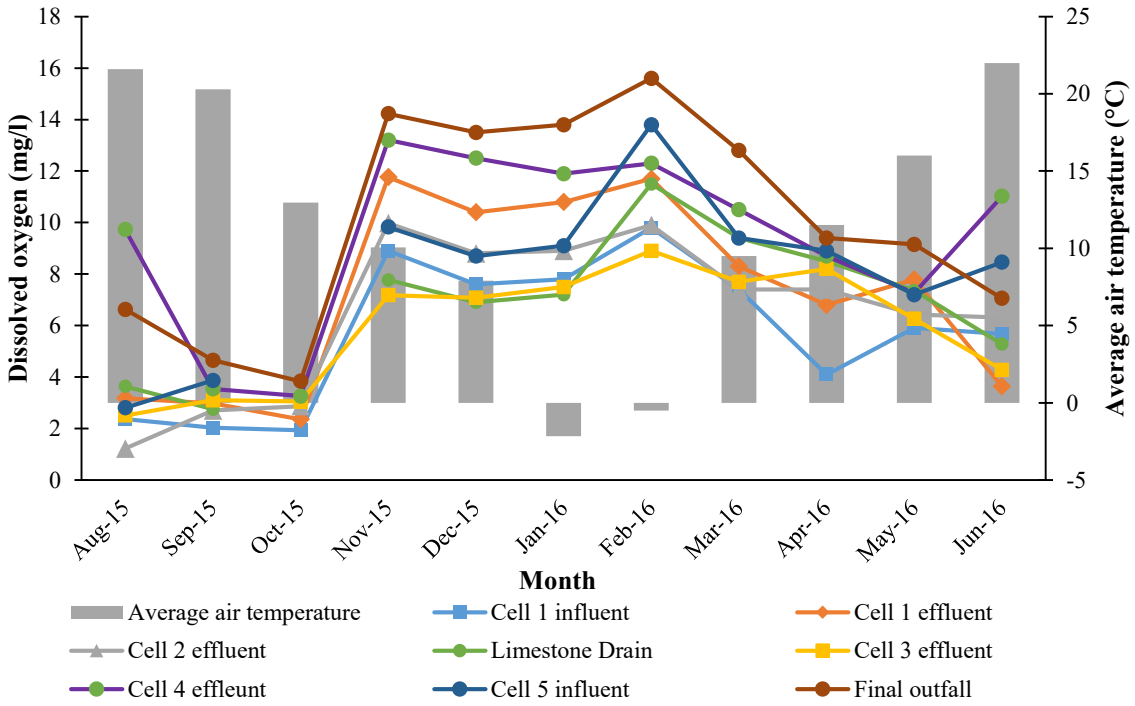

Figure 28. Dissolved oxygen at different sampling locations in accordance with monthly average temperature.

5.3.1.5 Acidity and Alkalinity

Acidity values were consistently below the detection limit (5 mg/l $CaCO_3$) in all samples collected from all wetland cells and four seasons. The results of alkalinity are shown in Table 15 and Figure 29. The initially high alkalinity in the leachate inflow to cell 1 decreased to 404, 340, 288, 258, 257, 214, and 188 mg/l on average in cell 1 effluent, cell 2, limestone drain, cell 3, cell 4, cell 5, and the final outfall, respectively. The alkalinity in each cell remained the same pattern for all season.

Table 15 Seasonal alkalinity concentrations (mg/l $CaCO_3$) at eight sampling locations.

Sampling event	Cell 1 influent	Cell 1 effluent	Cell 2 effluent	Limestone Drain	Cell 3 effluent	Cell 4 effluent	Cell 5 influent	Final outfall
Summer	549	545	442	-	266	230	217	236
Fall	364	353	298	265	264	190	44	44
Winter	287	279	240	232	238	286	283	225
Spring	442	438	382	366	375	321	313	247
Average	411	404	341	288	286	257	214	188

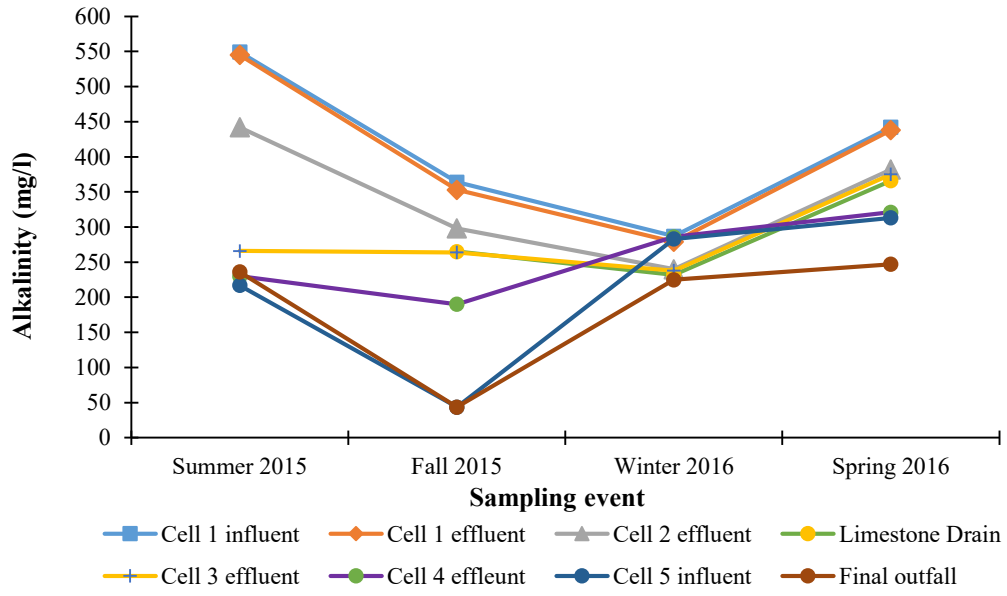

Figure 29. Alkalinity for eight sampling locations.

5.3.1.6 BOD_5 and COD

Table 16 and Figure 30 shows the concentrations of BOD_5 levels in each wetland cell and COD levels in cell 1 and the final outfall. BOD_5 concentrations were reduced significantly as water flowed through the treatment cells, from 6.1 mg/l (cell 1 influent) to 5 mg/l (cell 1 effluent), 4.8 mg/l (cell 2), 4.5 mg/l (cell 3), 4.6 mg/l (cell 4), 3.6 mg/l (cell 5), and 1.8 mg/l (outfall) in summer and fall 2015, indicating active treatment of BOD_5 in the wetland cells. BOD_5 levels below 2 mg/l in all cells and the final outfall in winter 2015-2016 indicating lack of bacterial activity in cold water (less than 14°C in December, January, and February). In spring 2016, BOD_5 levels greatly increased in all cells, suggesting active bacterial activity during the spring overturn in warm water (Qiu et al., 2005 and Vymazal, 2005). However, BOD_5 levels considerably decreased as water flowed through the cells, from 22 mg/l (cell 1 influent), to 20 mg/l (cell 1 effluent), 13 mg/l (cell 2), 9.9 mg/l (limestone drain), 7.7 mg/l (cell 3), 6.2 mg/l (cell 4), 6.3 mg/l (cell 5), and 7.3 mg/l (outfall), suggesting efficient treatment of BOD_5 in the wetland. Similarly, COD generally decreased as water flowed through the wetland cells. The COD concentration was 36.75 mg/l on average in cell 1 and decreased in final outfall to 27.5 mg/l.

Table 16 Seasonal BOD_5 and COD concentrations (mg/l) for eight sampling locations.

Sampling event	Cell 1 influent	Cell 1 effluent	Cell 2 effluent	Limestone Drain	Cell 3 effluent	Cell 4 effluent	Cell 5 influent	Final outfall
				BOD_5				
Summer	2.2	0.0	4.1	-	6.9	7.5	7.9	0.0
Fall	0.0	0.0	8.2	4.6	3.2	4.6	0.0	0.0
Winter	0.0	0.0	0.0	0.0	0.0	0.0	0.0	0.0
Spring	22.0	20.0	13.0	9.9	7.7	6.2	6.3	7.3
Average	6.1	5.0	6.3	4.8	4.5	4.6	3.6	1.8
				COD				
Summer	56.0	54.0	38.0	-	34.0	28.0	33.0	31.0
Fall	38.0	36.0	50.0	37.0	37.0	54.0	20.0	24.0
Winter	22.0	20.0	20.0	20.0	20.0	20.0	20.0	21.0
Spring	31.0	33.0	33.0	35.0	35.0	33.0	33.0	34.0
Average	36.8	35.8	35.3	30.7	31.5	33.8	26.5	27.5

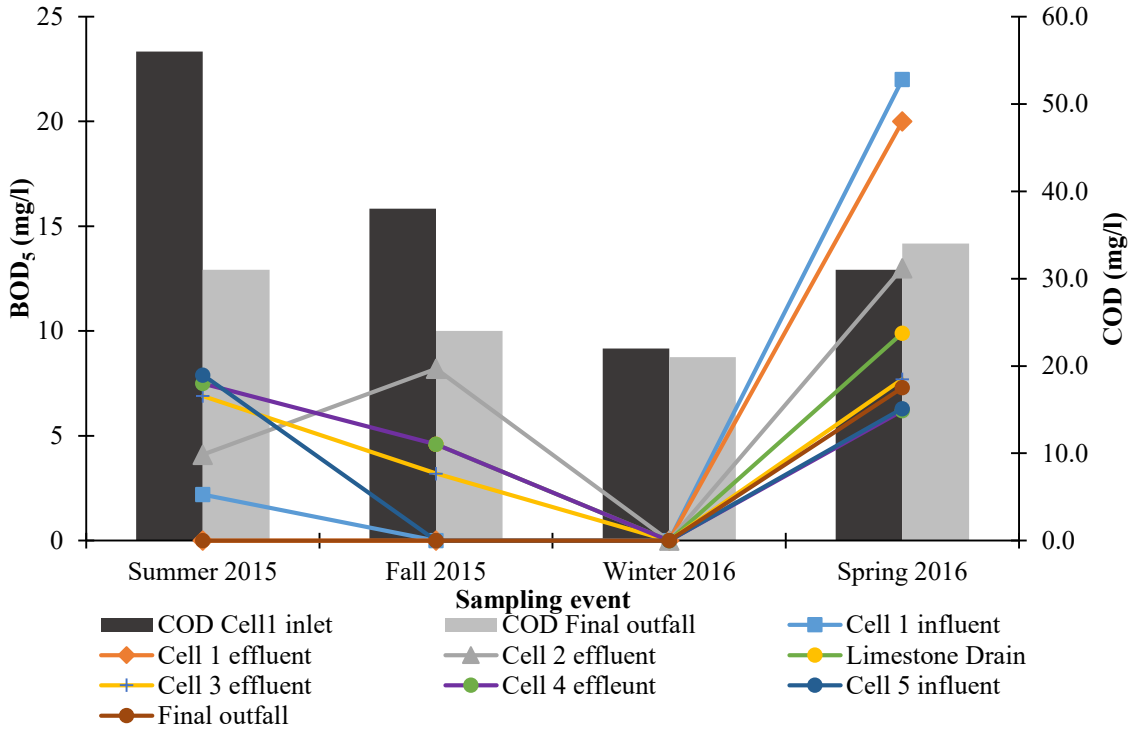

Figure 30. BOD_5 for eight sampling locations and COD concentrations for cell 1 influent and the final outfall.

5.3.1.7 Total Iron

Total iron concentrations at eight sampling locations ranged from 44 to 0.3 mg/l (Table 17 and Figure 31). Like conductivity, iron concentrations in the leachate were high in summer (44.2 mg/l) compared to winter (17.1 mg/l), suggesting more active leachate generation during warm season. The average iron concentration for four seasons in cell1 influent was 27 mg/l, which was similar to cell 1 effluent (22 mg/l). Outflows from other wetland cells showed decreasing iron concentrations as water flowed through the wetland cells. The average iron concentrations were 2.7 mg/l in cell 2, 1.8 mg/l in limestone drain, 1.5 mg/l in cell 3, 0.9 mg/l in cell 4, 1.5 mg/l in cell 5, and 1 mg/l in the final outfall. Iron removal rates for all seasons were 27% in cell 1, 88% in cell 2, 17% in cell 3, 40% in cell 4, and 27% in cells 5 and 6. High removal rates in cells 2 and 4 were attributed to the long residence time (73.3 hours in cell 2 and 233.8 hours in cell 4), which can provide more time for dissolved iron to precipitate as ferric hydroxide ($Fe(OH)_3$). However, cell 1 was the most efficient iron treatment system with small cell volume and high removal rates of iron.

Table 17 Seasonal total concentrations (mg/l) at eight sampling locations.

Sampling event	Cell 1 influent	Cell 1 effluent	Cell 2 effluent	Limestone Drain	Cell 3 effluent	Cell 4 effluent	Cell 5 influent	Final outfall
Summer	44.2	43.2	1.9	0.9	0.9	0.7	1.6	0.5
Fall	16.2	29.4	2.9	2.6	2.2	1.2	2.2	1.9
Winter	17.1	4.0	3.3	2.1	2.3	1.2	1.9	1.2
Spring	33.2	11.1	2.6	1.6	0.5	0.4	0.4	0.7
Average	27.7	21.9	2.7	1.8	1.5	0.9	1.5	1.1

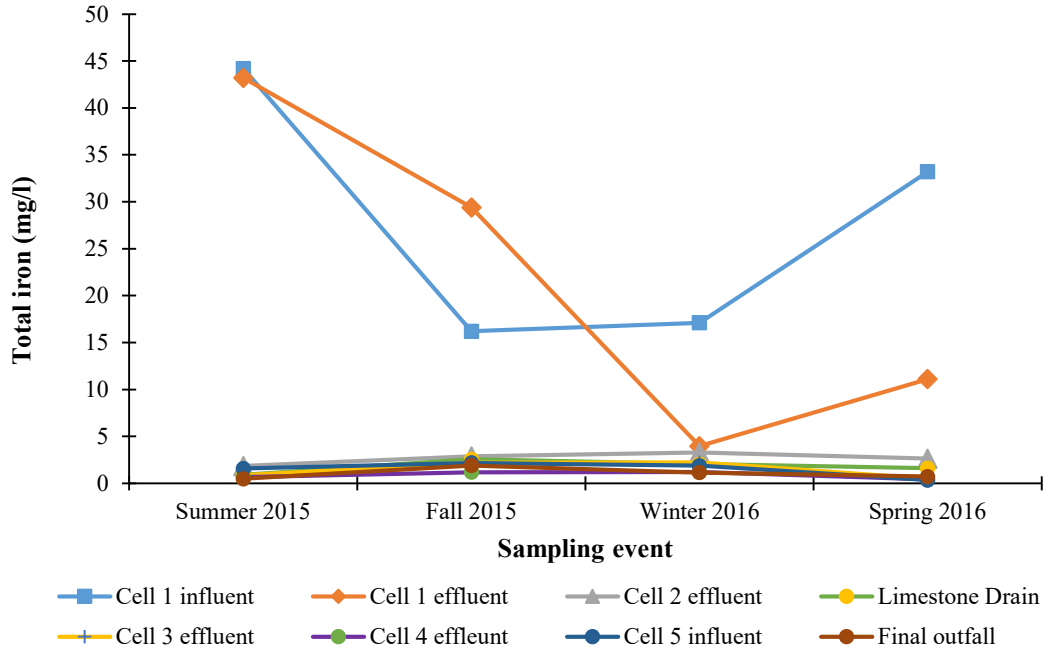

Figure 31. Total iron concentration at eight sampling locations.

5.3.1.8 Aluminum and Manganese

Aluminum concentrations were consistently below the detection limit (200 µg/l) in all samples collected from all wetland cells and four seasons. Manganese levels at all sampling locations for four seasons were low with the range of 0 to 3.8 mg/l (Table 18 and Figure 32). Average manganese concentrations generally decreased as water flowed through the wetland cells, from 2.3 mg/l (cell 1 influent) to 1.7 mg/l (cell 1 effluent), 1 mg/l (cell 2), 0.5 mg/l (limestone drain), 0.6 mg/l (cell 3), 0.5 mg/l (cell 4), 0.7 mg/l (cell 5), and 0.4 mg/l (final outfall). The results indicated high manganese was actively removed in limestone drain with the range of 0 to 1 mg/l. The oxidation of Mn(II) to Mn(IV) can occur in limestone drain at pH ranged from 6.5 to 7.8 which is optimal condition for manganese removal (Aziz and Smith, 1996).

Table 18 Seasonal manganese concentrations (mg/l) for eight sampling locations.

Sampling event	Cell 1 influent	Cell 1 effluent	Cell 2 effluent	Limestone Drain	Cell 3 effluent	Cell 4 effluent	Cell 5 influent	Final outfall
Summer	3.8	2.5	1.2	0.0	1.2	0.5	1.3	0.6
Fall	2.6	1.6	0.5	0.4	0.3	0.8	0.8	0.7
Winter	0.7	0.8	1.0	0.6	0.5	0.3	0.4	0.2
Spring	2.0	1.9	1.3	1.1	0.4	0.3	0.2	0.2
Average	2.3	1.7	1.0	0.5	0.6	0.5	0.7	0.4

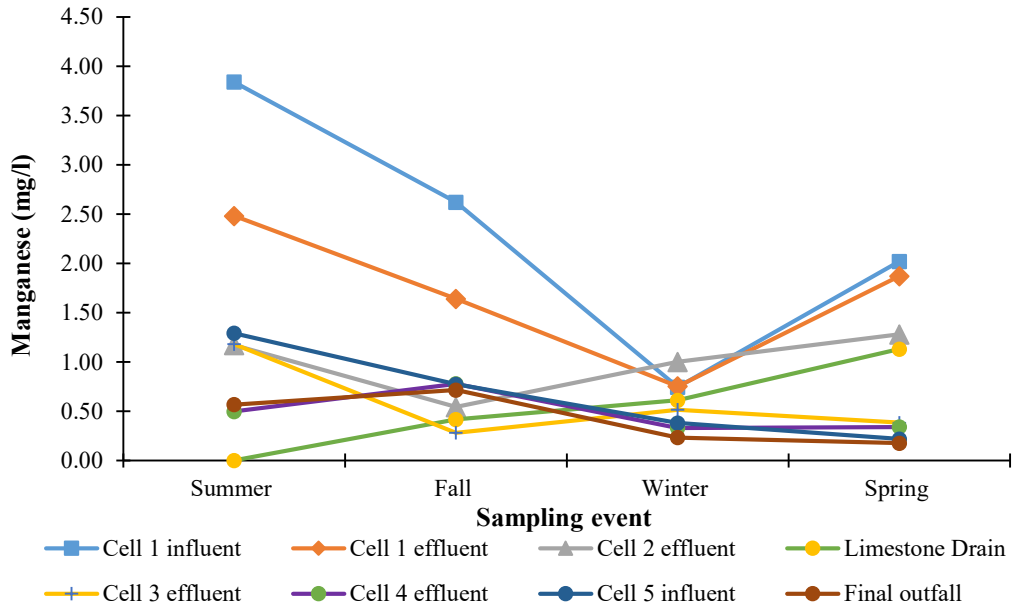

Figure 32. Manganese concentrations for eight sampling locations.

5.3.1.9 Ammonia and Nitrate

Ammonia concentrations were high in cell 1 influent ranged from 5.8 to 31.6 mg/l (Table 19 and Figure 33), indicating reducing condition in the landfill. Average ammonia concentrations decreased as water flowed through the cells, from 16.6 mg/l (cell 1 influent) to 16.2 mg/l (cell 1 effluent), 10.3 mg/l (cell 2), 6.5 mg/l (limestone drain), 5 mg/l (cell 3), 3.8 mg/l (cell 4), 3.6 mg/l (cell 5), 2.3 mg/l (final outfall), indicating active oxidation of ammonia the wetlands. The removal mechanisms of ammonia occurred in wetland plants through nitrification (Aziz et al., 2010). Ammonia

was oxidized to nitrite and nitrate in the root zone where sufficient oxygen was supplied. The observations suggested that ammonia was greatly decreased in cells 2, 3, 4, and 5 where wetland plants existed.

Nitrate concentrations were below the maximum contaminant level (10 mg/l) throughout the wetlands and showed seasonal variations with increased concentrations in cell 1 influent increased in fall and winter, compared to summer and spring. Such seasonal variations suggest that the source of nitrate in the wetlands is oxidation of ammonia in the leachate. Nitrate concentrations in the leachate inflow to cell 1 and final outfall were 0.05 mg/l and 0.17 mg/l in summer 2015, and 0.44 mg/l and 0.14 mg/l in fall 2015, and 0.67 mg/l and 0.48 mg/l in winter 2015, and 0.1 mg/l and 0.48 mg/l in spring 2016, respectively (Figure 34). Denitrification in the wetlands is known to reduce nitrate concentrations, especially during warm periods (Spalding and Exner, 1993). However, irregular variations of nitrate levels in the wetland cells suggest the occurrence of denitrification in the wetlands is not evident.

Table 19 Seasonal ammonia and nitrate concentrations (mg/l) for eight sampling locations.

Sampling event	Cell 1 influent	Cell 1 effluent	Cell 2 effluent	Limestone Drain	Cell 3 effluent	Cell 4 effluent	Cell 5 influent	Final outfall
				Ammonia				
Summer	31.6	31.8	16.6	-	1.1	0.4	0.3	0.1
Fall	11.6	9.7	7.6	4.8	4.7	0.6	0.2	0.1
Winter	5.8	5.8	4.6	4.2	3.6	5.5	5.5	4.3
Spring	17.7	17.6	12.7	10.5	10.7	9.0	8.8	4.9
Average	16.7	16.2	10.4	4.9	5.0	3.9	3.7	2.3

Table 19 continued

Sampling event	Cell 1 influent	Cell 1 effluent	Cell 2 effluent	Limestone Drain	Cell 3 effluent	Cell 4 effluent	Cell 5 influent	Final outfall
				Nitrate				
Summer	0.05	0.26	0.05	-	0.05	0.69	0.41	0.17
Fall	0.44	1.00	1.68	2.08	2.00	0.15	0.30	0.14
Winter	0.67	0.54	0.38	0.40	0.35	0.36	0.36	0.48
Spring	0.10	0.10	0.32	0.52	0.73	0.53	0.77	0.48
Average	0.32	0.48	0.61	1.00	0.78	0.43	0.46	0.32

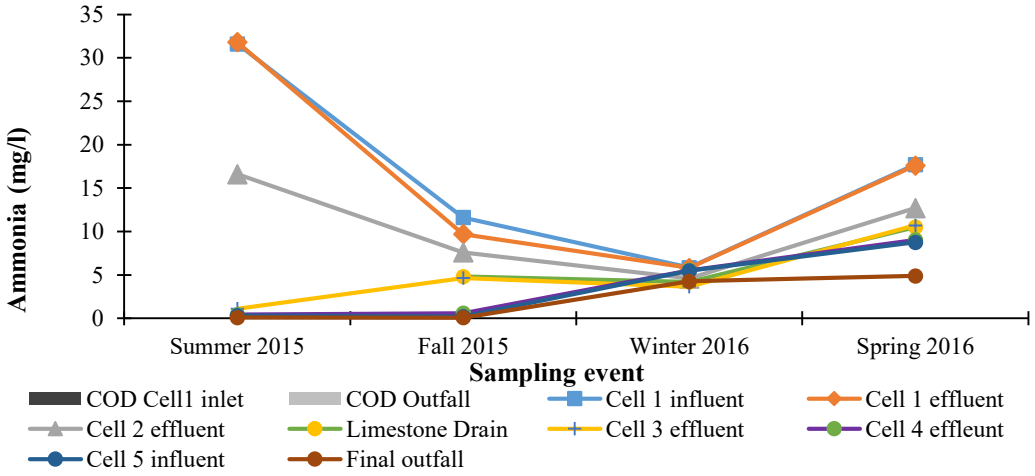

Figure 33. Ammonia concentrations in eight sampling locations for four seasons.

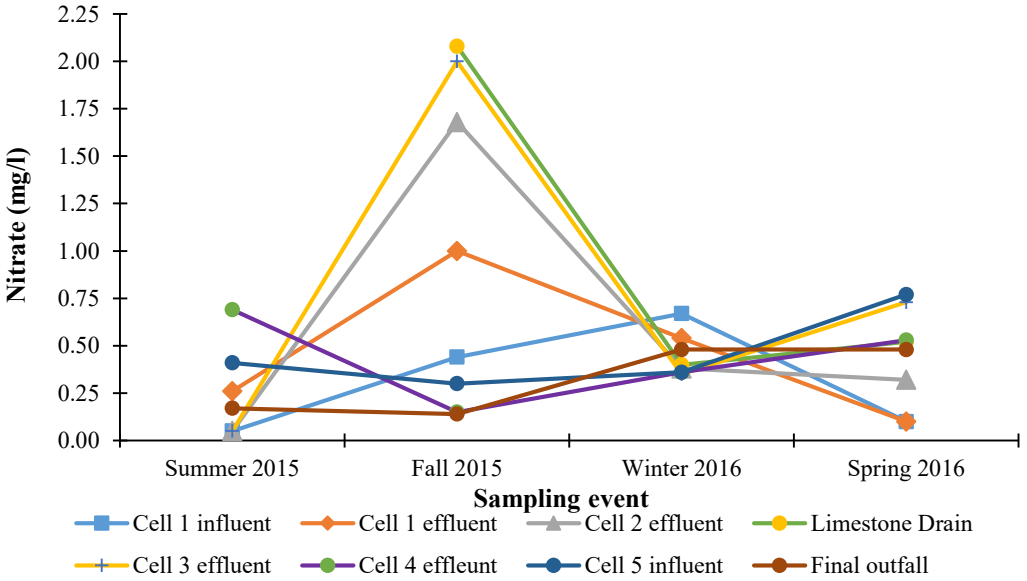

Figure 34. Nitrate concentrations in eight sampling locations for four seasons.

5.3.1.10 Sulfate and Chloride

Sulfate concentration in cell 1 influent ranged from 71 to 110 mg/l (Table 20 and Figure 35). Average sulfate levels for all seasons considerably decreased as water flowed through the cells, from 93.1 mg/l (cell 1 influent) to 78.5 mg/l (cell 1 effluent), 65.8 mg/l (cell 2), 58.5 mg/l (limestone drain), 58.2 mg/l (cell 3), 60.8 mg/l (cell 4), 56.5 mg/l (cell 5), and 64.9 mg/l (final outfall). Concentrations of sulfate were lower in summer 2015 than fall, winter, and spring, indicating dilution of wetland water by rain water.

Average chloride concentrations gradually decreased from 33.6 mg/l (cell 1 influent) to 33.4 mg/l (cell 1 effluent), 26.3 mg/l (cell 2), 19.8 mg/l (limestone drain), 19.6 mg/l (cell 3), 21.9 mg/l (cell 4), 16.4 mg/l (cell 5), 14.3 mg/l (final outfall).

Table 20 Seasonal sulfate and chloride concentrations (mg/l) for eight sampling locations.

Sampling event	Cell 1 influent	Cell 1 effluent	Cell 2 effluent	Limestone Drain	Cell 3 effluent	Cell 4 effluent	Cell 5 influent	Final outfall
				Sulfate				
Summer	71.2	46.4	29.2	14.2	16.3	25.1	8.9	4.6
Fall	99.1	90.8	83.6	73.0	73.5	50.1	48.6	103.0
Winter	110.0	95.2	75.6	73.2	72.4	92.9	92.7	84.4
Spring	92.2	81.8	74.8	73.7	70.8	75.4	75.9	67.8
Average	93.1	78.6	65.8	58.5	58.3	60.9	56.5	65.0
				Chloride				
Summer	61.9	67.0	45.2	26.6	25.4	24.9	24.7	23.3
Fall	32.9	28.2	30.8	24.6	24.6	26.7	5.0	5.0
Winter	12.2	12.2	9.7	9.4	8.9	15.3	15.6	13.0
Spring	27.5	26.4	19.8	18.7	19.6	20.9	20.5	16.2
Average	33.6	33.5	26.4	19.8	19.6	22.0	16.5	14.4

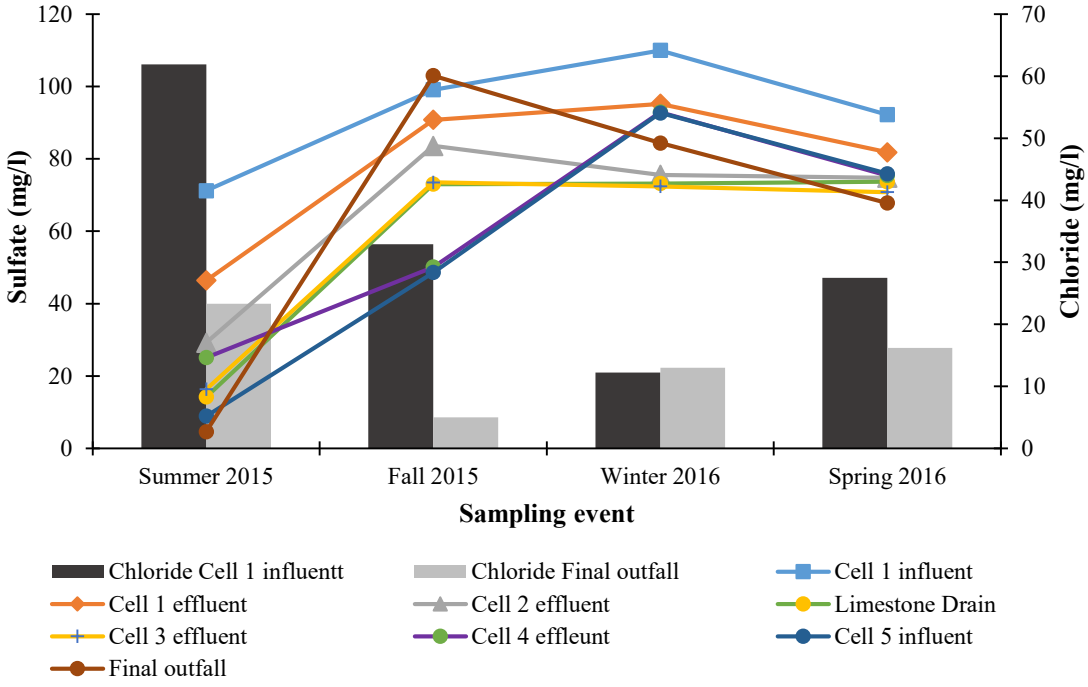

Figure 35. Sulfate concentrations for eight sampling locations and chloride concentrations at cell 1 influent and the final outfall.

5.3.2 Data Analysis

Pearson correlation coefficients were calculated using field parameters and water quality data distributions. Correlation coefficient (r) of parameters in cell 1 influent and the final outfall are presented in Table 21. According to the correlation coefficient values, parameters including temperature, pH, conductivity, DO, iron, manganese, ammonia, and nitrate were most frequently correlated.

The r values indicated negative correlation between parameter concentrations in cell 1 effluent and the final outfall of conductivity, iron, and ammonia, suggesting that the pollutants were removed as water flowed through the wetlands. Conversely, the r values indicated positive relationship between concentrations of DO in cell 1 effluent and the final outfall, indicating that the concentration of DO was increasing as the water

flowed through the wetlands. The changes in concentrations of iron, manganese, ammonia, and nitrate were dependent upon pH and water temperature. This was also indicated by the positive correlation of pH and water temperature with concentrations of iron, manganese, ammonia, and nitrate at the inflow and outflow.

5.3.2 Hydrochemical Modeling

Ion concentration data for total of four water samples collected from the wetland cells in summer 2015, fall 2015, winter 2015, and spring 2016 were used for hydrochemical modeling to characterize chemical processes occurring in the treatment wetland cells. PHREEQC Interactive program with WATQ4F database was used for the modeling.

Results of forward modeling can help identifying mineral species formed in the water and characterize phases of those minerals in terms of saturation indices. Figure 36-39 illustrate the mineral species and their saturation indices. Mineral species identified by the forward modeling include alunite ($KAl_3(SO_4)2(OH)_6$), calcite ($CaCO_3$), dolomite ($CaMg(CO_3)_2$), ferric hydroxide ($Fe(OH)_3$), gibbsite ($Al(OH)_3$), and magnesite ($MgCO_3$) for each season at each sampling location. Modeled saturation indices suggested that alunite was dissolving in summer and fall, but precipitating during winter and spring. Gibbsite was precipitating in every season at all sampling locations. Ferric hydroxide was precipitating at all sampling locations and in all seasons except in the winter when it was dissolving. A plausible explanation for this precipitation is that during the winter pH remained lower than 6 and ferric hydroxide cannot be present in that range of pH which causes it to precipitate.

Table 21
Correlation coefficient (r values) shows the correlation between parameters in Cell 1 influent and the final outfall.

	Temp in	Temp out	pH in	pH out	Cond. In	Cond. out	DO in	DO out	COD in	COD out
Temp in	1	0.8310158	0.724838	0.042251	0.997038	-0.71845	-0.91998	-0.94816	0.958562	0.296108
Temp out	0.8310158	1	0.329987	0.255646	0.852488	-0.212621	-0.81402	-0.82302	0.93983	0.736705
pH in	0.7248382	0.3299873	1	0.28093	0.732518	-0.897351	-0.80826	-0.80732	0.509673	-0.03964
pH out	0.0422512	0.2556463	0.28093	1	0.117649	0.1713589	-0.42422	-0.35072	0.030891	0.698323
Cond. In	0.9970379	0.8524881	0.732518	0.117649	1	-0.691611	-0.94542	-0.96792	0.959038	0.356548
Cond. out	-0.71845	-0.2126209	-0.89735	0.171359	-0.69161	1	0.629549	0.662159	-0.5011	0.36795
DO in	-0.919982	-0.8140203	-0.80826	-0.42422	-0.94542	0.6295486	1	0.9968	-0.85828	-0.49081
DO out	-0.948158	-0.8230241	-0.80732	-0.35072	-0.96792	0.6621589	0.9968	1	-0.88717	-0.45056
COD in	0.9585621	0.9398298	0.509673	0.030891	0.959038	-0.501101	-0.85828	-0.88717	1	0.466344
COD out	0.2961083	0.7367046	-0.03964	0.698323	0.356548	0.3679497	-0.49081	-0.45056	0.466344	1
Fe in	0.5179832	0.8966327	-0.11789	0.197133	0.541594	0.2205455	-0.48576	-0.49067	0.733205	0.829845
Fe out	-0.070594	-0.5697209	0.586954	-0.01098	-0.08515	-0.61485	-0.00158	0.003894	-0.35159	-0.68891
Mn^{2+} in	0.9633061	0.94431	0.60669	0.209455	0.976182	-0.519138	-0.93681	-0.95218	0.981156	0.53973
Mn^{2+} out	0.838287	0.3980091	0.916641	-0.09009	0.818776	-0.980788	-0.75979	-0.79063	0.653696	-0.19039
NO_3^- in	-0.557182	-0.9017358	-0.14361	-0.57452	-0.60603	-0.124276	0.681967	0.658981	-0.70555	-0.95587
NO_3^- out	-0.927226	-0.5646758	-0.88107	0.055011	-0.91221	0.9264525	0.841968	0.873656	-0.78652	0.030879
SO_4^{2-} in	-0.799668	-0.9937254	-0.24067	-0.17533	-0.81629	0.1575281	0.749599	0.763929	-0.9313	-0.72158
SO_4^{2-} out	-0.557911	-0.8398157	0.159854	0.149427	-0.55469	-0.104462	0.389836	0.421826	-0.76755	-0.58542
Cl^- in	0.9295109	0.9651668	0.442866	0.060778	0.933611	-0.418398	-0.83774	-0.86383	0.995612	0.53454
Cl^- out	0.2545094	0.6704802	-0.46397	-0.12465	0.257105	0.4271492	-0.11505	-0.13627	0.517895	0.618312
NH_3 in	0.7616936	0.9855765	0.176682	0.16041	0.778155	-0.098584	-0.70592	-0.72039	0.909723	0.735464
NH_3 out	-0.9209	-0.5508843	-0.82805	0.167233	-0.89788	0.9234117	0.790715	0.830732	-0.79056	0.088597
BOD_5 in	-0.318015	0.1530615	-0.31698	0.815577	-0.24784	0.7013035	0.004548	0.073663	-0.18223	0.780035
BOD_5 out	-0.384456	0.0635791	-0.31794	0.820576	-0.31449	0.7036896	0.057738	0.129598	-0.26606	0.718902
Rainfall	-0.184205	0.2129125	-0.10183	0.922704	-0.1088	0.5295055	-0.16781	-0.09428	-0.09607	0.793415

Table 21 continued

	Fe in	Fe out	Mn^{2+} in	Mn^{2+} out	NO_3^- in	NO_3^- out	SO_4^{2-} in	SO_4^{2-} out
Temp in	0.517983	-0.07059	0.963306	0.838287	-0.55718	-0.92723	-0.79967	-0.55791
Temp out	0.896633	-0.56972	0.94431	0.398009	-0.90174	-0.56468	-0.99373	-0.83982
pH in	-0.11789	0.586954	0.60669	0.916641	-0.14361	-0.88107	-0.24067	0.159854
pH out	0.197133	-0.01098	0.209455	-0.09009	-0.57452	0.055011	-0.17533	0.149427
Cond. In	0.541594	-0.08515	0.976182	0.818776	-0.60603	-0.91221	-0.81629	-0.55469
Cond. out	0.220546	-0.61485	-0.51914	-0.98079	-0.12428	0.926452	0.157528	-0.10446
DO in	-0.48576	-0.00158	-0.93681	-0.75979	0.681967	0.841968	0.749599	0.389836
DO out	-0.49067	0.003894	-0.95218	-0.79063	0.658981	0.873656	0.763929	0.421826
COD in	0.733205	-0.35159	0.981156	0.653696	-0.70555	-0.78652	-0.9313	-0.76755
COD out	0.829845	-0.68891	0.53973	-0.19039	-0.95587	0.030879	-0.72158	-0.58542
Fe in	1	-0.87307	0.703243	-0.03201	-0.90511	-0.16031	-0.92757	-0.93813
Fe out	-0.87307	1	-0.27743	0.471049	0.663011	-0.29682	0.639602	0.847583
Mn^{2+} in	0.703243	-0.27743	1	0.675637	-0.75939	-0.80168	-0.91597	-0.6775
Mn^{2+} out	-0.03201	0.471049	0.675637	1	-0.06842	-0.98142	-0.34298	-0.05882
NO_3 in	-0.90511	0.663011	-0.75939	-0.06842	1	0.239631	0.885936	0.719255
NO3 out	-0.16031	-0.29682	-0.80168	-0.98142	0.239631	1	0.516636	0.239462
SO_4^{2-}in	-0.92757	0.639602	-0.91597	-0.34298	0.885936	0.516636	1	0.895193
SO_4^{2-} out	-0.93813	0.847583	-0.6775	-0.05882	0.719255	0.239462	0.895193	1
Cl^- in	0.79348	-0.43303	0.975837	0.581158	-0.75834	-0.7264	-0.96117	-0.81367
Cl^- out	0.909716	-0.97199	0.422017	-0.27765	-0.66153	0.098285	-0.74303	-0.94262
NH_3 in	0.94877	-0.68829	0.887901	0.285437	-0.88947	-0.46398	-0.99786	-0.9182
NH_3 out	-0.16394	-0.26652	-0.78327	-0.97336	0.194009	0.993199	0.514215	0.281087
BOD_5 in	0.364816	-0.4417	-0.07052	-0.61417	-0.56515	0.539334	-0.13087	-0.05117
BOD_5 out	0.27275	-0.36675	-0.14791	-0.63344	-0.48867	0.576124	-0.03772	0.04447
Rainfall	0.330986	-0.30785	0.045397	-0.4381	-0.60602	0.372472	-0.16797	0.009024

Table 21 continued

	Cl^- in	Cl^- out	NH_3 in	NH_3 out	BOD_5 in	BOD_5 out	Rainfall
Temp in	0.929511	0.254509	0.761694	-0.9209	-0.31802	-0.38446	-0.18421
Temp out	0.965167	0.67048	0.985576	-0.55088	0.153062	0.063579	0.212912
pH in	0.442866	-0.46397	0.176682	-0.82805	-0.31698	-0.31794	-0.10183
pH out	0.060778	-0.12465	0.16041	0.167233	0.815577	0.820576	0.922704
Cond. In	0.933611	0.257105	0.778155	-0.89788	-0.24784	-0.31449	-0.1088
Cond. out	-0.4184	0.427149	-0.09858	0.923412	0.701304	0.70369	0.529505
DO in	-0.83774	-0.11505	-0.70592	0.790715	0.004548	0.057738	-0.16781
DO out	-0.86383	-0.13627	-0.72039	0.830732	0.073663	0.129598	-0.09428
COD in	0.995612	0.517895	0.909723	-0.79056	-0.18223	-0.26606	-0.09607
COD out	0.53454	0.618312	0.735464	0.088597	0.780035	0.718902	0.793415
Fe in	0.79348	0.909716	0.94877	-0.16394	0.364816	0.27275	0.330986
Fe out	-0.43303	-0.97199	-0.68829	-0.26652	-0.4417	-0.36675	-0.30785
Mn^{2+} in	0.975837	0.422017	0.887901	-0.78327	-0.07052	-0.14791	0.045397
Mn^{2+} out	0.581158	-0.27765	0.285437	-0.97336	-0.61417	-0.63344	-0.4381
NO_3^- in	-0.75834	-0.66153	-0.88947	0.194009	-0.56515	-0.48867	-0.60602
NO_3^- out	-0.7264	0.098285	-0.46398	0.993199	0.539334	0.576124	0.372472
SO_4^{2-} in	-0.96117	-0.74303	-0.99786	0.514215	-0.13087	-0.03772	-0.16797
SO_4^{2-} out	-0.81367	-0.94262	-0.9182	0.281087	-0.05117	0.04447	0.009024
Cl^- in	1	0.586181	0.944587	-0.72979	-0.10887	-0.19642	-0.0355
Cl^- out	0.586181	1	0.78459	0.054329	0.245796	0.160325	0.12775
NH_3 in	0.944587	0.78459	1	-0.46493	0.155559	0.061182	0.178761
NH_3 out	-0.72979	0.054329	-0.46493	1	0.615748	0.65523	0.465697
BOD_5 in	-0.10887	0.245796	0.155559	0.615748	1	0.995277	0.975453
BOD_5 out	-0.19642	0.160325	0.061182	0.65523	0.995277	1	0.972819
Rainfall	-0.0355	0.12775	0.178761	0.465697	0.975453	0.972819	1

Calcite and dolomite were dissolving in cells 1 and 2, but precipitating after flowing though limestone drain as indicated by precipitation occurring in the final outfall. Magnesite was dissolving at all sampling locations and in all seasons. The modeled data suggested that the constructed wetland is effective in removing iron and aluminum from water through enhanced precipitation of ferric hydroxide and gibbsite. The wetlands were also effective in removing sulfate and aluminum in the winter and spring at average water temperature ranging from 7 to 15 °C through precipitation of alunite. However, dissolution of alunite in the summer and fall occurred when water temperature increased (13°C to 23°C on average), appeared to make wetlands loss effective in removing sulfate and aluminum in these seasons.

pH affects dissolution and precipitation because it acts as a catalyst in the reaction or changes reaction pathway (Tsuzuki, 1967). According to pH modeling, the rate of dissolution of ferric hydroxide was increasing as pH increasing. The modeled results suggested that the concentration of H^+ which is described as pH is proportional to the rate of metal hydroxide (Stumm and Wieland, 1990). The rate of minerals precipitation and dissolution is also dependent on temperature. High temperature increases the rate of reaction by increasing the possibility of dehydration of $Al(OH^-)_4$ to AlO_2^- for example (Hemingway, 1982).

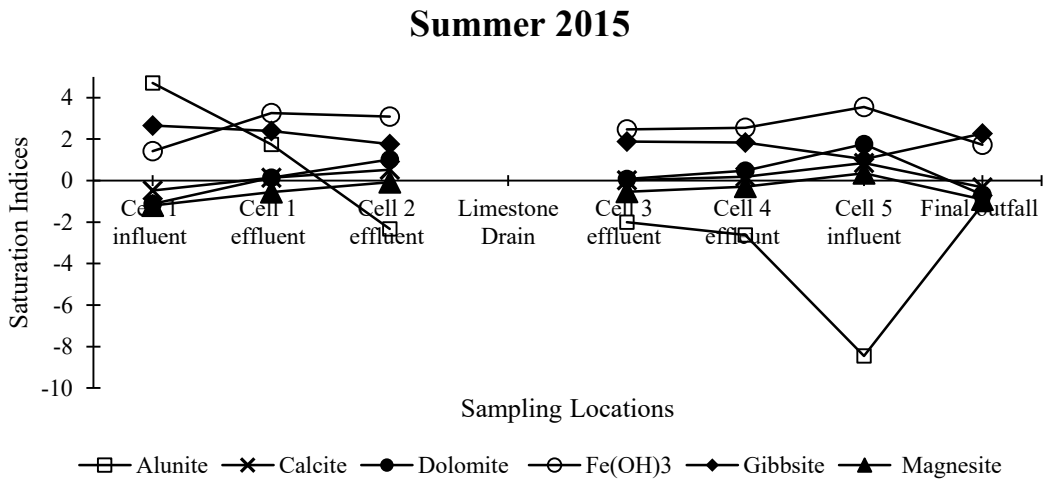

Figure 36. Saturation indices of selected minerals for summer 2015 sampling event.

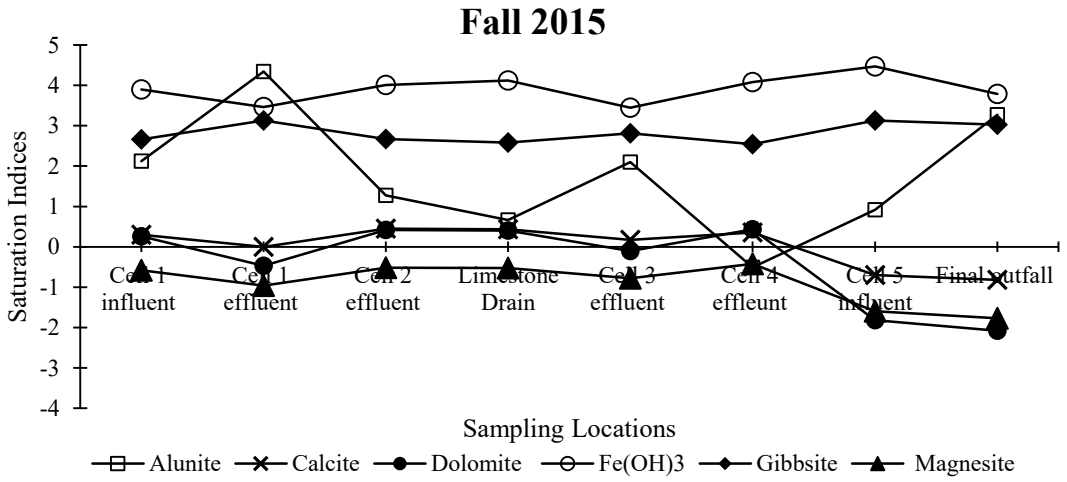

Figure 37. Saturation indices of selected minerals for fall 2015 sampling event.

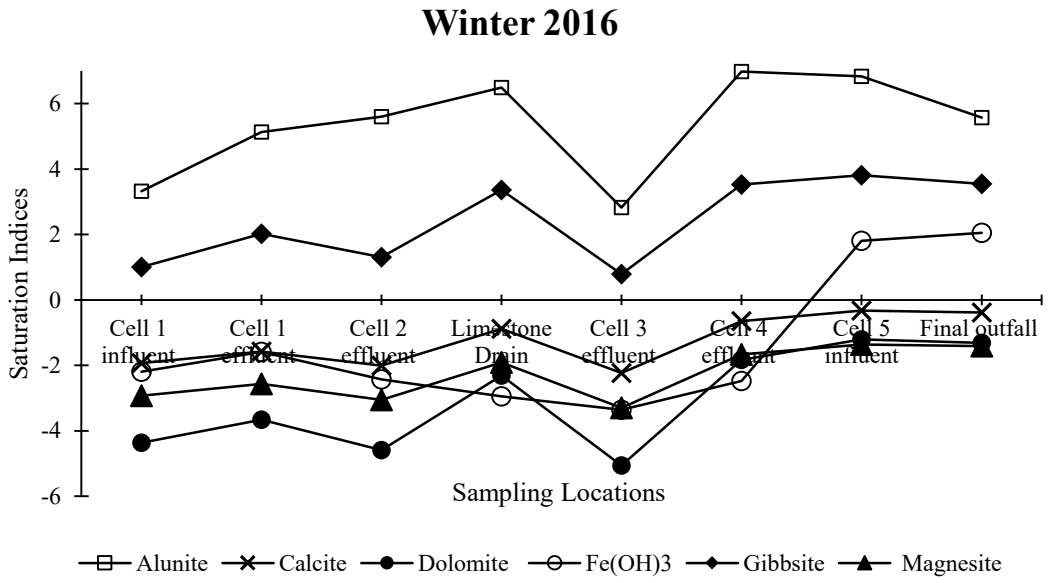

Figure 38. Saturation indices of selected minerals for winter 2016 sampling event.

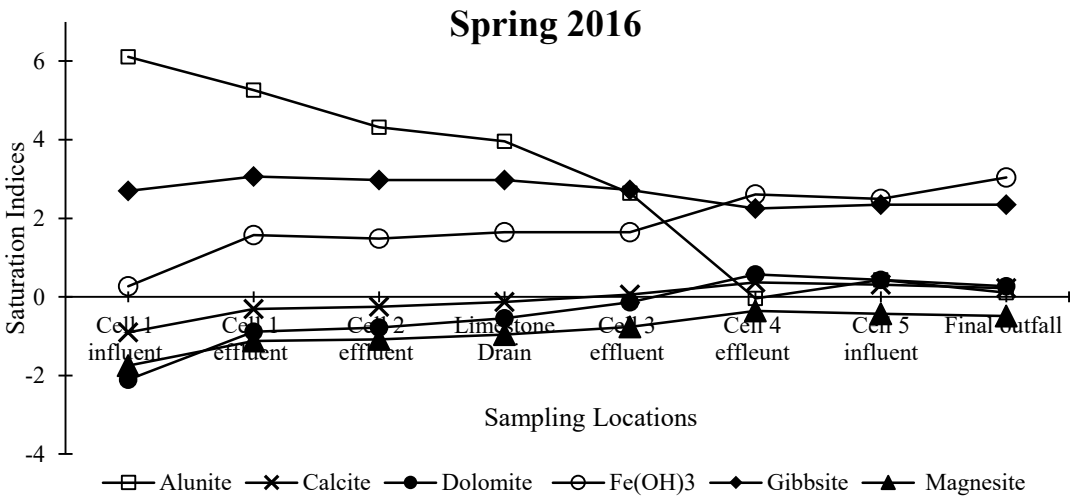

Figure 39. Saturation indices of selected minerals for spring 2016 sampling event.

5.3.3 Inverse Modeling

Hydrochemical inverse modeling was conducted in order to understand and identify mass transfer reactions that produced the compositional differences between inflows and outflows of the constructed wetland cells. In the mass balance modeling, it was assumed that chemical reactions were in steady states (Zhu and Anderson, 2002). In order to minimize kinetic effects, inflow and outflow of water samples for each wetland cell were collected almost simultaneously, and analyzed together at the same time. Mass transfers were assumed to occur within each wetland cell following the flow paths described by simple mass balance equation below.

Cell influent + reactants → Cell effluent + products

The results from PHREEQCI analyses yielded all possible inverse models. Table 22 is the summary of selected models for mass transfer within wetland cells in spring. Phase mole transfer was displayed in concentration (mol/kg of water). The negative sign (-) indicates precipitation only and positive sign (+) indicated dissolution only.

The main reaction in cell 1 is dissolution of $Fe(OH)_3$ and goethite with mole transfers of 3.96E-04 and -3.26E-05, respectively which increased dissolved iron in the landfill leachate. Most minerals dissolved in cell 2, which consumed CO_2 for 4.433e-03 mol. Precipitation of gypsum, dolomite, anhydrite occurred in limestone drain with mole transfers of 1.44E-04, 4.10E-06, and 5.88E-05, respectively, whereas barite, calcite, goethite, and siderite dissolved with mole transfers of 8.16E-07, 1.33E-04, 1.85E-05, and 1.85E-05, respectively. Large amount of magnesite and siderite precipitated in cell 3 with mole transfers of 4.10E-05 and 7.81E-03, respectively while barite and calcite dissolved

with mole transfers of 1.14E-06 and 1.12E-05, respectively. $Fe(OH)_3$, barite, and goethite dissolved more in cell 4 with mole transfers of 9.89E-06, 1.14E-06, and 1.98E-05, respectively which removed iron and sulfate. In cell 5 and 6, alunite, calcite, and dolomite dissolved with moles transfers of 1.37E-10, 1.27E-03, and 1.45E-03, respectively which removed aluminum and magnesium from the water.

According to several models observation, the outputs were varied depended on the mineral and gas phases assumed in the inputs. More models can be produced with different input constrains (Zhu and Anderson, 2002).

5.4 Removal Efficiencies

Removal rates of the treatment system were estimated for ammonia, BOD_5, COD, nitrate, chloride, iron, manganese, and sulfate by comparing concentrations (mg/l) and flow rates (l/day) of the leachate inflow to cell 1 and the final outfall from the wetland system are presented in Table 23 and Figure 40. In summer, fall, and winter, removal efficiencies ranged from 67 to 100 % for ammonia, 41 to 100 %, 33 to 100 % for chloride, BOD_5, 57 to 100 % for COD, 97 to 100 % in for iron, 86 to 100 % for manganese, 42 to 94 % for nitrate, and 17 to 100 %for sulfate, indicating generally efficient removal efficacy of the wetlands for treating those pollutants. BOD_5 levels in the leachate and the final outfall were below detection limit (0 mg/l) in fall and winter, so the removal efficiency of BOD_5 could not be estimated during those periods. However, the concentrations of COD and nitrate in the final outfall were higher than the leachate. The concentrations were increased from 31 mg/l to 34 mg/l for COD and from 0.1 mg/l to 0.2 mg/l for nitrate, resulting in removal efficiencies of -24 % and -98%, respectively. Lower

removal efficiencies of COD and nitrate removal efficiencies during spring were attributed to more active bacterial activity and potential inflow of surface runoff which elevated nitrate values.

Table 22 Results of inverse modeling at the constructed wetland cells in spring 2016. Concentration are moles per kilogram of water.

Mineral name	Mineral composition	Cell 1	Cell 2	Limestone Drain	Cell 3	Cell 4	Cell 5 and 6
Alunite	$KAl_3(SO_4)_2(OH)_6$	-2.08E-10	-2.80E-10		-2.74E-08		-1.37E-10
Anhydrite	$CaSO_4$	4.61E-04		5.88E-05	1.13E-04		
Aragonite	$CaCO_3$						
Barite	$BaSO_4$	-2.19E-07	-2.55E-07	-8.16E-07	-1.14E-06	-1.14E-06	
Calcite	$CaCO_3$			-1.33E-04	-1.12E-05		-1.27E-03
CO2(g)	CO_2		4.433e-03				6.74E-05
Diaspore	AlOOH						
Dolomite	$CaMg(CO_3)_2$			4.10E-06	4.12E-05		-1.45E-03
Ferric hydroxide	$Fe(OH)_3$	-3.96E-04	-1.52E-04		-1.98E-05	-9.89E-06	
Gibbsite	$Al(OH)_3$		-1.02E-04				
Goethite	FeOOH	-3.26E-05	-1.52E-04	-1.85E-05		-1.98E-05	
Gypsum	$CaSO_4{:}2H_2O$	4.75E-04	3.02E-04	1.44E-04		3.00E-05	1.08E-03
Halite	NaCl			5.22E-05	2.54E-05		
Hematite	$Fe2O_3$					2.54E-05	
Magnesite	$MgCO_3$			4.11E-06	4.10E-05	4.12E-05	1.34E-03
Siderite	$FeCO_3$	-1.68E-04	-4.56E-04	-1.85E-05	7.81E-03		

Table 23 Removal rates (%) of the pollutants for four sampling events.

Sampling event	Ammonia	BOD_5	Chloride	COD	Iron	Manganese	Nitrate	Sulfate
Summer 2015	100	100	100	99	100	100	88	100
Fall 2015	100	0	99	97	100	99	94	96
Winter 2016	67	0	52	57	97	86	84	65
Spring 2016	69	63	33	-24	98	90	-98	17
Average	84	41	71	57	99	94	42	69

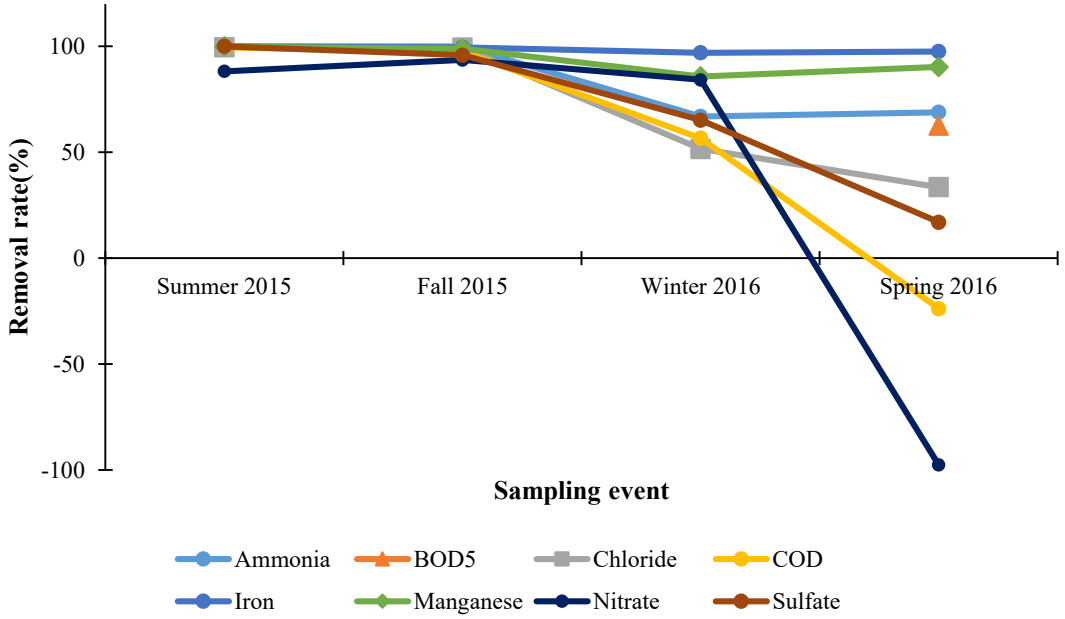

Figure 40. Removal efficiencies (%) of the wetland treatment system. Negative values indicate that concentrations were higher in final outfall than in the leachate.

CHAPTER 6: CONCLUSIONS

The purpose of this study was to investigate the performance efficiency of the constructed wetland in treating leachate generated from the Athens 691 Landfill. The assessment was performed through hydrological and hydrochemical characterizations of water in the wetlands.

The water balance of the entire treatment system was estimated using the following variables; precipitation, inflow rates, and groundwater inflow as hydrologic inputs, evapotranspiration, outflow rates, and groundwater outflow as hydrologic outputs. The results indicated that surface inflow and outflow were the major controlling factors of the water balance. During the observation period, high precipitation contributed to high surface inflow rates in August, September, and November 2015, and May 2016 with rates ranging from 1,700 to 2,700 m^3/month while low surface inflow rates occurred in October 2015 and January 2016 with rates ranging from 443 to 986 m^3/month due to low precipitation. Loss by evaporation and groundwater outflow caused low surface outflow rates in September and October 2015, and June 2016 with rates ranging from 3.5 to 5 m^3/month. The water balance estimation indicates that the constructed wetland lost water in December, January, March, April, and May. However, the calculation was not observed to be true since the water balance estimation suggested that all of the wetland cells should be dry in December 2015 and January 2016. The discrepancy between predicted and observed shows that the water balance equation may need to be altered to compensate for freezing temperature during winter months.

Hydraulic residence time is dependent upon inflow and outflow rates and volume of the wetland cells. The results indicated that cells 2 and 4 had the longest residence and yielded the highest removal efficiencies.

Water chemistry data suggested that the studied parameters were influenced by seasonal changes in temperature and precipitation. The levels of pH decreased during the dry season and increased during the wet season. Conductivity in the leachate was high in the summer and spring, suggesting more active generation of pollutants during these months due to high precipitation. In summer and spring, the levels dissolved oxygen concentrations decreased while water temperatures increased, suggesting that oxygen was used by plants during warm seasons. Acidity values were consistently below the detection limit (5 mg/l $CaCO_3$) in all samples collected from all wetland cells during all four seasons while alkalinity concentrations were high in the leachate inflow to cell 1 and generally decreased as water flowed through the wetlands. The BOD_5, COD, ammonia, and nitrate values also varied by season, depending on the temperature in each season. BOD_5 and COD concentrations were reduced as water flowed through the treatment cells, indicating active treatment of BOD_5 and COD in the wetland cells. During warm seasons, BOD_5 levels increased in all cells, suggesting bacterial activity in warm water which consumed oxygen to remove ammonia though nitrification. Nitrate concentrations in cell 1 influent increased in fall and winter, compared to summer and spring, suggesting that the source of nitrate in the wetlands is oxidation of ammonia.

The results of hydrochemical modeling using PHREEQCI indicated that ferric hydroxide ($Fe(OH)_3$) was precipitating in all sampling locations. Alunite

($KAl_3(SO_4)2(OH)_6$) and gibbsite ($Al(OH)_3$) were precipitating at the limestone drain removing sulfate and aluminum in water.

Overall, the pollutants levels (iron and manganese) were decreasing as water flowed through the treatment system. Removal efficiencies ranged from 97 to 100 % for iron and 86 to 100 % for manganese. Cell 1 provided the most efficient iron treatment system with high iron removal rates for all seasons in small volume of cell (5.3 m^3).

Results of this study suggested that the constructed wetland efficiently removes the major pollutants such as iron, manganese, sulfate, ammonia and BOD_5 in the landfill leachate.

Recommendations

1. Accurate water depth measurement tools should be installed for more accurately estimate water storage.

2. To determine hydraulic residence time for water within the wetland cells, dye tracing methods would be useful for actual time and monitoring the treatment performance.

3. A more detailed study in wetland plants, sediments, and bacterial activity would help understand the chemical, physical, and biological processes occurring with the constructed wetland.

4. Removing the mature sediment that has been coating by metals precipitated should be considered in maintenance procedure to improve porosity and penetration of wetland soil and plants.

REFERENCES

ARCADIS U.S., Inc., 2013, Athens County 691 Landfill, 2nd quarter 2013 corrective measures activities report. Columbus, Ohio.

ARCADIS U.S., Inc., 2014, Athens County 691 Landfill, 2nd quarter 2014 corrective measures activities report. Columbus, Ohio.

ARCADIS U.S., Inc., 2015, Athens County 691 Landfill, 2nd quarter 2015 corrective measures activities report. Columbus, Ohio.

Akinbile, C,. O., Yusoff, M., S., and Zuki, A., A., 2012, Landfill leachate treatment using sub-surface flow constructed wetland by *Cyperus haspan*: Waste Management, v. 32, p. 1387-1393.

Aziz, H.A, and Smith, P.G., 1996, Removal of manganese from water using crushed dolomite filtration technique: Water Resources, v. 30, p. 489-492.

Aziz, S.Q., Aziz, H.A., Yusoff, M.S., Bashir, M.J.K., and Umar, M., 2010, Leachate characterization in semi-aerobic and anaerobic sanitary landfills: Journal of Environmental Management, v. 91, p. 2608–2614.

Bradley, C., 2002, Simulation of the annual water table dynamics of a floodplain wetland, Narborough Bog, UK: Journal of Hydrology, v. 261, p. 150-172.

Bulc, T.G., 2006, Long term performance of a constructed wetland for landfill leachate treatment: Ecological Engineering, v. 26, p. 365-374.

Clark, I., and Fritz, P., 1997, Environmental Isotopes in Hydrology: Boca Raton, FL, Lewis Publishers, pp. 80-86.

Craig, H., 1961, Isotopic variations in meteoric waters: Science, v. 133, pp. 1702-1703.

Dunne, E.J., Culleton, N., O'Donovan, G., Harrington,R., and Olsen, A.E., 2005, An integrated constructed wetland to treat contaminants and nutrients from dairy farmyard dirty water: Ecological Engineering, v. 24, p. 221-234.

Faure, G., 1986, Principles of Isotope Geology, 2nd Ed., John Wiley and Sons, New York, 589 p.

Ford, K.L, 2003, Passive Treatment Systems for Acid Mine Drainage: Technical Note 409, Bureau of Land Management, http://www.blm.gov/nstc/library/techno2.htm

Glynn, P.D., and Brown, J.G., 1996, Reactive-transport modeling of acidic metal-contaminated ground water at a site with sparse spatial information, in Lichtner, P.C., Steefel, C.I., and Oelkers, E.H., eds., Reactive Transport in Porous Media: Washington, D.C., Mineralogical Society of America, Reviews in Mineralogy, v. 34, p. 377–438.

Hammer, D.A., and Bastion, R.K., 1989. Wetlands ecosystems: natural water purifiers? *In* Hammer, D.A., ed, Constructed Wetlands for Wastewater Treatment, USA, Lewis Publishers, p. 5–20.

Hammer, D.A., 1993, Designing constructed wetland systems to treat agricultural nonpoint source pollution *In* Olson R.K., ed, Created and Natural Wetlands for Controlling Point and Nonpoint Source Pollution, Boca Raton, C.K. Smoley, p. 71-112.

Hemingway, B.S., 1982,Gibbs free energies of formation for bayerite, nordstrandite, AI(OH)Z+, and AI(OH),+, aluminum mobility, and the formation of bauxites and laterites: Advanced Physical Geochemistry, v. 2, p. 283-316.

Ibanez, J.G., Hernandez, E.M., Doria, S.C, Fregoso, I.A., and Singh, M.M, 2007, Environmental Chemistry: Fundamentals: New York, Springer.

Kadlec, R.H. and Knight, R.L., 1996, Treatment Wetlands: Florida, CRC Press.

Kadlec, R.H., and Wallace, S., 2008, Treatment Wetlands second edition: Florida, CRC Press, 1016 p.

Karathanasis, A.D., 2003, Vegetation effects on fecal bacteria, BOD, and suspended solid removal in constructed wetlands treating domestic wastewater: Ecological Engineering, v. 20, p. 157-169.

Kjeldsen, P., Barlaz, M.A., Rooker, A.P., Baum, A., Ledin, A., and Christensen, T.H., 2002, Present and long-term composition of MSW landfill leachate: A review: Environmental Science and Technology, v. 32(4), p. 297-336.

Li, W., Zhou, Q., and Hua, T., 2010, Removal of Organic Matter from Landfill Leachate by Advanced Oxidation Processes: A Review. International Journal of Chemical Engineering, p. 10, http://dx.doi.org/10.1155/2010/270532

Liston, M.A., 2014, Distribution of $\delta^{18}O$ and δD Values of Precipitation in Central Ohio [BS thesis]: Columbus, Ohio State University, 19 p.

May, P.A., and Edwards, G.S., 2001, Comparison of heavy metal accumulation in a natural wetland and constructed wetlands receiving acid mine drainage: Ecological Engineering, v. 16, p. 487-500.

Mitsch, W.J., and Gosselink, J.G., 2000, Wetlands, 3d ed.: New York, John Wiley and Sons, 920 p.

Neuhaus, E., 2013, Evaluation of a water budget model for use in wetland design [MS thesis]: Blacksburg, Virginia Polytechnic Institute and State University, 110 p.

Niessen, W.R., and Chansky, S.H., 1970, The nature of refuse *In* 1970 National Incinerator Conference, American Society of Mechanical Engineering, NewYork, New York.

Nzengy, D.M., and Wishitemi, B.E.L., 2001, The performance of constructed wetlands for wastewater treatment: a case study of Splash wetland in Nairobi Kenya: Hydrological Processes, v. 15, p. 3239-3247.

Oiu, S., McComb, A.J., Bell, R.B., and Davis, J.A., 2005, Response of soil microbial activity to temperature, moisture, and litter leaching on a wetland transect during seasonal refilling: Wetland Ecology and Management, v. 13, p. 43-54.

Parkhurst, D.L. and Appelo, C.A.J., 2013, Description of input and examples for PHREEQC Version 3-A computer program for speciation, batch-reaction, one dimensional transport, and inverse geochemical calculations: U.S. Geological Survey Techniques and Methods, book 6, chap. A43, 497 p.

Schleich, K.L., 2014. Geochemical modeling of processes affecting water and sediment chemistry and their relationship to biological recovery in an acid mine drainage remediated stream [MS thesis]: Athens, Ohio University, 106 p.

Seaman, J.M, (1984). Evaluation of local and regional groundwater contamination at the Athens County Landfill. [MS thesis]: Athens, Ohio University. 190 p.

Shimala, J., 2000, Hydrogeochemical characterization of the carbonale wetland, Athens County, Ohio: Evaluation of acid mine drainage remediation alternatives [MS Thesis]: Athens, Ohio University, 345 p.

Spalding, R. F., and Exner, M. E., 1993. Occurrence of nitrate in groundwater a Review: Environmental Quality, v. 22, p. 392-402.

Speer, S., Champagne, P., and Anderson, B., 2012. Pilot-scale comparison of two hybrid-passive landfill leachate treatment systems operated in a cold climate: Biology Resource Technology, v. 104, p. 119-126.

Stumm, W., and Wieland, E.,1990, Dissolution of oxide and silicate minerals: rates depend on surface speciation. *In* Aquatic Chemical Kinetics (W. Stumm, ed.), p. 367-400. Wiley, New York.

Sturgeon, M., and Associates, 1958, The Geology and Mineral Resources of Athens County, Ohio: Ohio Department of Natural Resources, Division of Geological Survey, Columbus, v. 57.

Tsuzuki, Y., 1967, Solubility diagrams for explaining zone sequences in bauxite, kaolin, and pyrophyllite-diaspore deposits: Clays Clay Mineral, v. 24, p. 297-302.

United States Environmental Protection Agency, 1979, Methods for Chemical Analysis of Water and Waste*s*, USEPA Publication No.EPA-600/4-79-020, Office of Research and Development, 491 p.

United States Environmental Protection Agency, 1993, Subsurface flow constructed wetlands for wastewater treatment: A technology assessment, EPA/832-R-93-008, Office of Wastewater Enforcement and Compliance, 87 p.

United States Environmental Protection Agency, 1999, Free water surface wetlands for waste water treatment: A technology assessment, EPA/832-S-99-002, Arizona, Office of Wastewater Management, 167 p.

United States Environmental Protection Agency, 2000, Constructed wetland treatment of municipal wastewaters, EPA/625/R-99/010: Ohio, Office of Research and Development, Manual, 166 p.

Vymazal, J., 2005, Horizontal sub-surface flow and hybrid constructed wetland systems for wastewater treatment: Ecological Engineering, v. 25, p. 478-490

Watson, J.T., Reed, S.C., Kadlec, R.H., Knight, R.L., and Whitehouse, A.E., 1989, Performance, expectations and loading rates for constructed wetlands *In* Hammer, D.A., ed, Constructed Wetlands for Wastewater Treatment: Municipal, Industrial and Agricultural, Chelsea, Lewis Publishers, p. 319-349.

Zhang, B.Y, Zheng, J.S., Sharp, R.G., 2010, Phytoremediation in engineered wetlands: Mechanisms and application: Procedia Environmental Sciences, v. 2, p. 1315-1325.

Zhu, C., and Anderson, G., 2002, Environmental Applications of Geochemical Modeling: Thermodynamic Background: Cambridge, University Press, 284 p.

Zotarelli, L., Dukes, M.D., Romero, C.C., Migliaccio, K.W., and Morgan,K.T., 2009, Step by Step Calculation of the Penman-Monteith Evapotranspiraion (FAO-56 Method): Agricultural and Biological Engineering Department, Florida, University of Florida.

APPENDIX: PHREEQCI INPUT FILES

Analytical Compositions for Summer 2015

```
SOLUTION_SPREAD
    -units    mg/l
   Al  Alkalinity    Ba    Ca    Cd    Cl     Fe          K    Mg    Mn
N(3)   N(5)    Na    Pb  S(6)    Sr    Zn  Temperature         pH  N(-
3)
ug/l         mg/l  ug/l  mg/l  ug/l  mg/l   ug/l       mg/l  mg/l  ug/l
mg/l   mg/l  mg/l  ug/l  mg/l  ug/l  ug/l
  100         549   195   110   0.1  61.9  44200       21.8  43.8  3840
0.01   0.05  46.3     1  71.2   429     5        16.65       6.36
31.6
  100         545   224   107  0.02    67  43200         26  43.2  2480
0.01   0.26  44.6   0.7  46.4   398     5        18.01       6.97
31.8
  100         442   170  80.5   0.1  45.2   1850       18.6  36.1  1170
0.01   0.05  32.3   3.5  29.2   328     5        21.61       7.48
16.6
  100         266   111    57   0.1  25.4    887       11.5  27.7  1180
0.029  0.05  19.3   3.3  16.3   240     5        23.25       7.27
16.6
  205         230    72  49.9   0.1  24.9    676       10.5  27.2   497
0.01   0.69  18.5  10.3  25.1   228     5        25.59       7.52
1.11
  100         217    70  38.7   0.1  24.7   1540        6.4  25.5  1290
0.029  0.41  19.4  16.9   8.9   181     5        16.59       8.46
0.417
  100         236    52  49.5  0.02  23.3    481        9.5  25.1   566
0.011  0.17  17.6  12.4   4.6   203     4        19.31       7.06
0.307
END

INVERSE_MODELING 1 Cell1
    -solutions      1        2
    -uncertainty    -0.02    -0.02
    -phases
        Alunite          pre
        Anhydrite        dis
        Aragonite        dis
        Barite           pre
        Calcite          pre
        CO2(g)           dis
        Dolomite         pre
        Fe(OH)3(a)       pre
        Gibbsite         pre
        Goethite         pre
        Gypsum           pre
        Halite           dis
        Magnesite        dis
        Siderite         pre
```

```
    -balances
        Al          -0.02    -0.02
        Ba          -0.02    -0.02
        Ca          -0.02    -0.02
        Cd          -0.02    -0.02
        Cl          -0.02    -0.02
        Fe          -0.02    -0.02
        K           -0.02    -0.02
        Mg          -0.02    -0.02
        Mn          -0.02    -0.02
        N(3)        -0.02    -0.02
        N(5)        -0.02    -0.02
        Na          -0.02    -0.02
        Pb          -0.02    -0.02
        S(6)        -0.02    -0.02
        Sr          -0.02    -0.02
        Zn          -0.02    -0.02
        C           -0.02    -0.02
        H(0)        -0.02    -0.02
    -tolerance         1e-10
    -mineral_water     true
END
INVERSE_MODELING 5 Cell 2
    -solutions      2        3
    -uncertainty    -0.02    -0.02
    -phases
        Alunite           dis
        Anhydrite         dis
        Aragonite         pre
        Barite            pre
        Calcite           dis
        CO2(g)            dis
        Dolomite          pre
        Fe(OH)3(a)        pre
        Gibbsite          pre
        Goethite          pre
        Gypsum            dis
        Halite            dis
        Magnesite         dis
        Siderite          pre
    -balances
        Al          -0.02    -0.02
        Ba          -0.02    -0.02
        Ca          -0.02    -0.02
        Cd          -0.02    -0.02
        Cl          -0.02    -0.02
        Fe          -0.02    -0.02
        K           -0.02    -0.02
        Mg          -0.02    -0.02
        Mn          -0.02    -0.02
        N(3)        -0.02    -0.02
        N(5)        -0.02    -0.02
        Na          -0.02    -0.02
        Pb          -0.02    -0.02
```

```
        S(6)        -0.02    -0.02
        Sr          -0.02    -0.02
        Zn          -0.02    -0.02
        C           -0.02    -0.02
        H(0)        -0.02    -0.02
    -tolerance         1e-10
    -mineral_water     true
END
INVERSE_MODELING 2 Cell3
    -solutions      3        4
    -uncertainty    -0.02    -0.02
    -phases
        Alunite           dis
        Anhydrite         dis
        Aragonite         dis
        Barite            dis
        Calcite           pre
        CO2(g)            dis
        Dolomite          pre
        Fe(OH)3(a)        pre
        Gibbsite          pre
        Goethite          pre
        Gypsum            dis
        Halite            dis
        Magnesite         dis
        Siderite          pre
    -balances
        Al          -0.02    -0.02
        Ba          -0.02    -0.02
        Ca          -0.02    -0.02
        Cd          -0.02    -0.02
        Cl          -0.02    -0.02
        Fe          -0.02    -0.02
        K           -0.02    -0.02
        Mg          -0.02    -0.02
        Mn          -0.02    -0.02
        N(3)        -0.02    -0.02
        N(5)        -0.02    -0.02
        Na          -0.02    -0.02
        Pb          -0.02    -0.02
        S(6)        -0.02    -0.02
        Sr          -0.02    -0.02
        Zn          -0.02    -0.02
        C           -0.02    -0.02
        H(0)        -0.02    -0.02
    -tolerance         1e-10
    -mineral_water     true
END
INVERSE_MODELING 3 Cell4
    -solutions      4        5
    -uncertainty    -0.02    -0.02
    -phases
        Alunite           dis
        Anhydrite         dis
```

```
        Aragonite          pre
        Barite             dis
        Calcite            pre
        CO2(g)             dis
        Dolomite           pre
        Fe(OH)3(a)         pre
        Gibbsite           pre
        Goethite           pre
        Gypsum             dis
        Halite             dis
        Magnesite          dis
        Siderite           dis
    -balances
        Al           -0.02    -0.02
        Ba           -0.02    -0.02
        Ca           -0.02    -0.02
        Cd           -0.02    -0.02
        Cl           -0.02    -0.02
        Fe           -0.02    -0.02
        K            -0.02    -0.02
        Mg           -0.02    -0.02
        Mn           -0.02    -0.02
        N(3)         -0.02    -0.02
        N(5)         -0.02    -0.02
        Na           -0.02    -0.02
        Pb           -0.02    -0.02
        S(6)         -0.02    -0.02
        Sr           -0.02    -0.02
        Zn           -0.02    -0.02
        C            -0.02    -0.02
        H(0)         -0.02    -0.02
    -tolerance         1e-10
    -mineral_water     true
END
INVERSE_MODELING 4 Cell 5 and 6
    -solutions      6        7
    -uncertainty    -0.02    -0.02
    -phases
        Alunite            dis
        Anhydrite          dis
        Aragonite          dis
        Barite             dis
        Calcite            pre
        CO2(g)             dis
        Dolomite           dis
        Fe(OH)3(a)         pre
        Gibbsite           pre
        Goethite           pre
        Gypsum             dis
        Halite             dis
        Magnesite          dis
        Siderite           dis
    -balances
        Al           -0.02    -0.02
```

```
    Ba          -0.02    -0.02
    Ca          -0.02    -0.02
    Cd          -0.02    -0.02
    Cl          -0.02    -0.02
    Fe          -0.02    -0.02
    K           -0.02    -0.02
    Mg          -0.02    -0.02
    Mn          -0.02    -0.02
    N(3)        -0.02    -0.02
    N(5)        -0.02    -0.02
    Na          -0.02    -0.02
    Pb          -0.02    -0.02
    S(6)        -0.02    -0.02
    Sr          -0.02    -0.02
    Zn          -0.02    -0.02
    C           -0.02    -0.02
    H(0)        -0.02    -0.02
-tolerance         1e-10
-mineral_water     true
```

Analytical Compositions for Fall 2015

```
SOLUTION_SPREAD
    -units    mg/l
   Al  Alkalinity    Ba    Ca    Cd    Cl     Fe          K    Mg    Mn
N(3)   N(5)    Na    Pb  S(6)    Sr    Zn  Temperature         pH  N(-
3)
ug/l         mg/l  ug/l  mg/l  ug/l  mg/l   ug/l       mg/l  mg/l  ug/l
mg/l   mg/l  mg/l  ug/l  mg/l  ug/l  ug/l
  200         364   129   107   0.2  32.9  16200       13.8  34.1  2620
0.02   0.44  27.6     2  99.1   340    10        11.49       7.38
0.007
  200         353   148   107   0.2  28.2  29400       13.3  33.7  1640
0.02      1  24.7     2  90.8   337    10         6.08       7.17
9.69
  200         298   123    93   0.2  30.8   2870       13.9  29.8   543
0.044  1.68  24.3     2  83.6   303    10         4.96       7.75
7.59
  200         265   100  82.9   0.2  24.6   2570       12.3  26.1   415
0.076  2.08  18.4     2    73   265    10         5.28       7.82
4.8
  200         264    94  81.9   0.2  24.6   2210       12.1    26   281
0.095     2  18.2     2  73.5   264    10         5.96       7.55
4.65
  327         190   122  49.5   0.2  26.7   1180       11.7  24.4   778
0.02   0.15  17.9     2  50.1   209    10          5.6       8.07
0.597
  989        43.6    35  21.5   0.2     5   2180        2.9   8.2   773
0.02    0.3     5     2  48.6    76    10         3.79       8.07
0.193
  854        43.5    43    39   0.2     5   1900        4.8  12.3   714
0.02   0.14     5     2   103   137    38         6.47       7.67
0.07

END
INVERSE_MODELING 1 Cell1
    -solutions      1        2
    -uncertainty    -0.02    -0.02
    -phases
        Alunite           pre
        Anhydrite         dis
        Aragonite         dis
        Barite            pre
        Calcite
        CO2(g)            dis
        Dolomite          dis
        Fe(OH)3(a)        pre
        Gibbsite          pre
        Goethite          pre
        Gypsum            dis
        Halite            dis
        Magnesite         dis
        Siderite          pre
    -balances
```

```
        Al          -0.02    -0.02
        Ba          -0.02    -0.02
        Ca          -0.02    -0.02
        Cd          -0.02    -0.02
        Cl          -0.02    -0.02
        Fe          -0.02    -0.02
        K           -0.02    -0.02
        Mg          -0.02    -0.02
        Mn          -0.02    -0.02
        N(3)        -0.02    -0.02
        N(5)        -0.02    -0.02
        Na          -0.02    -0.02
        Pb          -0.02    -0.02
        S(6)        -0.02    -0.02
        Sr          -0.02    -0.02
        Zn          -0.02    -0.02
        C           -0.02    -0.02
        H(0)        -0.02    -0.02
    -tolerance         1e-10
    -mineral_water     true
END
INVERSE_MODELING 6 Cell 2
    -solutions      2        3
    -uncertainty    -0.02    -0.02
    -phases
        Alunite           pre
        Anhydrite         dis
        Aragonite         pre
        Barite            pre
        Calcite           pre
        CO2(g)            dis
        Dolomite          pre
        Fe(OH)3(a)        pre
        Gibbsite          pre
        Goethite          pre
        Gypsum            dis
        Halite            dis
        Magnesite         dis
        Siderite          pre
    -tolerance         1e-10
    -mineral_water     true
END
INVERSE_MODELING 2 Limestone drain
    -solutions      3        4
    -uncertainty    -0.02    -0.02
    -phases
        Alunite           pre
        Anhydrite         dis
        Aragonite         pre
        Barite            pre
        Calcite           pre
        CO2(g)            dis
        Dolomite          pre
        Fe(OH)3(a)        pre
```

```
        Gibbsite          pre
        Goethite          pre
        Gypsum            dis
        Halite            dis
        Magnesite         dis
        Siderite          pre
    -balances
        Al          -0.02    -0.02
        Ba          -0.02    -0.02
        Ca          -0.02    -0.02
        Cd          -0.02    -0.02
        Cl          -0.02    -0.02
        Fe          -0.02    -0.02
        K           -0.02    -0.02
        Mg          -0.02    -0.02
        Mn          -0.02    -0.02
        N(3)        -0.02    -0.02
        N(5)        -0.02    -0.02
        Na          -0.02    -0.02
        Pb          -0.02    -0.02
        S(6)        -0.02    -0.02
        Sr          -0.02    -0.02
        Zn          -0.02    -0.02
        C           -0.02    -0.02
        H(0)        -0.02    -0.02
    -tolerance         1e-10
    -mineral_water     true
END
INVERSE_MODELING 3 Cell 3
    -solutions      4        5
    -uncertainty    -0.02    -0.02
    -phases
        Alunite           pre
        Anhydrite         dis
        Aragonite         pre
        Barite            pre
        Calcite           pre
        CO2(g)            dis
        Dolomite          dis
        Fe(OH)3(a)        pre
        Gibbsite          pre
        Goethite          pre
        Gypsum            dis
        Halite            dis
        Magnesite         dis
        Siderite          pre
    -balances
        Al          -0.02    -0.02
        Ba          -0.02    -0.02
        Ca          -0.02    -0.02
        Cd          -0.02    -0.02
        Cl          -0.02    -0.02
        Fe          -0.02    -0.02
        K           -0.02    -0.02
```

```
        Mg          -0.02    -0.02
        Mn          -0.02    -0.02
        N(3)        -0.02    -0.02
        N(5)        -0.02    -0.02
        Na          -0.02    -0.02
        Pb          -0.02    -0.02
        S(6)        -0.02    -0.02
        Sr          -0.02    -0.02
        Zn          -0.02    -0.02
        C           -0.02    -0.02
        H(0)        -0.02    -0.02
    -tolerance         1e-10
    -mineral_water     true
END
INVERSE_MODELING 4 Cell4
    -solutions      5        6
    -uncertainty    -0.02    -0.02
    -phases
        Alunite           dis
        Anhydrite         dis
        Aragonite         pre
        Barite            pre
        Calcite           dis
        CO2(g)            dis
        Dolomite          pre
        Fe(OH)3(a)        pre
        Gibbsite          pre
        Goethite          pre
        Gypsum            dis
        Halite            dis
        Magnesite         dis
        Siderite          pre
    -balances
        Al          -0.02    -0.02
        Ba          -0.02    -0.02
        Ca          -0.02    -0.02
        Cd          -0.02    -0.02
        Cl          -0.02    -0.02
        Fe          -0.02    -0.02
        K           -0.02    -0.02
        Mg          -0.02    -0.02
        Mn          -0.02    -0.02
        N(3)        -0.02    -0.02
        N(5)        -0.02    -0.02
        Na          -0.02    -0.02
        Pb          -0.02    -0.02
        S(6)        -0.02    -0.02
        Sr          -0.02    -0.02
        Zn          -0.02    -0.02
        C           -0.02    -0.02
        H(0)        -0.02    -0.02
    -tolerance         1e-10
    -mineral_water     true
END
```

```
INVERSE_MODELING 5 cell 5 and 6
    -solutions      7        8
    -uncertainty    -0.02    -0.02
    -phases
        Alunite           pre
        Anhydrite         dis
        Aragonite         dis
        Barite            pre
        Calcite           dis
        CO2(g)            dis
        Dolomite          dis
        Fe(OH)3(a)        pre
        Gibbsite          pre
        Goethite          pre
        Gypsum            dis
        Halite            dis
        Magnesite         dis
        Siderite          dis
    -balances
        Al          -0.02    -0.02
        Ba          -0.02    -0.02
        Ca          -0.02    -0.02
        Cd          -0.02    -0.02
        Cl          -0.02    -0.02
        Fe          -0.02    -0.02
        K           -0.02    -0.02
        Mg          -0.02    -0.02
        Mn          -0.02    -0.02
        N(3)        -0.02    -0.02
        N(5)        -0.02    -0.02
        Na          -0.02    -0.02
        Pb          -0.02    -0.02
        S(6)        -0.02    -0.02
        Sr          -0.02    -0.02
        Zn          -0.02    -0.02
        C           -0.02    -0.02
        H(0)        -0.02    -0.02
    -tolerance         1e-10
    -mineral_water     true
END
```

Analytical Compositions for Winter 2015-2016

```
SOLUTION_SPREAD
    -units    mg/l
   Al  Alkalinity    Ba    Ca    Cd    Cl     Fe          K    Mg    Mn
N(3)   N(5)    Na    Pb  S(6)    Sr    Zn  Temperature         pH  N(-
3)
ug/l         mg/l  ug/l  mg/l  ug/l  mg/l   ug/l       mg/l  mg/l  ug/l
mg/l   mg/l  mg/l  ug/l  mg/l  ug/l  ug/l
  200         287    96  95.3   0.2  12.2  17100        7.1  26.2   743
0.02   0.67  12.5     2   110   260    10         7.23        5.34
5.84
  200         279    80  84.3   0.2  12.2   3960        7.2  25.1   751
0.02   0.54  12.3     2  95.2   239    10         5.78        5.76
5.85
  200         240    78  76.4   0.2   9.7   3280       1000  21.9  1000
0.02   0.38  10.1     2  75.6   213    10         3.11        5.54
4.59
  200         232    73  75.8   0.2   9.4   2060        6.5  21.8   610
0.02    0.4  10.3     2  73.2   214    10         3.76         6.6
4.19
  311         238    74  74.5   0.2   8.9   2250        6.1  20.7   515
0.02   0.35   9.4     2  72.4   211    10         1.86        5.28
3.64
  259         286    85  88.7   0.2  15.3   1200        8.4  26.6   329
0.02   0.36  14.4     2  92.9   260    10         3.17        6.71
5.53
  539         283    89  89.6   0.2  15.6   1880        8.3  26.2   380
0.02   0.36  14.5     2  92.7   262    10         3.19        7.03
5.48
  317         225    73  71.7   0.2    13   1150           7  21.9   233
0.02   0.48  11.4     2  84.4   213    38         1.95        7.18
4.25
END
INVERSE_MODELING 1 Cell 1
    -solutions      1        2
    -uncertainty    -0.02    -0.02
    -phases
        Alunite           pre
        Anhydrite         dis
        Aragonite         dis
        Barite            pre
        Calcite           dis
        CO2(g)            dis
        Dolomite          dis
        Fe(OH)3(a)        dis
        Gibbsite          pre
        Goethite          pre
        Gypsum            dis
        Halite            dis
        Magnesite         dis
        Siderite          dis
    -balances
        Al          -0.02    -0.02
```

```
        Ba          -0.02    -0.02
        Ca          -0.02    -0.02
        Cd          -0.02    -0.02
        Cl          -0.02    -0.02
        Fe          -0.02    -0.02
        K           -0.02    -0.02
        Mg          -0.02    -0.02
        Mn          -0.02    -0.02
        N(3)        -0.02    -0.02
        N(5)        -0.02    -0.02
        Na          -0.02    -0.02
        Pb          -0.02    -0.02
        S(6)        -0.02    -0.02
        Sr          -0.02    -0.02
        Zn          -0.02    -0.02
        C           -0.02    -0.02
        H(0)        -0.02    -0.02
    -tolerance         1e-10
    -mineral_water     true
END
INVERSE_MODELING 2 Cell 2
    -solutions      2        3
    -uncertainty    -0.02    -0.02
    -phases
        Alunite           pre
        Anhydrite         dis
        Aragonite         dis
        Barite            pre
        Calcite           dis
        CO2(g)            dis
        Dolomite          dis
        Fe(OH)3(a)        dis
        Gibbsite          pre
        Goethite          pre
        Gypsum            dis
        Halite            dis
        Magnesite         dis
        Siderite          dis
    -balances
        Al          -0.02    -0.02
        Ba          -0.02    -0.02
        Ca          -0.02    -0.02
        Cd          -0.02    -0.02
        Cl          -0.02    -0.02
        Fe          -0.02    -0.02
        K           -0.02    -0.02
        Mg          -0.02    -0.02
        Mn          -0.02    -0.02
        N(3)        -0.02    -0.02
        N(5)        -0.02    -0.02
        Na          -0.02    -0.02
        Pb          -0.02    -0.02
        S(6)        -0.02    -0.02
        Sr          -0.02    -0.02
```

```
        Zn          -0.02    -0.02
        C           -0.02    -0.02
        H(0)        -0.02    -0.02
    -tolerance         1e-10
    -mineral_water     true
END
INVERSE_MODELING 3 Limestone drain
    -solutions      3        4
    -uncertainty    -0.02    -0.02
    -phases
        Alunite           pre
        Anhydrite         dis
        Aragonite         dis
        Barite            pre
        Calcite           dis
        CO2(g)            dis
        Dolomite          dis
        Fe(OH)3(a)        dis
        Gibbsite          pre
        Goethite          pre
        Gypsum            dis
        Halite            dis
        Magnesite         dis
        Siderite          dis
    -balances
        Al          -0.02    -0.02
        Ba          -0.02    -0.02
        Ca          -0.02    -0.02
        Cd          -0.02    -0.02
        Cl          -0.02    -0.02
        Fe          -0.02    -0.02
        K           -0.02    -0.02
        Mg          -0.02    -0.02
        Mn          -0.02    -0.02
        N(3)        -0.02    -0.02
        N(5)        -0.02    -0.02
        Na          -0.02    -0.02
        Pb          -0.02    -0.02
        S(6)        -0.02    -0.02
        Sr          -0.02    -0.02
        Zn          -0.02    -0.02
        C           -0.02    -0.02
        H(0)        -0.02    -0.02
    -tolerance         1e-10
    -mineral_water     true
END
INVERSE_MODELING 4 Cell 3
    -solutions      4        5
    -uncertainty    -0.02    -0.02
    -phases
        Alunite           pre
        Anhydrite         dis
        Aragonite         dis
        Barite            pre
```

```
        Calcite           dis
        CO2(g)            pre
        Dolomite          dis
        Fe(OH)3(a)        dis
        Gibbsite          pre
        Goethite          pre
        Gypsum            dis
        Halite            dis
        Magnesite         dis
        Siderite          dis
    -balances
        Al          -0.02    -0.02
        Ba          -0.02    -0.02
        Ca          -0.02    -0.02
        Cd          -0.02    -0.02
        Cl          -0.02    -0.02
        Fe          -0.02    -0.02
        K           -0.02    -0.02
        Mg          -0.02    -0.02
        Mn          -0.02    -0.02
        N(3)        -0.02    -0.02
        N(5)        -0.02    -0.02
        Na          -0.02    -0.02
        Pb          -0.02    -0.02
        S(6)        -0.02    -0.02
        Sr          -0.02    -0.02
        Zn          -0.02    -0.02
        C           -0.02    -0.02
        H(0)        -0.02    -0.02
    -tolerance         1e-10
    -mineral_water     true
END
INVERSE_MODELING 5 Cell 4
    -solutions      5        6
    -uncertainty    -0.02    -0.02
    -phases
        Alunite           pre
        Anhydrite         dis
        Aragonite         dis
        Barite            pre
        Calcite           dis
        CO2(g)            dis
        Dolomite          dis
        Fe(OH)3(a)        pre
        Gibbsite          pre
        Goethite          pre
        Gypsum            dis
        Halite            dis
        Magnesite         dis
        Siderite          pre
    -tolerance         1e-10
    -mineral_water     true
END
INVERSE_MODELING 6 Cell 5 and 6
```

```
    -solutions      7        8
    -uncertainty    -0.02    -0.02
    -phases
        Alunite           pre
        Anhydrite         dis
        Aragonite         dis
        Barite            pre
        Calcite           dis
        CO2(g)            dis
        Dolomite          dis
        Fe(OH)3(a)        pre
        Gibbsite          pre
        Goethite          pre
        Gypsum            dis
        Halite            dis
        Magnesite         dis
        Siderite          dis
    -tolerance         1e-10
    -mineral_water     true
END
```

Analytical Compositions for Spring 2016

```
SOLUTION_SPREAD
    -units    mg/l
   Al  Alkalinity    Ba    Ca    Cd    Cl     Fe          K    Mg    Mn
N(3)   N(5)    Na    Pb  S(6)    Sr    Zn  Temperature         pH  N(-
3)
ug/l         mg/l  ug/l  mg/l  ug/l  mg/l   ug/l       mg/l  mg/l  ug/l
mg/l   mg/l  mg/l  ug/l  mg/l  ug/l  ug/l
  200         442   177   120   0.2  27.5  33200       14.9  39.9  2020
0.02    0.1  29.4     2  92.2   408    10        12.66       6.04
17.7
  200         438   147   114   0.2  26.4  11100       14.2  39.9  1870
0.02    0.1  29.1     2  81.8   239    10        14.13       6.62
17.6
  200         382   112  96.7   0.2  19.8   2640       10.7  31.1  1280
0.02   0.32  20.5     2  74.8   323    10        15.02       6.78
12.7
  249         366   156  97.2   0.2  18.7   1610       11.1  31.2  1130
0.064  0.52  21.7     2  73.7   369    63        15.14       6.91
10.5
  200         375   132  98.4   0.2  19.6    504       11.1  32.2   384
0.106  0.73  21.6     2  70.8   332    10        15.55       7.08
10.7
  200         321    93  82.6   0.2  20.9    439       11.1  31.8   339
0.109  0.53  22.3     2  75.4   296    10        17.29        7.5
9.02
  200         313    92  82.7   0.2  20.5    357       11.2  31.9   218
0.103  0.11  22.1     2  75.9   296    10         15.9       7.47
8.76
  200         247    22  67.9   0.2  16.2    720       10.1  29.3   175
0.066  0.48  19.4     2  67.8   254    10        13.85       7.58
4.88
END
INVERSE_MODELING 1 Cell1
    -solutions      1        2
    -uncertainty    -0.02    -0.02
    -phases
        Alunite           pre
        Anhydrite         dis
        Aragonite         dis
        Barite            pre
        Calcite           dis
        CO2(g)            dis
        Dolomite          dis
        Fe(OH)3(a)        pre
        Gibbsite          pre
        Goethite          pre
        Gypsum            dis
        Halite            dis
        Magnesite         dis
        Siderite          pre
    -balances
        Al          -0.02    -0.02
        Ba          -0.02    -0.02
```

```
        Ca          -0.02    -0.02
        Cd          -0.02    -0.02
        Cl          -0.02    -0.02
        Fe          -0.02    -0.02
        K           -0.02    -0.02
        Mg          -0.02    -0.02
        Mn          -0.02    -0.02
        N(3)        -0.02    -0.02
        N(5)        -0.02    -0.02
        Na          -0.02    -0.02
        Pb          -0.02    -0.02
        S(6)        -0.02    -0.02
        Sr          -0.02    -0.02
        Zn          -0.02    -0.02
        C           -0.02    -0.02
        H(0)        -0.02    -0.02
    -tolerance         1e-10
    -mineral_water     true
END
INVERSE_MODELING 2 Cell 2
    -solutions      2        3
    -uncertainty    -0.02    -0.02
    -phases
        Alunite           pre
        Anhydrite         dis
        Aragonite         dis
        Barite            pre
        Calcite           dis
        CO2(g)            dis
        Dolomite          dis
        Fe(OH)3(a)        pre
        Gibbsite          pre
        Goethite          pre
        Gypsum            dis
        Halite            dis
        Magnesite         dis
        Siderite          pre
    -balances
        Al          -0.02    -0.02
        Ba          -0.02    -0.02
        Ca          -0.02    -0.02
        Cd          -0.02    -0.02
        Cl          -0.02    -0.02
        Fe          -0.02    -0.02
        K           -0.02    -0.02
        Mg          -0.02    -0.02
        Mn          -0.02    -0.02
        N(3)        -0.02    -0.02
        N(5)        -0.02    -0.02
        Na          -0.02    -0.02
        Pb          -0.02    -0.02
        S(6)        -0.02    -0.02
        Sr          -0.02    -0.02
        Zn          -0.02    -0.02
        C           -0.02    -0.02
```

```
        H(0)        -0.02    -0.02
    -tolerance         1e-10
    -mineral_water     true
END
INVERSE_MODELING 3 Limestone drain
    -solutions      3        4
    -uncertainty    -0.02    -0.02
    -phases
        Alunite           pre
        Anhydrite         dis
        Aragonite         dis
        Barite            pre
        Calcite           pre
        CO2(g)            dis
        Dolomite          dis
        Fe(OH)3(a)        pre
        Gibbsite          pre
        Goethite          pre
        Gypsum            dis
        Halite            dis
        Magnesite         dis
        Siderite          pre
    -balances
        Al          -0.02    -0.02
        Ba          -0.02    -0.02
        Ca          -0.02    -0.02
        Cd          -0.02    -0.02
        Cl          -0.02    -0.02
        Fe          -0.02    -0.02
        K           -0.02    -0.02
        Mg          -0.02    -0.02
        Mn          -0.02    -0.02
        N(3)        -0.02    -0.02
        N(5)        -0.02    -0.02
        Na          -0.02    -0.02
        Pb          -0.02    -0.02
        S(6)        -0.02    -0.02
        Sr          -0.02    -0.02
        Zn          -0.02    -0.02
        C           -0.02    -0.02
        H(0)        -0.02    -0.02
    -tolerance         1e-10
    -mineral_water     true
END
INVERSE_MODELING 4 Cell 3
    -solutions      4        5
    -uncertainty    -0.02    -0.02
    -phases
        Alunite           pre
        Anhydrite         dis
        Aragonite         dis
        Barite            pre
        Calcite           pre
        CO2(g)            dis
        Dolomite          dis
```

```
        Fe(OH)3(a)        pre
        Gibbsite          pre
        Goethite          pre
        Gypsum            dis
        Halite            dis
        Magnesite         dis
        Siderite          dis
    -balances
        Al          -0.02    -0.02
        Ba          -0.02    -0.02
        Ca          -0.02    -0.02
        Cd          -0.02    -0.02
        Cl          -0.02    -0.02
        Fe          -0.02    -0.02
        K           -0.02    -0.02
        Mg          -0.02    -0.02
        Mn          -0.02    -0.02
        N(3)        -0.02    -0.02
        N(5)        -0.02    -0.02
        Na          -0.02    -0.02
        Pb          -0.02    -0.02
        S(6)        -0.02    -0.02
        Sr          -0.02    -0.02
        Zn          -0.02    -0.02
        C           -0.02    -0.02
        H(0)        -0.02    -0.02
    -tolerance         1e-10
    -mineral_water     true
END
INVERSE_MODELING 5 Cell 4
    -solutions      4        5
    -uncertainty    -0.02    -0.02
    -phases
        Alunite           dis
        Anhydrite         dis
        Aragonite         pre
        Barite            pre
        Calcite           pre
        CO2(g)            dis
        Dolomite          pre
        Fe(OH)3(a)        pre
        Gibbsite          pre
        Goethite          pre
        Gypsum            dis
        Halite            dis
        Magnesite         dis
        Siderite          dis
    -balances
        Al          -0.02    -0.02
        Ba          -0.02    -0.02
        Ca          -0.02    -0.02
        Cd          -0.02    -0.02
        Cl          -0.02    -0.02
        Fe          -0.02    -0.02
        K           -0.02    -0.02
```

```
        Mg          -0.02    -0.02
        Mn          -0.02    -0.02
        N(3)        -0.02    -0.02
        N(5)        -0.02    -0.02
        Na          -0.02    -0.02
        Pb          -0.02    -0.02
        S(6)        -0.02    -0.02
        Sr          -0.02    -0.02
        Zn          -0.02    -0.02
        C           -0.02    -0.02
        H(0)        -0.02    -0.02
    -tolerance         1e-10
    -mineral_water     true
END
INVERSE_MODELING 6 Cell 5 and 6
    -solutions      7        8
    -uncertainty    -0.02    -0.02
    -phases
        Alunite           pre
        Anhydrite         dis
        Aragonite         pre
        Barite            dis
        Calcite           pre
        CO2(g)            dis
        Dolomite          pre
        Fe(OH)3(a)        pre
        Gibbsite          pre
        Goethite          pre
        Gypsum            dis
        Halite            dis
        Magnesite         dis
        Siderite          pre
    -balances
        Al          -0.02    -0.02
        Ba          -0.02    -0.02
        Ca          -0.02    -0.02
        Cd          -0.02    -0.02
        Cl          -0.02    -0.02
        Fe          -0.02    -0.02
        K           -0.02    -0.02
        Mg          -0.02    -0.02
        Mn          -0.02    -0.02
        N(3)        -0.02    -0.02
        N(5)        -0.02    -0.02
        Na          -0.02    -0.02
        Pb          -0.02    -0.02
        S(6)        -0.02    -0.02
        Sr          -0.02    -0.02
        Zn          -0.02    -0.02
        C           -0.02    -0.02
        H(0)        -0.02    -0.02
    -tolerance         1e-10
    -mineral_water     true
END
```

Thesis and Dissertation Services